

Aus der Gruppe Vaskuläre Signaltransduktion und Krebs
des Deutschen Krebsforschungszentrums (DKFZ) Heidelberg
Arbeitsgruppenleiter: Prof. Dr. med. Andreas Fischer

**The role of Semaphorin 3C in the activation of hepatic stellate cells
and liver fibrosis**

Inauguraldissertation
zur Erlangung des medizinischen Doktorgrades
der
Medizinischen Fakultät Mannheim
der Ruprecht-Karls-Universität
zu
Heidelberg

vorgelegt von
Max Ole Hubert

aus
Kaarst
2022

Dekan: Prof. Dr. med. Sergij Goerd
Referent: Prof. Dr. med. Andreas Fischer

MEINEN ELTERN, SCHWESTERN UND OMIS.

TABLE OF CONTENTS

page

DECLARATION – PUBLISHED CONTENT OF THE DISSERTATION ...	1
LIST OF FIGURES & TABLES	2
ABBREVIATIONS	4
1 INTRODUCTION	8
1.1 The liver	8
1.1.1 Anatomy and histology of the liver	8
1.1.2 Hepatic stellate cells	10
1.2 Liver fibrosis.....	12
1.2.1 Pathogenesis of liver fibrosis	12
1.2.2 Hepatic stellate cells and liver fibrosis	14
1.2.3 Progression	19
1.2.4 Therapeutic strategies	20
1.3 Hepatocellular carcinoma and hepatic stellate cells	22
1.4 Semaphorin protein family	23
1.4.1 Vertebrate Semaphorins	24
1.4.2 Class 3 Semaphorins.....	26
1.5 Aim.....	28
2 MATERIAL AND METHODS	31
2.1 Material	31
2.1.1 Solutions and Buffers	31
2.1.2 Chemicals	33
2.1.3 Consumables	34
2.1.4 Kits & Reagents	35

2.1.5	Oligonucleotid primers for qPCR	35
2.1.6	Genotyping primers.....	36
2.1.7	Plasmids	36
2.1.8	Antibodies	36
2.1.9	Bacteria, cell lines, growth media	37
2.1.10	Mouse strains.....	38
2.1.11	Equipment and software	38
2.2	Methods.....	40
2.2.1	Cell Culture	40
2.2.2	Biochemical and molecularbiological methods	41
2.2.3	Mouse Experiments	48
2.2.4	Statistical analysis.....	51
2.2.5	Bioinformatic analysis	52
	Gene set enrichment analysis.....	52
	Overall survival analysis	52
2.2.6	Ethical statement	53
3	RESULTS	54
3.1	The role of Semaphorin 3C in liver fibrosis.....	54
3.1.1	Semaphorin 3C is enriched in cirrhotic patients.....	54
3.1.2	Semaphorin 3C correlates with worse fibrotic state in patients	55
3.2	The role of Semaphorin 3C in the activation of hepatic stellate cells	56
3.2.1	Semaphorin 3C exacerbates TGF- β signaling response in fibroblasts 56	
3.2.2	Semaphorin 3C overexpression upregulates TGF- β related gene expression in activated fibroblasts	57
3.2.3	Semaphorin 3C upregulation in activated hepatic stellate cells.....	59
3.2.4	Semaphorin 3C receptor downregulation in activated hepatic stellate cells 61	
3.2.5	Regulation of class 3 Semaphorins in activated hepatic stellate cells 62	
3.2.6	Semaphorin 3C knock out decreases activatability of hepatic stellate cells 63	
3.3	The role of Neuropilin 2 in the activation of hepatic stellate cells	64
3.3.1	Neuropilin 2 alters Neuropilin 1 expression in fibroblasts	64
3.3.2	Neuropilin 2 alters activatability of hepatic stellate cells	66

3.4	Semaphorin 3C expression correlates with overall survival in patients with hepatocellular carcinoma	67
4	DISCUSSION	69
4.1	Correlation of Semaphorin 3C and chronic liver disease.....	69
4.2	Role of Semaphorin 3C in fibroblast signaling and activation.....	70
4.3	The relevance of Semaphorin 3C in activation and transdifferentiation of hepatic stellate cells.....	71
4.4	Other Class 3 semaphorins in activated hepatic stellate cells.....	73
4.5	Semaphorin 3C in hepatocellular carcinoma	73
4.6	Study limitations.....	74
4.7	Conclusion and outlook	75
5	SUMMARY	77
6	ZUSAMMENFASSUNG.....	79
7	REFERENCES	81
8	APPENDIX	97
9	CURRICULUM VITAE	98
10	DANKSAGUNG	99

DECLARATION – PUBLISHED CONTENT OF THE DISSERTATION

Partial results of the work at hand were published in:

*De Angelis Rigotti F, Wiedmann L, **Hubert MO**, et al. Semaphorin 3C exacerbates liver fibrosis [published online ahead of print, 2023 Apr 15]. Hepatology.2023;10.1097/HEP.000000000000407.doi:10.1097/HEP.000000000000407*

LIST OF FIGURES & TABLES

List of figures

Figure 1 - Organization of the liver	9
Figure 2 - Mechanistic concepts of liver fibrosis	14
Figure 3 - Functions, features, and phenotypes of HSCs following activation	17
Figure 4 - Therapeutic opportunities for blocking fibrosis development.....	21
Figure 5 - Proposed mechanisms by which HSCs promote HCC.....	23
Figure 6 – Semaphorins and their receptors: Plexins and Neuropilins	24
Figure 7 - Semaphorin 3C and its role in development.....	28
Figure 8 - HSC isolation overview.....	50
Figure 9 - HSC isolation, perfusion step	51
Figure 10 – Semaphorin and Plexin targets enriched in cirrhotic liver samples.....	54
Figure 11 - Cirrhosis signature genes enriched in SEMA3C high expressing patients with alcoholic hepatitis	55
Figure 12 – GRX cells show elevated levels of TGF- β signaling upon SEMA3C overexpression.....	56
Figure 13 – SEMA3C overexpressing cells show elevated levels of TGF- β related gene expression.....	58
Figure 14 - Semaphorin 3C is upregulated in activated primary HSC upon activation by culture time.....	59
Figure 15 - <i>Nrp2</i> is maintained while <i>Nrp1</i> and <i>Plxnd1</i> are clearly downregulated upon activation	61
Figure 16 - <i>Sema3a</i> and <i>Sema3e</i> are upregulated, <i>Sema3b</i> and <i>Sema3f</i> downregulated in activated hepatic stellate cells	62
Figure 17 - HSCs with SEMA3C knock-out express lower levels of activation and transdifferentiation markers.....	64
Figure 18 - Neuropilin 2 knock down alters activatability of fibroblasts and downregulates Neuropilin 1.....	65
Figure 19 - HSCs with NRP2 knock out express lower levels of activation and transdifferentiation markers.....	66
Figure 20 – SEMA3C low expressing patients show longer overall survival than SEMA3C high expressing patients.....	67

Figure 21 - Automatic cutoff determination of KM OS plot in HCC patients.....	97
---	----

List of tables

Table 1 - Consumables	34
Table 2 - Kits and reagents	35
Table 3 - Oligonucleotid primers	35
Table 4 - genotyping primers	36
Table 5 – Plasmids.....	36
Table 6 – Antibodies Western Blot.....	36
Table 7 – Bacteria	37
Table 8 - Cell lines	37
Table 9 - Growth media, solutions, buffers	37
Table 10 - Mouse strains.....	38
Table 11 - Laboratory equipment	38
Table 12 – Software	39
Table 13 - Master mix composition cDNA transcription	43
Table 14 - qPCR reaction protocol.....	44
Table 15 - Genotyping mix for SM22a-CRE, SEMA3C-flox, NRP2-flox mutant, NRP2-flox WT	45
Table 16 - PCR program for SM22a-CRE genotyping	45
Table 17 - PCR program for SEMA3C-flox genotyping.....	45
Table 18 - PCR program for NRP2-flox mutant genotyping.....	46
Table 19 - PCR program for NRP2-flox Wildtype genotyping	46

ABBREVIATIONS

A

AB	<i>antibody</i>
ASH	<i>alcoholic steatohepatitis</i>

B

BSA	<i>bovine serum albumin</i>
-----	-----------------------------

C

CRE	<i>cyclization recombinase</i>
CTGF	<i>connective tissue growth factor</i>

D

d	<i>days</i>
DNA	<i>deoxyribonucleic acid</i>
DAPI	<i>4',6-Diamidin-2-phenylindol</i>
DMEM	<i>Dulbecco modified eagle medium</i>

E

EBS	<i>enzyme buffer solution</i>
ECM	<i>extra cellular matrix</i>

F

FCS	<i>fetal calf serum</i>
FDR	<i>false discovery rate</i>
fl	<i>flox</i>
FLNA	<i>filamin a</i>

G

g	<i>grams</i>
g	<i>g – force</i>
GAPDH	<i>Glyceraldehyde 3-phosphate dehydrogenase</i>
GBBS/A	<i>Gey's balanced salt solution A</i>
GBBS/B	<i>Gey's balanced salt solution B</i>
GSEA	<i>gene set enrichment analysis</i>

H

h	<i>hour</i>
---	-------------

HBV	<i>hepatitis b virus</i>
HCC	<i>hepatocellular carcinoma</i>
HSC	<i>hepatic stellate cell</i>
HEK 293T	<i>human-embryonic kidney cells 293 with SV40-large T-antigen</i>
HR	<i>hazard ratio</i>
I	
IVC	<i>inferior vena cava</i>
K	
ko	<i>knock-out</i>
KC	<i>Kupffer cell</i>
L	
l	<i>liter</i>
LB	<i>lysogeny broth</i>
LC	<i>liver cirrhosis</i>
LF	<i>liver fibrosis</i>
LSEC	<i>liver sinusoidal endothelial cell</i>
M	
min	<i>minute</i>
ml	<i>milliliter</i>
μl	<i>microliter</i>
mg	<i>milligramm</i>
μg	<i>microgram</i>
mRNA	<i>messenger ribonucleic acid</i>
N	
NAFL	<i>non-alcoholic fatty liver</i>
NAFLD	<i>non-alcoholic fatty liver disease</i>
NASH	<i>non-alcoholic steatohepatitis</i>
NES	<i>normalized enrichment score</i>
NRP	<i>Neuropilin</i>
NRP1	<i>Neuropilin 1</i>
NRP2	<i>Neuropilin 2</i>

O

OS *overall survival*

P

pSMAD2/3

PAGE *polyacrylamide gel electrophoresis*

PAI-1 *plasminogen activator inhibitor 1*

PBS *phosphate buffered saline*

PCR *polymerase chain reaction*

PDGF *platelet derived growth factor*

PLXND1 *Plexin D1*

PMSF *phenylmethylsulfonyl flouride*

PV *portal vein*

P/S *penicillin / streptomycin*

Q

q-PCR *quantitative polymerase chain reaction*

R

Rpm *revolutions per minute*

RT *reverse transcription / transcriptase*

S

S100A6 *S100 calcium binding protein A 6*

SDS *sodium dodecyl sulfate*

SEMA3A *Semaphorin 3A*

SEMA3B *Semaphorin 3B*

SEMA3C *Semaphorin 3C*

SEMA3D *Semaphorin 3D*

SEMA3E *Semaphorin 3E*

SEMA3F *Semaphorin 3F*

shRNA *small hairpin Ribonucleic acid*

α -SMA *α – smooth muscle actin*

T

TAGLN *transgelin*

TGF- β *transforming growth factor β*

TME *tumor microenvironment*

V

VCP *valosin containing protein*

VEGF *vascular endothelium-derived growth factor*

W

WB *Western blot*

Wt *wildtype*

1 INTRODUCTION

1.1 The liver

The liver is a complex and multifunctional organ. More than 30% of the body's total blood volume passes through the liver per minute (Sheth and Bankey, 2001). It efficiently regulates the lipid household, biotransforms and metabolizes drugs, breaks down and stores nutrients, and synthesizes proteins (Tannapfel and Klöppel, 2020). These numerous functions play a pivotal role for the human organism. Given the vast variety of hepatic functions, it becomes clear how severe the implications of hepatic diseases and consequential hepatic malfunction, or even hepatic failure, are (Bosoi and Rose, 2013; Ginès and Schrier, 2009; Helmy et al., 2000; Jalan et al., 2012).

1.1.1 Anatomy and histology of the liver

The liver locates in the upper peritoneal cave, made up of two lobes and eight segments. Liver tissue consists of a range of different parenchymal and non-parenchymal cell types. The parenchymal fraction of hepatic cells are hepatocytes; hepatic stellate cells (HSCs) (or Ito-cells), Kupffer cells (KCs), liver sinusoidal endothelial cells (LSECs), hepatic lymphocytes (HLs), dendritic cells (DCs), and biliary cells (BCs) built the non-parenchymal fraction of hepatic cells. 60-80% of the liver's total cell population are hepatocytes, with 20-40% non-parenchymal cells (Racanelli and Rehmann, 2006). The liver has a unique dual blood supply receiving oxygen-rich blood from the hepatic artery and nutrient-rich blood from the portal vein (DeLeve, 2011). Together with the outflowing biliary duct, the hepatic artery and the portal vein flow into the liver in the hepatic portal. This trias can be traced up into the small organizational unit of the liver - the hepatic lobule. Each lobule has a hexagonal architecture with a central vein (CV) in its center and periportal triads at the corners (**Figure 1A**). Portal triads are also called Glisson triads: a small branch of the hepatic artery, the portal vein, and a biliary canaliculus. From the Glisson trias, arteriovenous blood flows through the liver sinusoids towards the central vein (**Figure 1B**). A layer of hepatocytes frames each liver sinusoid. The liver sinusoids are formed by LSECs, highly specialized and fenestrated endothelial cells that built the barrier between sinusoids and the space of Disse (Maslak et al., 2015).

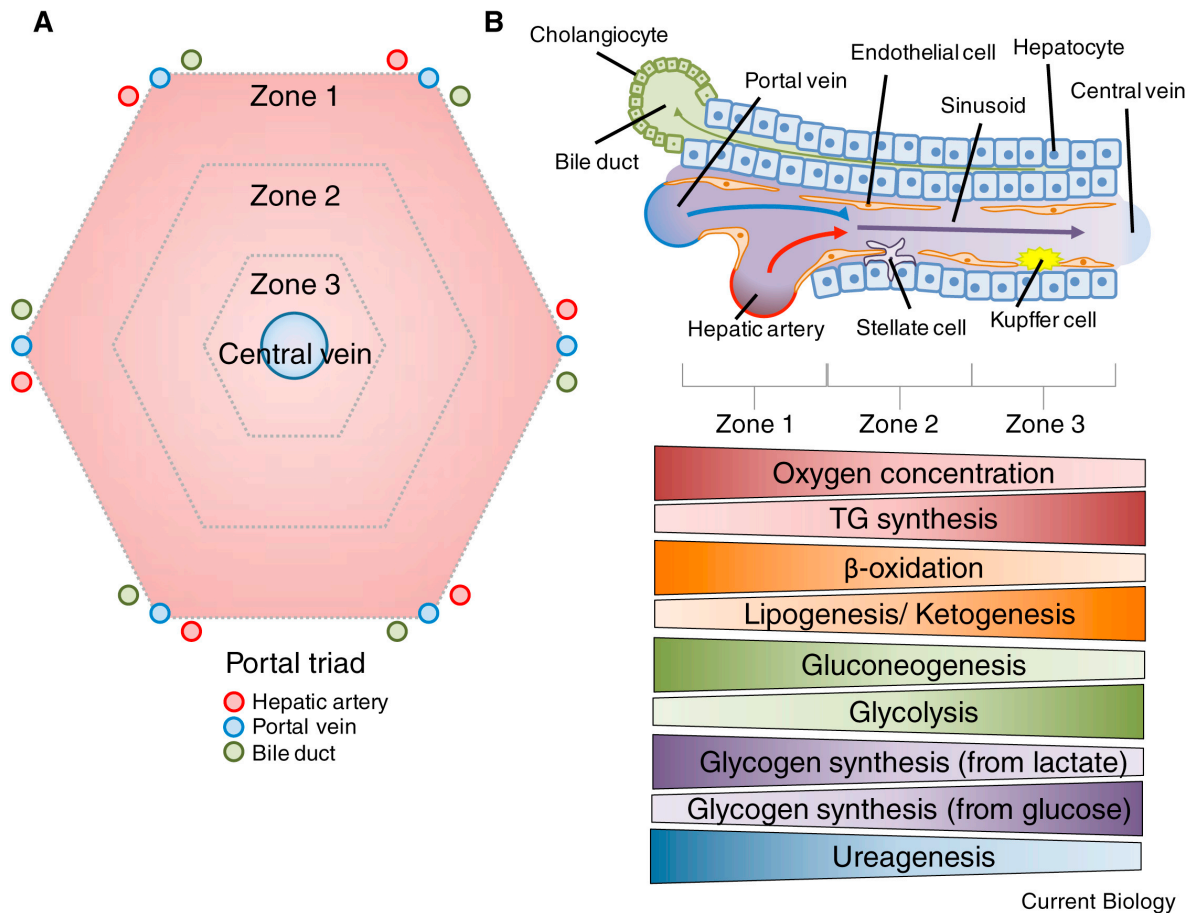


Figure 1 - Organization of the liver

Overview of the liver's microanatomical architecture. **(A)** The hexagonal liver lobule is divided into three zones, with the periportal triads at the borders and the central vein in the lobule's center. Mixed arteriovenous blood from the hepatic artery and the portal vein flows from the periportal triads towards the central vein; bile flows opposite. **(B)** Sinusoids are formed by LSECs and surrounded by layers of hepatocytes that also frame the minor ductal units for bile transport (the canaliculus) towards the bile ducts. Hepatic stellate cells and Kupffer cells sit within the space of Disse or between LSECs at the edge of a sinusoid. Liver functions and processes vary from zone to zone due to different oxygen and nutrient levels. Reprinted with permission from (Trefts et al., 2017).

LSECs: liver sinusoidal endothelial cells

The space of Disse is a perivascular niche located between each sinusoid and the surrounding hepatocytes and contains a variety of cells, including hepatic stellate cells, Kupffer cells, and hepatic lymphocytes. These various cell types are embedded into the liver's extracellular matrix (ECM) that scaffolds the space of Disse. The ECM's complex composition consists of different types of collagens (especially collagen IV), secreted proteins, proteoglycans, glycosaminoglycans (hyaluronan), and glycoproteins (Geerts, 2001). This precisely structured and balanced environment directs the different cells' positional specialization, development, and migration and

drives wound healing and tissue regeneration (Schuppan et al., 2001; Stamenkovic, 2003). In healthy liver condition, the total ECM weight measures only about 0.5% of the organ's total weight (Rojkind et al., 1979). The close positional relation and, thereby, the interaction between parenchymal and non-parenchymal hepatic cells is the basis of the ECMs composition. In general, it builds the functional framework for physiological and pathophysiological mechanisms in liver function and disease. In a hepatological, clinical context, HSCs stand out among the non-parenchymal cells with their well-recognized role in liver fibrosis.

1.1.2 Hepatic stellate cells

First described by German anatomist Karl Wilhelm von Kupffer in 1876 as perivascular cells of the connective tissue (Pinzani and Gandhi, 2015), HSCs gained more and more attention over the last centuries over their increasingly understood and regarded role as critical agents in chronic liver diseases, especially fibrosis. HSCs are non-parenchymal resident liver cells and make up roughly 10% of the liver's non-parenchymal cells (Giampieri et al., 1981; Wake, 1971; Yin et al., 2013). Remarkably only 1.5% of total liver mass is composed of HSCs – a relatively low percentage considering the cells' vital role in organ homeostasis and their crucial importance for fibrotic mechanisms (Puche et al., 2013). In healthy livers, HSCs are in a quiescent and inactivated state. However, acute or chronic liver injury initiates hepatic stellate cell activation, with HSCs undergoing transdifferentiation into a proliferatory, myofibroblast-like state (Friedman et al., 1985; Mederacke et al., 2013). To understand the central role of HSCs in the creation and progression of liver fibrosis, it is of the essence to first envision their physiological characteristics and functions to then understand the morphological and pathophysiological changes in activated HSCs that contribute to fibrosis.

HSCs are mesenchymal cells (Asahina et al., 2009), likely to be embryologically originating from the septum transversum mesenchyme (STM) (Asahina et al., 2011). Different morphological features are typical for HSCs. Their eponymous stellate or star-shaped cytoplasmatic processes are easily detectable under a light microscope. Their most characteristic feature is the high cytoplasmatic lipid level. Hepatic stellate cells typically contain many circular-shaped vacuoles, storing vitamin A within the HSCs' cytoplasm and being responsible for the characteristic autofluorescence of HSCs

(Friedman et al., 1992; Shang et al., 2018). The high lipid content of HSCs facilitates their microscopic detection under specific wavelengths (Lua et al., 2016) and the density-based isolation of the cells (Friedman and Roll, 1987). The somewhat poorly developed smooth endoplasmic reticulum suggests that the cytoplasmic lipids are not synthesized by the HSCs themselves but endocytosed from the sinusoids (Wake, 1971). HSCs have a well-developed rough endoplasmic reticulum and Golgi apparatus, indicating their strong ability to synthesize and secrete proteins. HSCs express a variety of nuclear transcription factor receptors such as farnesoid X receptor (FXR), peroxisome proliferator-activated receptors (PPARs), or liver X receptor (LXR) that ensure HSC quiescence by suppression of activatory pathways (Tsuchida and Friedman, 2017). For example, in quiescent HSCs, PPAR γ downregulates the expression of transforming growth factor – β (TGF- β), Collagen I and alpha smooth muscle actin (α SMA) (Hazra et al., 2004). Besides these characteristic morphological features of HSCs, there are various molecular markers for quiescent and activated HSCs facilitating the precise identification of HSCs. Many studies have described Desmin (Yokoi et al., 1984), glial fibrillary acidic protein (GFAP) (Gard et al., 1985), and platelet-derived growth factor receptor β (PDGFR- β) (Heldin et al., 1991; Pinzani et al., 1994) among others to be typical markers for quiescent HSCs. Distinct features and markers for activated HSCs will be discussed in *chapter 1.2 liver fibrosis*.

In a healthy liver, quiescent HSCs fulfill a variety of functions. The retinoid storing cells contain more than 80% of the body's total vitamin A (Hendriks et al., 1985). Along with LSECs, Kupffer cells and hepatocytes, HSCs play a decisive role in maintaining ECM homeostasis in the space of Disse (Puche et al., 2013) by secreting not only ECM components such as collagens but also matrix metalloproteinases. These proteinases are crucial for balancing ECM production and degradation (Arthur et al., 1989; Knittel et al., 1999; Stamenkovic, 2003). Furthermore, HSCs release various mediators that affect surrounding cells in a paracrine manner. For example, HSCs synthesize and release vascular endothelial growth factor (VEGF) and hepatocyte growth factor (HGF). With HGF being the most potent mitogen for hepatocytes (Schirmacher et al., 1992) and VEGF's crucial role in vasculo- and angiogenesis (Apte et al., 2019), the pivotal role of hepatic stellate cells for liver homeostasis and regeneration becomes clear (Puche et al., 2013).

Acute or chronic liver injury can initiate hepatic stellate cell activation, with HSCs undergoing transdifferentiation into a proliferatory, myofibroblast-like state (Friedman et al., 1985; Mederacke et al., 2013). To understand the activation process of HSCs and the dynamic morphological and pathophysiological changes the cells undergo, several protocols for murine HSC isolation and subsequent culturing have been developed (Friedman et al., 1985; Mederacke et al., 2015; Weiskirchen et al., 2017). Cultivating isolated primary murine hepatic stellate cells was observed to sufficiently activate hepatic stellate cells and initiate transdifferentiation towards a proliferative and myofibroblast phenotype (De Minicis et al., 2007). Hence, the cultivation of isolated HSCs is regarded as an appropriate *ex vivo* model to simulate profibrotic processes and liver fibrosis.

1.2 Liver fibrosis

Liver fibrosis is a pathological remodeling process of liver tissue. It results from chronic liver inflammation and injury caused by virus hepatitis, metabolic disorders, abusive alcohol consumption or biliary obstruction, and the subsequent wound healing response by the liver (Kisseleva and Brenner, 2021). Liver fibrosis is characterized by excessive secretion of extracellular matrix resulting in replacement of liver tissue by scar tissue (Friedman, 2003). Progressing liver fibrosis can ultimately lead to liver cirrhosis, resulting in hepatic decompensation, liver failure, and hepatocellular carcinoma. Patients with decompensated cirrhosis have a 5-year mortality of 50% (Fattovich et al., 1997), and nowadays, chronic liver diseases account for more than 2 million deaths per year, making chronic liver diseases a global and significant health challenge to hepatologists and doctors in general (Asrani et al., 2019).

1.2.1 Pathogenesis of liver fibrosis

While the fibrosis' etiology differs from patient to patient and is distinct, etiology specific fibrotic patterns are known (Pinzani and Macias-Barragan, 2010), central pathophysiological and molecular mechanisms of fibrosis development are regarded to be the same (Kisseleva and Brenner, 2021): An overshooting hepatic response to injury and inflammation leads to massive ECM deposition by myofibroblastic cells forming a fibrotic scar. Fate trace analysis proved HSCs to be the primary source of hepatic myofibroblasts - upon activation, they transdifferentiate out of quiescent HSCs (Mederacke et al., 2013).

Chronic injuring noxae such as vast amounts of lipids, ethanol, viral particles, or iron amplify the production of reactive oxygen species, trigger hepatocyte damage and cause damage to the sinusoidal-endothelial barrier (Friedman, 2008; Sánchez-Valle et al., 2012). In response, damaged, apoptotic, and, above all, necrotic hepatocytes induce the transdifferentiation of quiescent hepatic stellate cells into myofibroblasts by the secretion of danger or damage-associated molecular patterns (DAMPs, **Figure 2**) (Mihm, 2018; Roehlen et al., 2020). Besides the hepatocyte-mediated HSC activation, various cell types, cytokines and pathways contribute to the activation of HSCs. Activated, proliferative and contractile HSCs start secreting vast amounts of extracellular matrix such as collagen I and III, contribute to altered matrix degradation, thereby recomposing the finely balanced hepatic ECM structure and thus disturbing the homeostasis between sinusoidal endothelium, non-parenchymal cells in the space of Disse and the parenchymal hepatocytes (**Figure 2**) (Roehlen et al., 2020). The imbalanced ECM composition causes LSECs to initiate sinusoidal capillarization - LSEC's form a basement membrane, which causes a loss of sinusoidal fenestration. Thereby nutrient exchange with and oxygen supply of the space of Disse and the surrounding hepatocytes is impaired (Dewidar et al., 2019). Hypoxia and lack of nutrients subsequently further trigger hepatocyte damage and HSCs activation (Rosmorduc and Housset, 2010). After initial activation of HSCs', going in hand with a changing phenotype, various intra- and extracellular stimuli perpetuate the activation of hepatic stellate cells and promote the fibrotic remodeling (Tsuchida and Friedman, 2017).

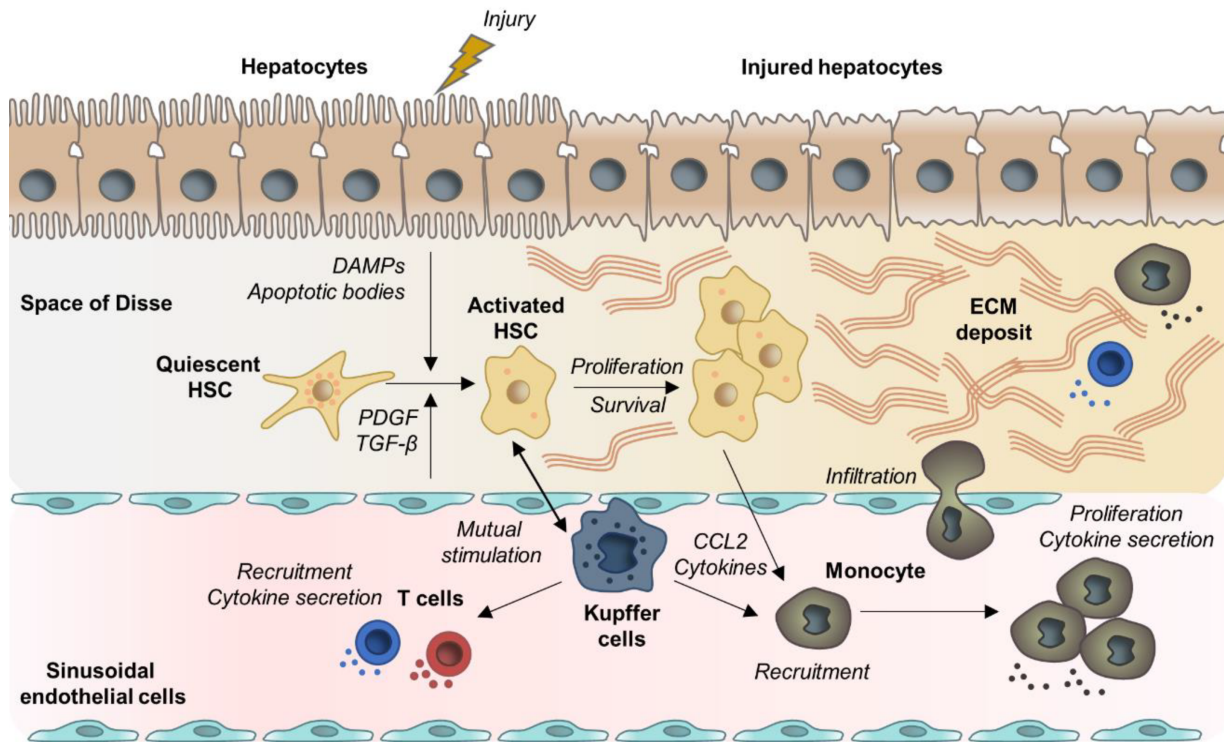


Figure 2 - Mechanistic concepts of liver fibrosis

Hepatocytes secrete DAMPs and apoptotic bodies following hepatic injury. These activate quiescent HSCs into a myofibroblast phenotype. Mutual stimulation by Kupffer cells perpetuates the activated state of HSCs. These activated HSCs secrete massive amounts of ECM, and together with Kupffer cell-secreted chemokines, monocytes and T-cells are recruited. These immunological cells further perpetuate HSC activation and amplify the inflammatory process in the space of Disse. Reprinted with permission from (Roehlen et al., 2020).

ECM: extracellular matrix; HSCs: hepatic stellate cells

Continuous ECM secretion by activated HSCs causes increasing disturbance to the liver's homeostasis, sinusoidal structures, the structural balance of the space Disse, and the parenchyma's functionality. In the further course, deposited ECM forms a growing fibrotic scar. Scar-like connective tissue infiltrates in periportal areas and replaces a growing share of liver tissue (Ferrell, 2000). Eventually, these liver fibrosis induced pathological changes in hepatic microarchitecture progress into synthetic insufficiency, hemodynamic obstruction (portal hypertension), and metabolic hypofunction (Bataller and Brenner, 2005). As already described, hepatic stellate cells play a pivotal role in this development and progression of fibrosis, making them one of the critical targets for fibrosis inhibition and treatment.

1.2.2 Hepatic stellate cells and liver fibrosis

Before the 1970's hepatic stellate cells were mainly considered the liver's Vitamin A storing compartment and their role in the body's retinoid metabolism (Pinzani and

Gandhi, 2015; Wake, 1971). Only in the late 1970s and early 1980s did first research groups recognize hepatic stellate cells' transitional potential going in hand with the secretory and proliferatory activity of HSCs (Pinzani and Gandhi, 2015). As described, the activation of HSCs by externally secreted stimuli and the perpetuation of the activated state of HSCs is laying the fundament to the long-term development of fibrosis. The widely regarded mechanisms underlying these two steps will now be elucidated further.

To understand the exact cascade of HSC's contribution to liver fibrosis development, one can subdivide the life cycle of hepatic stellate cells in fibrosis into three stages: HSC activation, perpetuation, and eventual regression (**Figure 3**) (Hasegawa et al., 2015). As mentioned, HSCs are activated by multiple factors. External stimuli secreted by injured and activated cells like hepatocytes, LSECs, Kupffer cells, and hepatic monocytes, along with ECM bound mediators, trigger HSC activation. Infiltrating immune cells, further secretion of extracellular stimuli and intracellular signaling perpetuates the activation of HSCs. Upon eventual removal of noxae and injuring stimuli, activated HSCs might resolute and either reverse into quiescent-like HSCs or go into apoptosis.

Activation and perpetuation of hepatic stellate cells

HSCs lose their cytoplasmatic retinoid vacuoles upon activation, change their surface receptor composition, upregulate profibrotic genes, and start secreting inflammatory chemokines and excess ECM. Among many different secreted fibrogenic and proliferative cytokines triggering HSC activation, TGF- β , PDGF and CTGF stand out (Tsuchida and Friedman, 2017). With its multitude of effects in fibrosis, TGF- β is considered the central fibrogenic mediator, which is why some also refer to TGF- β as 'the master profibrogenic cytokine' (Chang and Li, 2020; Dewidar et al., 2019). TGF- β in its latent form is apparent and retained in the ECM. Upon activation of the latent TGF- β complex, TGF- β binds to TGF- β receptor II (T β -RII), for example, on hepatic stellate cells. The binding of TGF- β to T β -RII induces the recruitment of TGF- β receptor I (T β -RI), and consequentially T β -RII phosphorylates T β -RI (Huse et al., 1999). Upon phosphorylation, T β -RI acts as a kinase and activates SMAD2/3 through phosphorylation (Heldin and Moustakas, 2016; Ruiz-Ortega et al., 2007). When activated, SMAD2/3 dissociate from T β -RI immediately after phosphorylation and form a complex with SMAD4. The SMAD complex then translocates into the nucleus and

acts as a transcriptional regulator (Derynck and Budi Erine, 2019; Dewidar et al., 2019). Even though there also exist SMAD independent cascades of TGF- β signaling, SMADs are widely regarded as the primary effector in TGF- β signaling, transducing ligand binding on TGF- β receptors into transcriptional upregulation or inhibition of TGF- β related target genes (Hill, 2016; Kitamura and Ninomiya, 2003; Massagué, 2012).

In activated myofibroblasts, SMADs directly induce the transcription of TGF- β target genes *Acta2* (α SMA), *Tagln* (SM22), *PAI-1*, and *CTGF* (Duncan et al., 1999; Hu et al., 2003; Leyland et al., 1996; Liu et al., 2013; Lund et al., 1987; Shafer and Towler, 2009) and directly and indirectly influence upregulation of fibrogenic *COL1* (Collagen I) for example via interaction with the hippo signaling pathway (Carthy, 2018). As S100 calcium-binding protein A 6 (*S100A6*) is highly expressed by hepatic myofibroblasts, while little or no expression of *S100A6* is found in quiescent HSCs, it serves as an excellent further marker for transdifferentiation and activation of HSCs (Krenkel et al., 2019). The upregulation of these target genes is the transcriptional correlate to a variety of functional and phenotypical aspects that characterize the activated state of HSCs and can be ascribed to their transdifferentiation into myofibroblast (**Figure 3**).

The described markers can be linked with certain functional aspects of profibrotic myofibroblasts, such as proliferation, contractility, fibrogenesis, altered matrix degradation, chemotaxis, and inflammatory signaling (**Figure 3**). These features worsen fibrosis and progression into liver cirrhosis in the long term. The exact role of fibrosis marker genes and proteins in HSC derived, activated myofibroblasts will be discussed in the following.

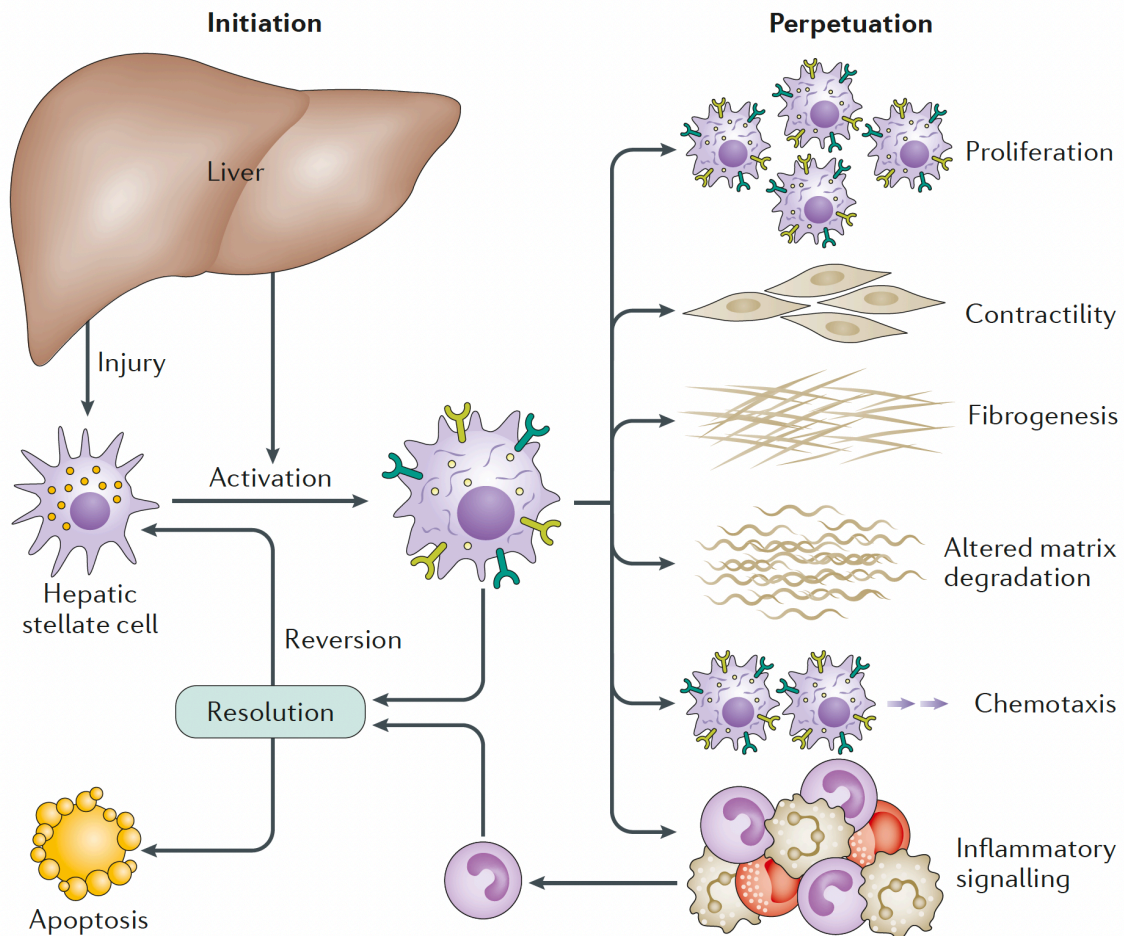


Figure 3 - Functions, features, and phenotypes of HSCs following activation

Liver injury initiates the transdifferentiation of quiescent hepatic stellate cells (HSCs) to their activated phenotype. Perpetuation follows, characterized by specific phenotypic changes including proliferation, contractility, fibrogenesis, altered matrix degradation, chemotaxis, and inflammatory signaling. During the resolution of hepatic fibrosis, activated HSCs can be cleared by apoptosis or reversion to an inactivated phenotype (Tsuchida and Friedman, 2017). Reprinted with permission from (Tsuchida and Friedman, 2017).

Functional characteristics of activated hepatic stellate cells

Increased contractility of activated HSCs contributes to the progression of liver fibrosis by constricting hepatic sinusoids (Racine-Samson et al., 1997; Reynaert et al., 2002). Increased contractility of cells is evoked by a contractile cytoskeletal architecture composed of myosin and actin. By expressing myosin and α SMA upon activation, HSCs acquire a contractile phenotype (Saab et al., 2002). Above that, the balance between the most potent contractile mediator endothelin 1 (ET-1) (Racine-Samson et al., 1997) and its relaxing counterpart nitric oxid (NO) (synthesized by quiescent HSCs ensuring relaxation) is imbalanced towards overproduction of ET-1, resulting in further HSC contractility (Gupta et al., 1998).

Fibrogenesis describes an excessive accumulation of ECM components, especially collagens, accompanied by changing composition of ECM. Activated HSCs secrete collagens of type I and III and fibronectins replacing ECM components of the healthy liver. Activated HSCs upregulate CTGF expression upon TGF- β exposition. As CTGF triggers Collagen I secretion, ECM accumulation is further amplified (Duncan et al., 1999; Liu et al., 2013). Such severe changes in ECM composition come along with loss of hepatic microarchitecture and less tissue elasticity (Klaas et al., 2016).

Altered matrix degradation arises from excess fibrillary proteins such as collagen and elastin and simultaneously impaired fibrinolytic processes (Schuppan et al., 2001). In healthy tissue, specifically in non-fibrotic, healthy liver, ECM homeostasis and composition are regulated precisely, and constant ECM turnover and degradation by matrix metalloproteinases (MMPs) ensures a stable ECM architecture. However, in fibrotic livers, plasminogen activator inhibitor (PAI) affects physiological, MMP-mediated ECM degradation and triggers fibrotic remodeling of the liver's parenchyma. Plasmin is a powerful enzyme for MMPs (Dong et al., 2002) and is activated from its inactive proenzyme plasminogen by tissue or urokinase plasminogen activators (tPA/uPA). As PAI is a potent inhibitor of tPA and uPA (Cubellis et al., 1989; Irigoyen et al., 1999) and consequentially of MMPs, upregulated PAI levels in liver disease go in hand with reduced fibrinolysis and ECM degradation and thus elevated ECM accumulation and fibrosis formation. Also, activated HSCs express tissue inhibitor of matrix metalloproteinase 1 (TIMP-1), further inhibiting physiological ECM degradation (Hazra et al., 2004).

Chemotaxis and inflammatory signals are critical to the recruitment of immune cells during liver injury and fibrosis formation. Studies have shown that HSCs play a pivotal role in mediating immune cell recruitment by secreting various chemokines and inflammatory signals that enhance immune cell infiltration of the subendothelial space in fibrotic areas (Friedman, 2008). For example, the secretion of CCL2 and CXCL1 has a chemotactic effect on monocytes, respectively, neutrophils. The invasion of the hepatic parenchyma, precisely the space of Disse, contributes to hepatic inflammation in general, activates other hepatic stellate cells, and contributes to the perpetuation of already activated HSCs (Weiskirchen and Tacke, 2016).

Reversion of activated HSCs

For many years liver fibrosis was perceived to be a progressing, irreversible state of liver damage. However, a growing number of studies demonstrate regression of liver fibrosis in rodent models and patients upon removing the injuring and inflammatory stimuli (Ellis and Mann, 2012; Kisseleva and Brenner, 2021; Lo and Kim, 2017). Fibrosis is characterized by fibrotic scar formation. As described, HSCs are the primary source of scar tissue in the liver. Therefore, the reversion of activated HSCs is a central feature of fibrosis regression. When the injuring noxa is removed, damage to LSECs and hepatocytes halts, less inflammatory chemokines and mediators are secreted, and TGF- β levels drop. In the absence of 'the master profibrogenic cytokine' HSCs', ECM secretion quickly decreases, and MMP mediated ECM degradation returns to exceed ECM accumulation (Kisseleva and Brenner, 2021). While still subject to discussion, the fate of activated HSCs in fibrosis regression activated HSCs is becoming increasingly apparent. External and internal factors induce either a non-fibrogenic state of formerly activated HSCs or apoptosis of activated HSCs (Higashi et al., 2017). Approximately 50% of activated HSCs do not undergo apoptosis and acquire an inactivated phenotype similar to quiescent HSCs in a healthy liver. While staying increasingly responsive to potential new fibrogenic stimuli, inactivated HSCs express little contractile and fibrogenic markers and restore Vitamin A in their cytoplasm, one of the main morphological characteristics of quiescent HSCs (Kisseleva et al., 2012).

1.2.3 Progression

Untreated and worsening liver fibrosis can progress into liver cirrhosis. Fibrosis initially changes microarchitecture and ECM in locally limited areas of the liver. In the further course, fibrotic scars begin to form, and the fibrotic regions occupy increasing shares of liver tissue. Eventually, fibrotic remodeling results in the formation of septae and hepatic nodules, pathognomic for liver cirrhosis (Pinzani, 2015). Cirrhosis might initially be compensated and hence without severe symptomatology. With decreasing disease severity, patients often develop portal hypertension. They might shift into decompensated cirrhosis with oesophageal varices (Villanueva et al., 2016), ascites (Zipprich et al., 2012), hepatic encephalopathy (Jepsen et al., 2010), and renal malfunction (Appenrodt and Lammert, 2018; Morales-Ruiz et al., 2015). These complications illustrate why decompensated liver cirrhosis is the 14th most common cause of death worldwide, causing more than 1 million deaths globally and 140.000 in

Europe annually (Lewis et al., 2017). Also, as 70% of deaths in patients with compensated liver cirrhosis occur from hepatocellular carcinoma (HCC) (Benvegnù et al., 2004), it becomes clear that the compensated stage of liver cirrhosis already comes along with considerable increases in morbidity and mortality risk. This underlines why halting or reversing chronic liver disease in fibrotic stages is essential to the patient's complication-free survival and prognosis. Considering the typical progression course of fibrosis over cirrhosis to HCC, an efficient, antifibrotic drug would function as a direct fibrosis therapy and as a prevention for cirrhosis and HCC development.

1.2.4 Therapeutic strategies

In the context of fibrosis therapy, the fundamental concept and aim that underlies all therapeutic strategies is preserving or returning to functional, non-inflammatory and parenchymatous hepatic tissue. The complex cascade from the injuring noxa, over cell damage and chemokine secretion, the HSC activation and transdifferentiation, and the fibrotic scar formation offer a multitude of therapeutic opportunities (**Figure 4**). Although many candidates for more impactful antifibrotic therapies have been tested in the recent years, they failed to proof sufficient antifibrotic effects in patients, which is why to date there are still no direct antifibrotic therapies in the clinic (Zhang et al., 2016).

One strategy in liver fibrosis therapy is removing the etiological source, as regression of liver fibrosis and even cirrhosis was demonstrated upon the removal of the injuring and inflammatory agent (Kisseleva and Brenner, 2021). For example, antiviral drugs proved impressively sufficient to revert damage from viral hepatitis (D'Ambrosio et al., 2012; Kim et al., 2019), and NASH patients clearly profit from bariatric surgery combined with or diet and weight loss. Still, the need for a direct antifibrotic agent is pressing.

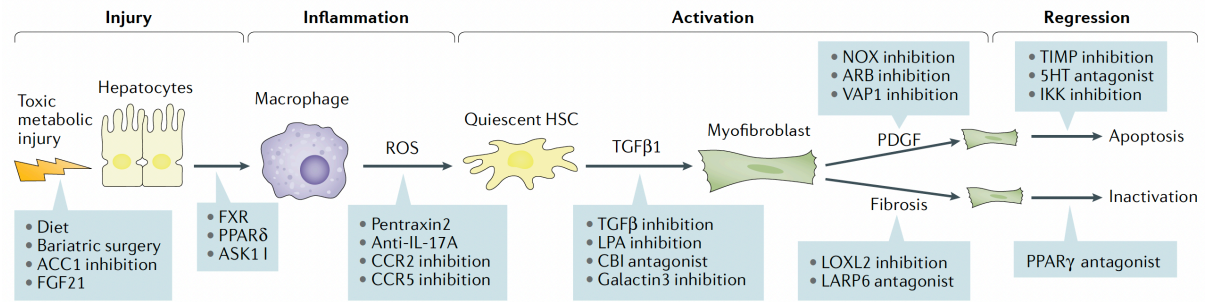


Figure 4 - Therapeutic opportunities for blocking fibrosis development

Injuring and inflammatory noxae cause hepatocytic damage. Damaged hepatocytes activate Kupffer cells, which release reactive oxygen species (ROS) upon activation. Together with hepatocytes, Kupffer cell-released ROS induce HSC activation and transdifferentiation to myofibroblast. Activations strongest inducers are TGF- β and PDGF signaling leading to profibrotic remodeling of the liver. If the liver-injuring trigger is removed, fibrosis regression eventually follows with HSCs becoming apoptotic or inactivated. Therapeutic agents interfere at all stages of the fibrosis and activation cascade, beginning with removing the injuring agent. Reprinted with permission from (Kisseleva and Brenner, 2021).

5-HT: 5-hydroxytryptamine; ACC1: Acetyl-CoA carboxylase 1; ARB: angiotensin II receptor blocker; ASK1: Apoptosis signal-regulating kinase 1; CBI: cannabinoid receptor-1; CCR: CC-receptor; FGF21: fibroblast growth factor 21; FXR: farnesoid X receptor; IKK: inhibitor of nuclear factor- κ B (I κ B) kinase; LARP6: La ribonucleoprotein domain family member 6; LOXL2: Lysyle Oxidase Like 2; LPA: lysophosphatidic acid; NOX: NADPH Oxidases; PPAR: peroxisome proliferator-activated receptors TGF- β : TIMP: Tissue inhibitor of metalloproteinase; VAP1: Vascular adhesion protein - 1

As HSCs are the cellular driver of fibrosis, nearly all therapy concepts directly or indirectly target HSC activation, perpetuation, or resolution. Promising candidates in clinical trial stage III drugs like PPAR α/δ and FXR agonists (trigger the anti-inflammatory effect of quiescent HSCs), LOXL 2 inhibitors (inhibit cross-linking of HSC-secreted-collagen in the ECM) or CCR2/5 inhibitors (inhibit monocyte recruitment that perpetuates HSC activation) (**Figure 4**) address different signaling steps in the fibrotic cascade, however their effect is yet to be confirmed, or studies have already been terminated due to lacking therapeutic effects (for links to clinical trials see chapter 8 - Appendix). Given the pathomechanism of fibrosis with TGF- β being the most potent profibrotic activation trigger and mediator with multiple effects on HSCs and other involved cell types, TGF- β signaling and its inhibition is one of the central targets in anti-fibrotic drug development. Unselective and direct TGF- β antagonization proved to be highly complex and often involves severe adverse effects for patients due to the expression of TGF- β and its receptors in nearly all organs (Dewidar et al., 2019). For example, it was demonstrated that general TGF- β inhibition increases the risk for tumor formation (Chang and Li, 2020). Targets interfering with TGF- β signaling while

having at least a certain level of expressive exclusiveness in hepatic tissue or specifically hepatic stellate cells could solve this problem. These TGF- β related targets can be co-receptors, agents that influence receptor-ligand interaction and TGF-signaling pathway components.

1.3 Hepatocellular carcinoma and hepatic stellate cells

Hepatocellular carcinoma causes 700.000 deaths worldwide per year, and 80-90% of HCCs develop in patients with preexisting liver fibrosis or cirrhosis (Bray et al., 2018; Fattovich et al., 2004). HSCs not only indirectly contribute to HCC development by being one of the causative cell types in fibrosis and cirrhosis as HCC precursors lesions, but also play a crucial and multiform role in the direct promotion of HCC (Barry et al., 2020; Tsuchida and Friedman, 2017). Cancer cells typically do not autonomously form tumors and retain growth but are decisively influenced by the peritumoral zone called the tumor microenvironment (TME) (Spill et al., 2016). In HCC the tumor microenvironment consists of different residual hepatic cells and the hepatic ECM surrounding the tumor. The interaction between TME and HCC cells includes growth signals, angiogenesis regulation, and immunological regulation (Barry et al., 2020). HSCs influence the HCC TME and promote HCC development in various ways (**Figure 5**). For example, HSCs help HCC to create an immunological escape niche, ensuring tumor growth by secreting cytokines which attract myeloid-derived suppressor cells (MDSCs) and T regulatory cells (Tregs) (Zhao et al., 2014). Furthermore, HSCs induce HCC angiogenesis by secreting Angiopoietin-1 (Lin et al., 2020). Also, HSCs produce cytokines that create a growth-stimulating TME enhancing HCC growth (Amann et al., 2009; Mikula et al., 2006) (**Figure 5**). Taking these examples of HSCs triggering HCC growth and development into consideration, inhibition of HSC activation represents a promising target in HCC therapy. Hence, HSC-targeted fibrosis and cirrhosis therapy are to be seen as an efficient HCC prevention.

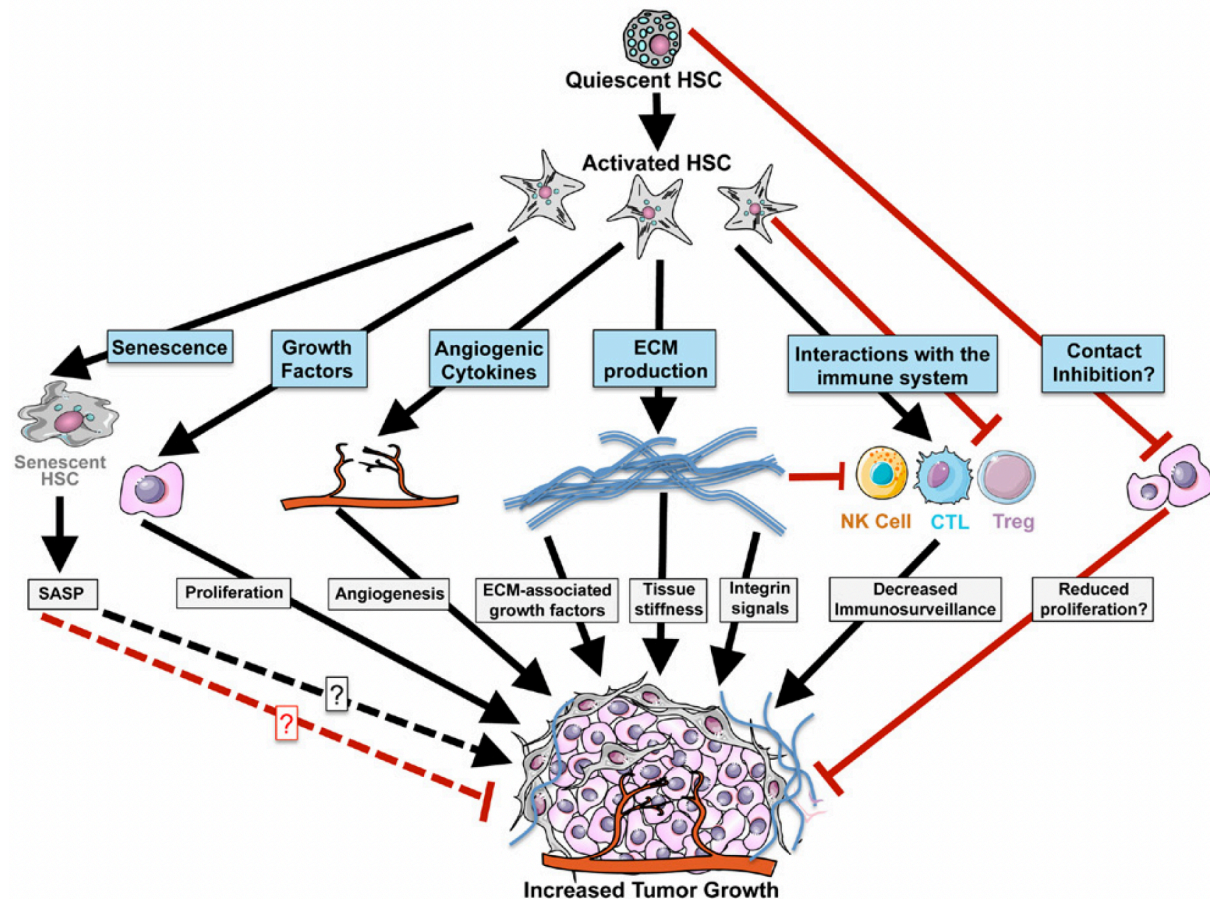


Figure 5 - Proposed mechanisms by which HSCs promote HCC

Activated HSCs unfold their tumor-promoting effect in multiple ways. Potentially they support tumor growth by secreting proliferation and activation factors (TGF- β , HGF). HSC secreted-proangiogenic factors like Angiopoietin-1 and VEGF induce vasculogenesis and angiogenesis, supplying HCC cells with nutrients. ECM remodeling further stimulates HCC growth, and immunomodulation avoids an adequate immune response against HCC cells. Reproduced with permission from (Dapito and Schwabe, 2015)

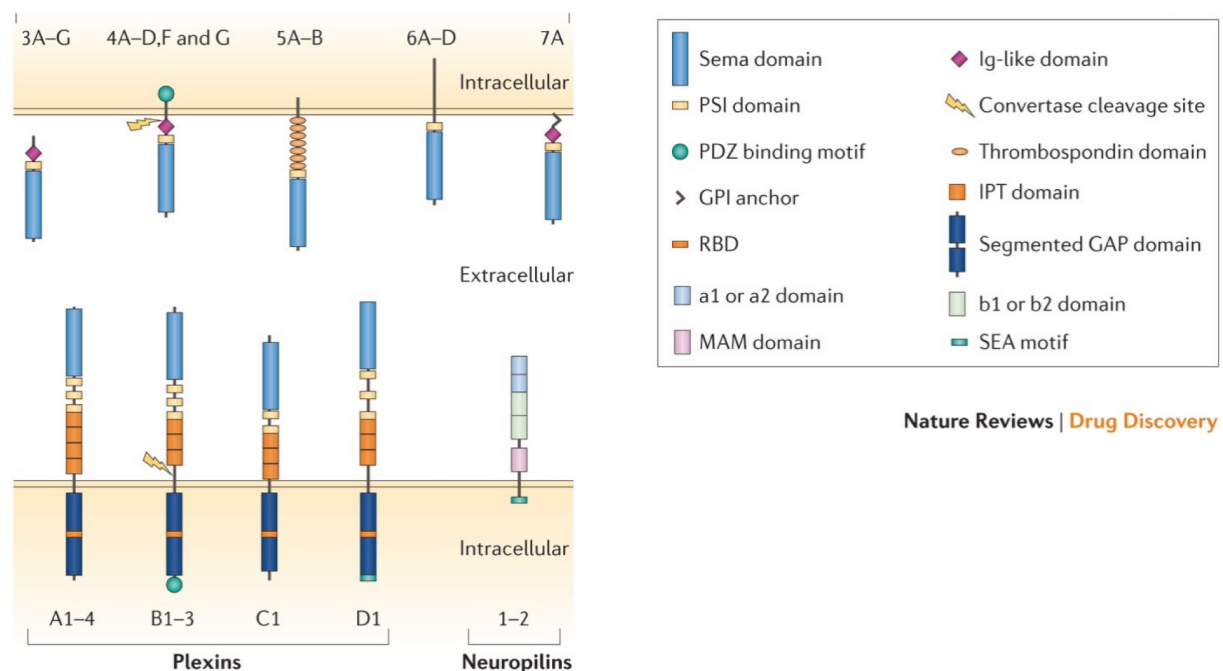
CTL: Cytotoxic T-cell; ECM: extracellular matrix; HCC: hepatocellular carcinoma; HSC: hepatic stellate cell; NK Cell: Natural killer cell; Treg: Regulatory T cell

1.4 Semaphorin protein family

Semaphorins are a family of secreted or transmembrane proteins (Goodman et al., 1999; Kolodkin et al., 1993). Initially discovered as axonal guidance proteins (Püschel et al., 1995), Semaphorins are now known to play various roles in cell-cell interaction, vital cellular functions, and the regulation of diseases such as fibrosis and tumor development (Worzfeld and Offermanns, 2014b).

1.4.1 Vertebrate Semaphorins

The Semaphorin protein family is divided into eight subclasses according to distinct structural features. Semaphorins from class 1 and 2 are proteins of invertebrate species, while Semaphorins from class 3 to 7 are expressed in vertebrates and Semaphorin V in viruses (Goodman et al., 1999). Each class of Semaphorins contains several members that share specific characteristics. Class 3 Semaphorins (SEMA3) are secreted proteins, Class 4-6 Semaphorins (SEMA4-6) are transmembrane proteins, and class 7 Semaphorins (SEMA7) are bound to the plasma membrane via a glycosylphosphatidylinositol anchor (GPI anchor).



Nature Reviews | Drug Discovery

Figure 6 – Semaphorins and their receptors: Plexins and Neuropilins

This figure focuses on vertebrate SEMAs 3 to 7. The 500 amino acids long Sema domain is common to the 20 Semaphorins of all classes. SEMA3s are secreted, non-membrane-bound proteins that interact with Plexin and Neuropilin receptors. SEMA4, 5, and 6 are transmembrane proteins with PDZ binding motifs, thrombospondin domains and PSI domains as anchoring units. SEMA7 is surface-bound via a GPI anchor. The central SEMA receptors are Plexins and Neuropilins, with Plexins being divided into four classes and the two Neuropilin receptors. All Plexins contain an intracellular GTPase activating protein (GAP) transducing Plexin signaling. Some Semaphorins and Plexins (SEMA4s and Plexin B1-3) can be cleaved at a convertase cleavage site. Reprinted with permission of (Worzfeld and Offermanns, 2014b).

GPI: glycosylphosphatidylinositol; Ig: immunoglobulin; IPT: immunoglobulin–plexin–transcription factor; MAM: meprin–A-5 protein–receptor protein tyrosine phosphatase mu; PSI: plexin–semaphorin–integrin; SEA motif: a motif consisting of the amino acids Ser, Glu and Ala; SEMA: Semaphorin (Worzfeld and Offermanns, 2014a).

No matter the subclass, all Semaphorins contain a specific 500-amino acid long extracellular domain, the Sema domain, and have a class-specific C terminus (Goodman et al., 1999; Worzfeld and Offermanns, 2014b).

Semaphorin receptors

Semaphorins mainly signal via two different receptor families: Plexins (PLXNs) and Neuropilins (NRPs) (Harvey, 2012; He and Tessier-Lavigne, 1997; Tamagnone et al., 1999b). However Neuropilins do not have an independent, standalone signaling function due to their very short intracellular domains. Instead NRPs are co-receptors of actual receptors and modulate their signaling by interacting with them (Gitler et al., 2004; Takahashi et al., 1999; Tamagnone et al., 1999a). Invertebrate SEMA1 and SEMA2, transmembranous SEMA4, 5 and 6 and membrane-bound SEMA7 signal directly through one of nine Plexin receptors (Tamagnone et al., 1999b). Apart from SEMA3E (which is able to signal independently of NRPs) (Gu et al., 2005), all SEMA3s need Neuropilins as co-receptors in addition to the Semaphorin-Plexin interaction, stabilizing the signaling complex – SEMA3s will bind NRPs which then bind to Plexin receptors and signal via these. (Falk et al., 2005; He and Tessier-Lavigne, 1997; Neufeld et al., 2016; Takahashi et al., 1999). Aside from their co-receptor function in SEMA signaling, NRP1 and 2 are known to be involved in cellular TGF- β response and are coreceptors for a variety of other (growth factor) receptors such as VEGF (Klagsbrun et al., 2002), placenta growth factor (Migdal et al., 1998), fibroblast growth factor (West et al., 2005), hepatocyte growth factor (Matsushita et al., 2007) and TGF- β . NRP1 is a co-receptor for TGF- β receptor 1, enhancing SMAD2/3 phosphorylation (Glinka and Prud'homme, 2008; Glinka et al., 2011) and promoting liver fibrosis and cirrhosis upon enhanced TGF- β signaling in HSCs (Cao et al., 2010; Wang et al., 2019). While NRP2 amplifies TGF- β response by increased SMAD2/3 phosphorylation in colorectal cancer (Grandclement et al., 2011b), its role in liver fibrosis and cirrhosis is not known to date. Remarkably there is no single holoreceptor for a SEMA subclass; instead, each SEMA subclass and even different SEMAs within one subclass form individual Semaphorin-Plexin-Neuropilin complexes to conduct signaling (Harvey, 2012). The diversity of potential ligand-co-receptor-receptor combinations illustrates the massive variety of subsequent signaling in the context of SEMAs.

1.4.2 Class 3 Semaphorins

As described, SEMA3s are the only secreted members of the SEMA family, with NRPs as stabilizers and modulators of Plexin-mediated signaling (Neufeld et al., 2016; Smolkin et al., 2018). The functionality of SEMA3s is regulated by the activity of proteases. It is assumed that SEMA3s are bound to the ECM and only unfold their effect upon cleavage by furin-like endoproteases that release SEMA3s from the ECM (Adams et al., 1997; Esselens et al., 2010). SEMA3s are widely expressed in different organs and tissues, physiologically regulating neural development (Pasterkamp and Giger, 2009; Schwamborn et al., 2004; Yamashita et al., 2007), angiogenesis (Toledano et al., 2019), and cell migration and morphology (Tran et al., 2007). Axonal guidance functions of SEMA3s are long known and well described. SEMA3s trigger inhibitory growth cone guidance during neurodevelopment (He and Tessier-Lavigne, 1997); they induce dendritic branching and growth in the adult hippocampus and play a role in neuronal regeneration and neural scar formation (De Winter et al., 2002). Increasing attention is drawn to the effects of SEMA3 proteins in (embryonic) angiogenesis and vasculogenesis. SEMA3A and SEMA3F inhibit endothelial cell motility and survival by outcompeting VEGF for the interaction with NRP1 (De Minicis et al., 2007; Guttmann-Raviv et al., 2007; Miao et al., 1999). SEMA3E is regarded to be essential for patterns in developmental vasculogenesis (Gu et al., 2005), and SEMA3C delivery ameliorates pathological angiogenesis (Yang et al., 2015).

Class Semaphorin 3 in disease

At the same time, SEMA3s are known to be broadly involved in pathological processes such as angiogenesis associated diseases (Jiao et al., 2021), tumorigenesis (Jiao et al., 2021; Potiron et al., 2009; Toledano et al., 2019), and fibrotic diseases (Jeon et al., 2020; Papic et al., 2018; Yagai et al., 2014).

As mentioned, several studies have shown the involvement of class 3 SEMAs in the pathogenesis of organ fibrosis. SEMA3A was demonstrated to amplify fibrotic remodeling in the wounded cornea, leading to tissue fibrosis and eventually blindness (Jeon et al., 2020). SEMA3E secretion by injured hepatocytes in chronic liver disease increases LSEC contractility. It hence potentiates HSC activation in liver fibrosis via described mechanisms (chapter 1.2.2) (Yagai et al., 2014) and SEMA3C was observed

to induce epithelial-to-mesenchymal transition (Tam et al., 2017) and to be associated with liver fibrosis (Papic et al., 2018).

Semaphorin 3C

As for all SEMA3 proteins, SEMA3C is a secreted protein. SEMA3C signals via NRP1, NRP2, and Plexin D1 (PLXND1). Like other class-3 SEMAs, SEMA3C has two cleavage sites (Toledano et al., 2016). When cleaved at the C terminus, SEMA3C is released from the ECM and binds to either NRP1 or NRP2 receptors as a ligand with similar affinity (Esselens et al., 2010; Nasarre et al., 2014; Smolkin et al., 2018). SEMA3C is involved in developing several organ systems, fulfilling a variety of directive and regulative functions in the central nervous system, the cardiovascular system, the lung, kidney (**Figure 7**), and gastrointestinal system. In neuronal development, SEMA3C is the attracting counterpart to the repellent SEMA3A, regulating and directing axonal growth (Bagnard et al., 1998). Interestingly SEMA3C deficient mice develop cardiac outflow malfunctions indicating SEMA3C's role in cardiac development (Feiner et al., 2001). Correlation of SEMA3C upregulation with loss of sympathetic nerves in enteric mucosa in Crohn's disease and SEMA3C loss of function mutations associated with Hirschsprung disease illustrate the involvement of SEMA3C in the enteric development and regulation (Jiang et al., 2015). SEMA3C was found to be upregulated in glioma and lung-, breast and ovarian cancer (Rehman and Tamagnone, 2013) and to induce epithelial-to-mesenchymal transition (EMT) in prostate cancer (Tam et al., 2017). SEMA3C also appears to be involved in liver fibrosis. Papic et al. describe an association between SEMA3C serum levels and fibrosis in hepatitis C patients. However, neither functional relation with fibrosis nor a mechanism was shown in the study (Papic et al., 2018). These studies and their findings - especially the SEMA3C mediated EMT induction and association with liver fibrosis – as well as the described involvement of other class 3 semaphorins indicate a potential role of Semaphorin 3C in the promotion and regulation of liver fibrosis and, more specifically the activation and transdifferentiation of hepatic stellate cells.

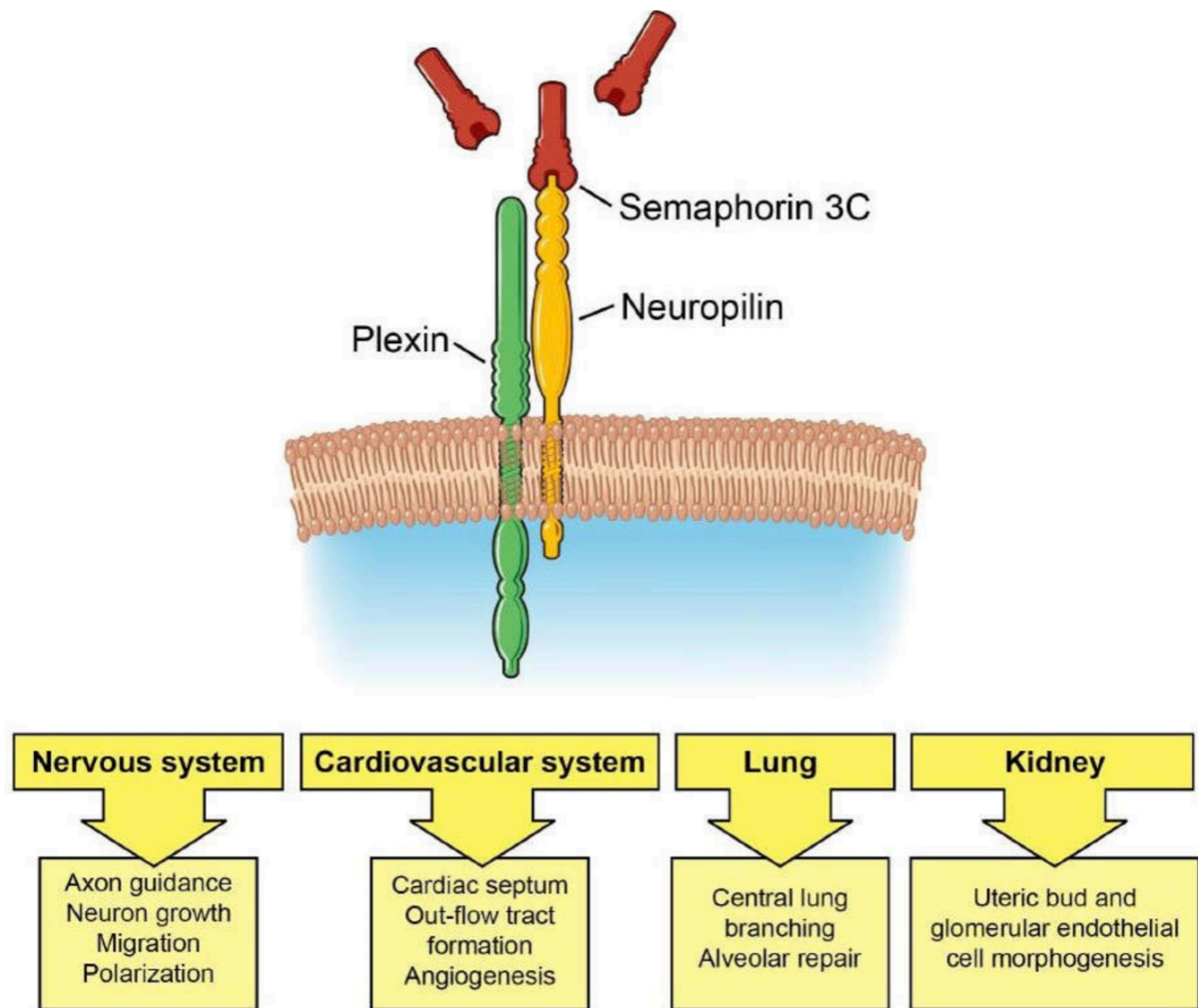


Figure 7 - Semaphorin 3C and its role in development

Secreted Semaphorin 3C binds to a complex of Neuropilin 1 or 2 with Plexin D1. It is involved in various regulative and directive functions during development in the nervous system, the cardiovascular system, the lung, and the kidney. Reprinted with permission from (Hao and Yu, 2018).

1.5 Aim

Given the striking and described relevance of chronic liver diseases as a global pandemic (Marcellin and Kutala, 2018; Mokdad et al., 2014) and the increased risk for liver fibrosis patients to develop HCC (Ellis and Mann, 2012), the ultimate goal of research in the field of liver fibrosis and chronic liver disease has to be the discovery of potential new markers for earlier and more precise diagnosis of fibrosis in patients and therapeutic targets that allow efficient, and above all direct antifibrotic, treatment. Although many studies in the past twenty years have contributed to our more and more

detailed understanding of liver fibrosis, additional in-depth analysis of further activation cascades will be necessary to develop future treatments for liver fibrosis.

In the case of hepatitis B and C, it was shown that the removal of the liver injuring agent proved sufficient to halt the progression and even initiate reversion of fibrosis. In scenarios with an unclear specific pathogenic driver or agent, inhibition of upstream signaling targets could mimic the removal of the pathogenic agent (Pinzani and Gandhi, 2015). For example, inhibiting TGF- β signaling lowers the extracellular matrix produced and reduces fibrosis amount and progression (de Gouville et al., 2005; Yata et al., 2002). However, long-term non-selective blocking of TGF- β signaling would come with severe side effects, impairing general and crucial wound healing mechanisms (de Gouville et al., 2005; Pinzani and Gandhi, 2015). Therefore, there is a pressing need for novel targets and markers to inhibit downstream signaling in activated HSCs, thereby laying the foundation for fibrosis reversion. With the involvement of different class 3 semaphorins in liver fibrosis and the association of SEMA3C serum levels with fibrosis, SEMA3C and its signaling might be involved in HSC activation and consequentially be a potential candidate for a novel fibrosis diagnosis marker and therapy target. Thus this project's aims are as follows:

- I. *To identify whether Semaphorin 3C correlates with severity of chronic liver fibrosis in cirrhosis patients.*
- II. *To investigate the molecular mechanisms and effects of Semaphorin 3C signaling in a hepatic stellate cell (HSC) cell line to explain the potential effects of Semaphorin 3C in liver fibrosis.*
- III. *To confirm potentially identified mechanisms and effects of Semaphorin 3C in primary hepatic stellate cells.*

By answering these questions, the project aims at discovering a novel marker for fibrosis and its progression. By understanding the mechanism of Semaphorin 3C signaling in and activation of HSC cell lines and, more importantly in/of primary hepatic stellate cells the project will investigate if it is a promising target for future therapies, potentially inhibiting the activation of hepatic stellate cells and thus target the major pathomechanism underlying liver fibrosis.

The analysis of publicly available patient data sets of liver fibrosis patients laid the fundament of this study. Results were then used to set up cell culture experiments on the fibroblast-like GRX cells, including Semaphorin 3C overexpression and Neuropilin 2 knockout. Isolation and activation of primary hepatic stellate cells followed to apply and verify outcomes from cell line experiments with GRX cells in primary and freshly isolated cell populations.

2 MATERIAL AND METHODS

2.1 Material

2.1.1 Solutions and Buffers

EGTA Solution

NaCl	8000mg/L
KCl	400mg/L
NaH ₂ PO ₄ .H ₂ O	88.17mg/L
Na ₂ HPO ₄	120.45mg/L
HEPES	2380 mg/L
NaHCO ₃	350 mg/L
EGTA	190 mg/L
Glucose	900 mg/L

GBBS/A solution

KCl	370 mg/L
MgCl ₂ .6H ₂ O	210 mg/L
MgSO ₄ .7H ₂ O	70 mg/L
Na ₂ HPO ₄	59.6 mg/L
KH ₂ PO ₄	30 mg/L
Glucose	991 mg/L
NaHCO ₃	227 mg/L
CaCl ₂ .2H ₂ O	225 mg/L

GBBS/B solution

NaCl	8000 mg/L
KCl	370 mg/L
MgCl ₂ .6H ₂ O	210 mg/L
MgSO ₄ .7H ₂ O	70 mg/L
Na ₂ HPO ₄	59.6 mg/L
KH ₂ PO ₄	30 mg/L
Glucose	991 mg/L
NaHCO ₃	227 mg/L
CaCl ₂ .2H ₂ O	225 mg/L

Histodenz solution

Per mouse:

Histodenz	4.94 g
GBBS/A	Fill up to 17 ml

Enzyme buffer solution (EBS)

NaCl	8000mg/L
KCl	400mg/L
NaH ₂ PO ₄ .H ₂ O	88.17mg/L
Na ₂ HPO ₄	120.45mg/L
HEPES	2380 mg/L
NaHCO ₃	350 mg/L
CaCl ₂ .2H ₂ O	560 mg/L

DNaseI Solution

DNaseI	100 mg
GBBS/B	50 ml

Pronase solution

Per mouse:

Pronase	14 mg
EBS	30 ml

Liberase solution

Per mouse:

Liberase	1.25 mg
EBS	30 ml

Running gel

30% polyacrylamide	12.45 ml
Tris buffer 1.5M, pH 8.8	9.45 ml
H ₂ O	14.85 ml
SDS (10%)	375 µl
APS (10%)	375 µl
TEMED	15 µl

Stacking gel

30% polyacrylamide	1.245 ml
Tris buffer 1 M, pH 6.8	0.945 ml
H ₂ O	5.1 ml
SDS (10%)	75 µl
APS (10%)	75 µl
TEMED	7,5 µl

Laemmli buffer (4x)

Tris buffer, pH 6.8	62.5 mM
SDS	2%
Glycerol	10%
β-mercaptoethanol	10%

Low glucose DMEM

1g glucose / L DMEM	500ml
FCS	50 ml
PenStrep	5 ml

High glucose DMEM

4,5g glucose / L DMEM	500ml
FCS	50 ml
PenStrep	5 ml

Protein lysis buffer

PMSF	1mM
Cell lysis buffer (Cell Signaling)	

Electrophoresis running buffer (10x)

Glycine	1.92 M
Tris	250 mM
SDS	1 %
ddH ₂ O	1 L

TBS (10x)

Tris, pH 7.4	0.5 M
NaCl	1.5 M

TBS-T

TBS	1x
Tween 20	0.05%

Transfer buffer

Glycine	1.42M
Tris	250mM
ddH ₂ O	1L

2.1.2 Chemicals

Chemical	Molecular formula	Manufacturer
1,4-Dithiothreitol (DTT)	C ₄ H ₁₀ O ₂ S ₂	Serva, Heidelberg
Ammoniumpersulfat (APS)	(NH ₄) ₂ S ₂ O ₈	Carl Roth
Blasticidin-S-Hydrochlorid	-	Carl Roth
Dimethyl sulfoxid (DMSO)	C ₂ H ₆ OS	Sigma-Aldrich
Disodium phosphate	Na ₂ HPO ₄ *H ₂ O	Sigma-Aldrich
ethylene glycol tetraacetic acid (EGTA)	C ₁₄ H ₂₄ N ₂ O ₁₀	Sigma-Aldrich
Ethanol 96%	C ₂ H ₅ OH	Sigma-Aldrich
Ethylen diamin tetraacetic acid (EDTA)	C ₁₀ H ₁₆ N ₂ O ₈	Merck
Glycin	C ₂ H ₅ NO ₂	Carl Roth
Isopropanol	C ₃ H ₈ O	Merck
Potassium chloride	KCl	Merck
Potassium phosphate	KH ₂ PO ₄	Merck
Calcium chloride	CaCl ₂	Sigma-Aldrich
Magnesium sulfate	MgSO ₄	Carl Roth
Magnesium chloride	MgCl ₂	Sigma-Aldrich
Magnesium phosphate	Mg ₃ (PO ₄) ₂	Carl Roth
Methanol	CH ₃ OH	Sigma-Aldrich
Sodium chloride	NaCl	Carl Roth
Monosodium phosphate	NaH ₂ PO ₄	Carl Roth
Sodium dodecyl sulfate (SDS)	NaC ₁₂ H ₂₅ SO ₄	Carl Roth
Sodium hydroxide	NaOH	Carl Roth
Penicillin/Streptomycin	-	Sigma-Aldrich
Polyethylenimin (PEI)	(C ₂ H ₅ N) _n	Carl Roth
Hydrochloric acid 37%	HCl	Sigma-Aldrich
β-Mercaptoethanol	C ₂ H ₆ OS	Carl Roth
Tetramethylenediamine (TEMED)	C ₆ H ₁₆ N ₂	Sigma-Aldrich
Triton X-100	C ₁₄ H ₂₂ O(C ₂ H ₄ O) _n	Sigma-Aldrich
Trypan blue	C ₃₄ H ₂₈ N ₆ O ₁₄ S ₄	Sigma-Aldrich

Tween-20	$C_{58}H_{114}O_{26}$	Sigma-Aldrich
-----------------	-----------------------	---------------

2.1.3 Consumables

Table 1 - Consumables

Consumable	Company
Cell culture flask T75	Greiner Bio-one
Cell Scraper	Sarstedt
Cell strainer 70 μm	Falcon
CELLSTAR 24-well culture plate	Greiner Bio-one
CELLSTAR 12-well culture plate	Greiner Bio-one
CELLSTAR 6-well culture plate	Greiner Bio-one
Cell culture dish 10 cm	Greiner Bio-one
Cell culture dish 15 cm	Greiner Bio-one
Cryogenic vials	Star Lab
Insulin syringes, 29G	VWR
Nitrocellulose blotting membrane	GE Healthcare LifeScience
Pasteur pipettes (glass)	WU Mainz
PCR 8er-CapStripes and Tubes	Biozym
Pipette tips (1000 μl, 200 μl, 10 μl)	StarLab
Safe seal tips (1000 μl, 200 μl, 10 μl)	Biozym
Reaction tubes (2ml, 1,5ml, 0,5ml)	Eppendorf
Scalpel	LabAider
Butterfly 29G	Braun
Rotilab syringe filter (0.22μm)	Roth
Pipettes 50 ml, 25 ml, 10 ml, 5 ml	Eppendorf
Whatman paper 3mm	Whatman

2.1.4 Kits & Reagents

Table 2 - Kits and reagents

Kit or reagent	Company
Protein ladder	Thermo Fisher Scientific
Cell lysis buffer	Cell Signaling
SYBR Green	Sigma Aldrich
Pico Pure RNA isolation kit	Thermo Fisher Scientific
innuPREP RNA Mini kit	Jena Analytics
Transforming growth factor - β	Thermo Fisher Scientific

2.1.5 Oligonucleotid primers for qPCR

Table 3 - Oligonucleotid primers

Gene	Forward primer	Reverse primer
<i>mActa2</i>	GAGAAGCCCAGCCAGTCG	CTCTTGCTCTGGGCTTCA
<i>mCol1a2</i>	TGTAAACTCCCTCCACCCCA	TCGTCTGTTTCCAGGGTTGG
<i>mCtgf</i>	CTTCTGCGATTTCCGGCTCC	TACACCGACCCACCGAAGA
<i>mHprt</i>	TGTTGTTGGATATGCCCTTG	ACTGGCAACATCAACAGGACT
<i>mMmp12</i>	CTCATGATGATTGTGTTCTTACAG G	GACAAGTACCATTTCAGCAAATTCA C
<i>mNrp1</i>	GGAGCTACTGGGCTGTGAAG	ATGTCGGGAAGTCTGATTGG
<i>mNrp2</i>	GGCATTGTACGCAAGTTCA	GGGCTTTGAGTCTGTCCAGTC
<i>mPai-1</i>	TCGTGGAAGTCCCTACCAG	ATGTTGGTGAGGGCGGAGAG
<i>mPlexD1</i>	CGCAACCGTAGCCTAGAAGAC	GGTTAAGGTCGAAGGTGAAGAG
<i>mS100a6</i>	AAGCTGCAGGATGCTGAAAT	CCCTTGAGGGCTTCATTGTA
<i>mSema3 a</i>	ATATGCAAGAATGACTTTGGAGGA C	AAGGAACACCCTTCTTACATCACT C
<i>mSema3 b</i>	GCTGTCTTCTCCACCTCCAG	ACATGCCAGGTCTTGGGTAG
<i>mSema3 c</i>	AGACGTGAGACACGGGAATC	AGACGTGAGACACGGGAATC

<i>mSema3d</i>	CTGTATCCCCTTTTTGGGTTTCAT	AACCAGACTGAGCAGGAAGAC
<i>mSema3e</i>	GCGTCAGTGATGGCTACAGA	CAAACCCGGACATAATTGG
<i>mSema3f</i>	CTCTTCCAAGAGGCAACAACACTG	TTTGCATTGGAATTGAAACCAC
<i>mSm22a</i>	TCCAGTCCACAAACGACCAAGC	GAATTGAGCCACCTGTTCCATCT

2.1.6 Genotyping primers

In the following the used genotyping primers are enlisted. All protocols and master mix compositions can be found in 2.2.2.10 *genotyping PCR*.

Table 4 - genotyping primers

Gene	Primer
<i>SM22a^{CRE} fw</i>	GCGGTCTGGCAGTAAAACTATC
<i>SM22a^{CRE} rev</i>	GTGAAACAGCATTGCTGTCACTT
<i>SEMA3C flox fw</i>	GAATCTGGCAAAGGACGATG
<i>SEMA3C flox rev</i>	GACCACTGGGCTTGAGAGAG
<i>NRP2 flox common fw</i>	AGCTTTTGCCTCAGGACCCA
<i>NRP2 flox mutant rev</i>	CCTGACTACTCCCAGTCATAG
<i>NRP2 flox wildtype rev</i>	CAGGTGACTGGGGATAGGGTA

2.1.7 Plasmids

Table 5 – Plasmids

Plasmid Name	Parent vector	Sequence / NCBI Acc. No.
mNRP2 shRNA	TRC1 pLKO.1-puro	CCGGCCAGAGAAGTATCCACACAATCTC GAGATTGTGTGGATACTTCTCTGGTTTT
mSEMA3C closed	pDONR221	DQ890847

2.1.8 Antibodies

Table 6 – Antibodies Western Blot

Epitope	Host	Dilution	Manufacturer
pSMAD 2/3	Rabbit	1:1000	CellSignaling
NRP1	Mouse	1:1000	R&D
NRP2	Mouse / Rat	1:1000	R&D
VCP	Rabbit	1:1000	Abcam
GAPDH	Mouse	1:1000	Abcam
SM22	Rabbit	1:20	Abcam

2.1.9 Bacteria, cell lines, growth media

Table 7 – Bacteria

Bacteria

Stbl3

Table 8 - Cell lines

Cell lines

GRX

HEK293T

Table 9 - Growth media, solutions, buffers

Growth media	Manufacturer
DMEM low glucose (1%)	Thermo Fisher Scientific
DMEM high glucose (4,5%)	Thermo Fisher Scientific
IMEM basal	Thermo Fisher Scientific
S.O.C. medium	Sigma-Aldrich
LB (lysogeny broth)	Sigma-Aldrich
Penicillin (10.000 units/mL)	Thermo Fisher Scientific
Fetal calf serum, heat inactivated	Sigma-Aldrich

Streptomycin (10mg/mL)	Thermo Fisher Scientific
Trypsin-EDTA-0.05%	Thermo Fisher Scientific

2.1.10 Mouse strains

Table 10 - Mouse strains

Abbreviation	Full Strain Name
SM22α^{CRE}xSEMA3C^{fl/fl}	B6-Tg(Tagln-cre)1Her SEMA3Ctm1a(KOMP)Wtsi / Afis
SM22α^{CRE}xNRP2^{fl/fl}	B6-Tg(Tagln-cre)1Her NRP2tm1.1Mom/ Afis
Wildtype (wt)	C57BL/6J

2.1.11 Equipment and software

Laboratory equipment

Table 11 - Laboratory equipment

Equipment	Company
Balance	Mettler Toledo
Balance	Kern & Sohn
Centrifuge 5415	Eppendorf
Centrifuge Rotina 420R	Hettich
Consort EV231 power supply	Sigma-Aldrich
Electrophoresis chamber	BioRad
Erlenmeyer Flask 1.0l	Thermo Fisher Scientific
Freezer -20°	Liebherr
Freezer -80°	Thermo Fisher Scientific
Heat block	Carl Roth
Histo Star	Thermo Fisher
Incubator for cell culture	Thermo Fisher
Magnetic	Janke and Kunkel
Milli-Q Water	Milipore

Nanodrop1000	Thermo Fisher Scientific
Neubauer counting chamber	Marienfeld
PCR Thermocycler	Biozym
Perfusion pump	ISMATEC
pH meter	Eppendorf
QuantStudio3 qPCR machine	Thermo Fisher Scientific
Refrigerator 4°	Liebherr
StepOnePlus qPCR machine	Roth
Thermal block	DITABIS
Tubing for pump	ISMATEC
Ultra-centrifuge	Thermo Fisher Scientific
Vortex	StarLab
Water bath	GFL
Western blot blotting chamber	PegLab Biotechnology
Western blot equipment	PegLab Biotechnology

Software

Table 12 – Software

Software	Developer
BioRender	Biorender.com
Endnote20	Clarivate
GSEA	Broad Institute (Cambridge, Massachusetts)
Image Lab 3.0	Biorad
Kaplan-Meier Plotter	Balazs Gyorffy (Semmelweis University)
Microsoft Office 2013	Microsoft
Prism 9.1.1 for MacOS	GraphPad Software
Quant Studio3	Thermo Fisher Scientific
Real-time Analysis	Agilent

2.2 Methods

2.2.1 Cell Culture

General techniques

Using sterile techniques, all cell culture work was performed under a sterile laminar flow cell culture hood (see Material section). Cells were cultured in their respective media at 37°, 5% CO₂. Cells were checked for viability, confluence, and potential contaminations under a light microscope every day. Cell splitting was done whenever confluence was reached. To split cells, cell culture medium was discarded and cells were washed with PBS. In the following, cells were incubated with Trypsin-EDTA for 3-5 min. After incubation, Trypsin EDTA was inactivated with DMEM cell culture medium (ratio 10:1), cells were resuspended, and centrifuged at 200g for five minutes. The supernatant was discarded and the cell pellet was resuspended in fresh medium. The cell concentration in the suspension was determined by counting a 1:5 or 1:10 dilution with the help of a Neubauer counting chamber. After counting, the necessary amount of cells were plated onto a new cell culture plate or cell culture flask.

Cryoconservation and thawing of cells

Aliquots of cells were stored with 10% DMSO in a -80° freezer for shorter periods or in liquid nitrogen for longer storage times. To plate out a frozen cell line, the frozen aliquot was thawed at 37° and resuspended in a prewarmed, fresh cell culture medium. Cells were pelleted down at 200g for five minutes, the supernatant was discarded and the cell pellet was resuspended in the respective cell culture medium. Cells were then plated out on cell culture plates, or flasks, and viability (and attachment) was checked the following day.

Cultivation of HEK293-T cells

HEK293-T cells are plated in high glucose (4,5g Glucose/L) DMEM cell culture medium (with 10%FCS and 1% P/S) into 175 cm² cell culture flasks. Cells are stored in the incubator with splitting the cells in a 1:4 ratio every three days.

Cultivation of GRX cells

GRX cells are plated onto cell culture dishes or plates in a low glucose DMEM cell culture medium. Cells are stored in the incubator, splitting the cells in a 1:4 ratio every two to three days.

Cultivation of primary HSCs

Primary HSCs are plated for culturing immediately after isolation in low glucose DMEM cell culture medium into 12 or 6 well cell culture dishes. Cells are then put in the incubator for four days without media change to allow ideal attachment. In further course, half of the cell culture medium is changed every second day.

2.2.2 Biochemical and molecularbiological methods

Heat shock transformation and plasmid isolation

For transformation, Stbl3 bacteria were thawed on ice. 5µl of the plasmid of interest were added to Stbl3 bacteria on ice and then incubated for 30 min. After incubation, the bacteria were heat-shocked for 30 sec at 42 °C on a heat block to internalize the plasmid of interest. Directly after the heat shock, bacteria were put back on ice and cooled down for 5 min. Afterwards 250 µl of S.O.C. medium were added to the bacteria, then incubated in a heat block shaking 300 rpm at 37 °C for 1 h. Subsequently, 20 µl of bacteria were plated onto an agar plate with a selection medium and were incubated overnight at 37 °C. The following day a single colony was picked with a pipet tip and dropped onto a vial with 5ml lysogeny broth medium (LB-medium) and selection medium and was incubated over a day for at least 8 h. After incubation, 3 ml of the miniprep culture were added into 500 ml LB-medium and selection. The culture was then left growing overnight at 37 °C and 180 rpm. The next day 1 ml of the overnight culture was added into 1 ml of glycerol and stored at -80 °C.

Production of lentiviral particles

To produce lentiviral particles for stable overexpression or knock-down, HEK293-T were seeded on a 15cm dish. Cells were kept in culture until 90% confluency was reached. Polyethyleneimine (PEI) was used to transfect cells with the plasmids. A PEI solution and a DNA solution were prepared for each plate and construct. To prepare

the PEI solution 168 μ l of PEI were diluted in 2,5 ml IMEM basal (no FCS, no P/S) per construct and dish. Furthermore, a DNA solution containing the plasmid was prepared: per construct, and dish, 21 μ g psPAX2 (encoding for packaging), 14 μ g pMD2 (encoding for envelope), and 21 μ g plasmid of interest were diluted in 2,5ml IMEM basal. PEI solution was then added to the DNA solution, creating the transfection mix. The transfection mix was incubated for 30 min at room temperature. During incubation time cell culture medium of the HEK293-T cells was refreshed with 10ml culture medium containing 15% FCS. 5 ml of the incubation mix were added to the HEK293-T cells. Transfected HEK293-T cells were kept in the cell culture incubator for 12h at 37°C. After 12h, the culture medium is discarded and replaced with fresh IMEM cell culture medium containing 10% FCS. After 24h and 48h, cell culture medium containing the lentiviral particles was harvested, stored at 4°C, and new IMEM culture medium containing 10% FCS was added to the cells. Following the second collection after 48h, cells were trashed and harvested cell culture medium from both collection days was filtered through a 0,22 μ m sterile filter. The filtered medium was then centrifuged in an ultracentrifuge at 25,000g for 120 min at 4 °C. Afterwards, the supernatant was discarded, the virus particles resuspended in PBS and then stored in aliquots of 10-50 μ l at -80°C.

Lentiviral knockdown

To knockdown proteins in GRX cells, cells were treated with an aliquot of before generated lentivirus coding for shRNA. After 48h of incubation, medium was changed and a selective antibiotic is added to the cells. Cells were kept in culture and selection medium was refreshed every other day until all cells died in the negative control (cells not expressing the resistance gene). Subsequently, RT-qPCR was performed comparing potential knockdown and control cells to check successful knockdown.

Lentiviral overexpression

To overexpress proteins in GRX cells, cells were treated with an aliquot of before generated lentivirus. After 48 of incubation with the virus, medium was changed and selection started. Cells were kept in culture and selection medium was refreshed every other day until all cells died in the negative control (cells not expressing the resistance gene). Subsequently, RT-qPCR was performed comparing potentially overexpressing and control cells to check successful overexpression.

RNA isolation from cell lines

RNA isolation from cell lines was performed to analyze gene expression changes and patterns. Cells were washed with PBS twice and then lysed with RNA lysis buffer. RNA was then isolated with the innuPREP RNA Mini kit (Jena Analytics) according to the manufacturer's instructions.

RNA isolation from primary murine cells

Cells were washed with PBS twice and then lysed with RNA lysis buffer. RNA was then isolated with the PicoPure RNA isolation kit (ThermoFisher Scientific) according to the manufacturer's instructions.

Nucleic acid measurement

The nucleic acid concentration in isolated RNA samples was measured with the help of the NanoDrop to synthesize constant amounts of cDNA throughout a variety of samples. After initial measurement calibration with water, 1µl of the sample was pipetted onto the measurement spot of the NanoDrop. Concentrations were used to dilute samples to 100 ng/µl of RNA to proceed with cDNA synthesis.

cDNA synthesis

cDNA was synthesized to run RT-qPCRs and thereby analyze gene expression levels by measuring the abundance of mRNA of a specific gene. Isolated mRNA was transcribed into cDNA with the high-capacity cDNA reverse transcription (RT) kit from Thermo Fisher Scientific. According to the manufacturer's recommendation, the following master composition and mRNA concentration was used for cDNA transcription:

Table 13 - Master mix composition cDNA transcription

Reagent	Volume
100mM dNTP mix	0,8 µl
10x RT buffer	2 µl

10x random primer mix	2 μ l
20x reverse transcriptase	1 μ l
RNA	1000ng
ddH ₂ O	Fill up to 20 μ l

The reverse transcription reaction was then performed using a thermal cycler using the following reaction protocol: 25 °C for 10 min, 37 °C for 120 min and 85 °C for 5 min. Synthesized cDNA was diluted 1:40 in ddH₂O and stored at -20 °C.

Quantitative real time PCR (RT-qPCR)

To analyze the mRNA levels respectively, RT- qPCR was performed. 4 μ l of cDNA sample, 5 μ l of SyberGreen master mix and 1 μ l of the respective primer pair (respective forward and reverse primer, dilution of 1:40 in ddH₂O) were pipetted into a well of a 96-wellplate. The suspension was centrifuged at 300g for 30 seconds to ensure a sufficient mixture of all reagents. Then quantitative real-time PCR (RT-qPCR) was performed using Thermal Cycler. All reactions were performed in duplicates using the following reaction protocol:

Table 14 - qPCR reaction protocol

Step	Temperature	Time
Initial Denaturation	95°	10 min
Denaturation	95°	30 s
Annealing	60°	30 s
Elongation	72°	30 s
Final Elongation	72°	6 min

Denaturation, annealing and elongation steps were repeated in 40 or 50 cycles. After the reaction a melt curve was generated and analyzed to ensure specific amplification of the target gene mRNA and rule out amplification of contaminating DNA or by unspecific primer binding. All gene expression levels were calculated using the $2^{-\Delta\Delta C_t}$ method and the gene expression levels were normalized to the levels of housekeeping genes *Hprt* or *Rpl13a*. Statistics were calculated based on gene expression of the control from each biological set being equal to 1.

Genotyping PCR

Genotyping was performed by lysing tail or ear clipping of the mice. Samples were lysed in 100 µl lysis buffer and boiled at 95° for 30 minutes. Afterwards the lysed samples were centrifugated and cooled down. 100 µl neutralization buffer is added. In the following tables mastermix composition and protocols for genotyping PCRs are enlisted; all primers used are found in *Table 6*.

Table 15 - Genotyping mix for SM22a-CRE, SEMA3C-flox, NRP2-flox mutant, NRP2-flox WT

Reagent	1xPCR
5x Puffer	5.00 µl
dNTPs (2,5mM)	0.50 µl
Primer forward (10µm)	1.25 µl
Primer reverse (10µm)	1.25 µl
MgCl ₂	1.50 µl
Taq	0.10 µl
ddH ₂ O	14.40 µl
	24.00 µl

Table 16 - PCR program for SM22a-CRE genotyping

Step	Temperature	Time
Initial Denaturation	94°	2 min
Denaturation	94°	30 s
Annealing	65°	30 s
Elongation	72°	30 s <i>repeat step 2-4 for 35 cycles</i>
Final Elongation	72°	2 min
Hold	8°	

Table 17 - PCR program for SEMA3C-flox genotyping

Step	Temperature	Time
Initial Denaturation	94°	3 min

Denaturation	94°	30 s	
Annealing	63°	60 s	
Elongation	72°	60 s	<i>repeat step 2-4 for 35 cycles</i>
Final Elongation	72°	5 min	
Hold	8°		

Table 18 - PCR program for NRP2-flox mutant genotyping

Step	Temperature	Time	
Initial Denaturation	94°	3 min	
Denaturation	94°	30 s	
Annealing	60°	60 s	
Elongation	72°	60 s	<i>repeat step 2-4 for 30 cycles</i>
Final Elongation	72°	2 min	
Hold	8°		

Table 19 - PCR program for NRP2-flox Wildtype genotyping

Step	Temperature	Time	
Initial Denaturation	94°	3 min	
Denaturation	94°	30 s	
Annealing	64°	60 s	
Elongation	72°	60 s	<i>repeat step 2-4 for 30 cycles</i>
Final Elongation	72°	2 min	
Hold	8°		

Protein lysis

Cells were washed once in PBS and lysis buffer (Cell Signaling) containing 1mM PMSF was added. Cells were incubated on ice for five minutes. Lysis was followed by centrifugation at 4 °C for 15 min at 15,000g. The supernatant was transferred to a new Eppendorf tube and used to measure protein concentrations by BCA assay (Thermo Fisher Scientific). Protein samples were diluted 1:10 in ddH₂O and 10 µl of this dilution were pipetted onto a 96-well plate in duplicates in addition to BSA standards. 200 µl BCA working reagent were added to each well and incubated at 37 °C for 30 min. Absorbance of samples and BSA standards was measured using a plate reader at 562

nm (BMG Labtech). A BSA standard curve was generated using the known concentrations of the BSA standards to calculate the protein concentration in each sample. Lysed, isolated and measured protein samples were then stored at -20 or -80 °C.

SDS-PAGE

A sodium dodecyl sulfate polyacrylamide gel electrophoresis (SDS-PAGE) was used to separate proteins according to their mass. Protein samples were boiled in 4x Laemmli Buffer (ratio 3:1) for 5 min at 95°C. A gel consisting of two layers (5 % stacking gel and 10 % running gel (*recipes see 2.1.1 solutions and buffers*)) was poured. Samples and 2.5 or 5 µl protein ladder (Thermo Fisher Scientific) were loaded with equal amounts of protein onto the gel. The gel was then run in running buffer at 80 V for 30min followed by 2 h at 120 V in gel electrophoresis chambers (BioRad).

Western blotting

Western blot was performed by setting up a sandwich out of two meshes each side, two Whatman papers, SDS-PAGE gel and a PVDF membrane in protein transfer buffer containing 20 % methanol (*recipes see 2.1.1 solutions and buffers*). Proteins were transferred in a Western blotting chamber running an overnight transfer at 100 mA at 4 °C. The next day the PVDF membrane was blocked for one hour with 5% skim milk dissolved in TBS-T (*recipes see 2.1.1 solutions and buffers*). Primary antibodies were added in respective concentrations diluted in 5% skim milk dissolved in TBS-T and then incubated on a shaker at 4° overnight. The next day membranes were washed two to three times before adding the horseradish peroxidase-conjugated secondary antibodies in respective concentrations diluted in 5% skim milk dissolved in TBS-T and then incubated on a shaker for one hour at room temperature. After two membrane washes in TBS-T and one washing step in PBS, membranes were incubated with chemiluminescence substrate (Pierce Biotechnology) for 3 min. Imaging of membranes was performed using chemiluminescence detection with the ChemiDoc imaging system (BioRad). Intensity of the chemiluminescence signal was quantified with Image Lab software (BioRad). All quantifications thus protein expression levels were normalized to housekeeping proteins VCP or β-actin.

2.2.3 Mouse Experiments

Isolation of primary hepatic stellate cells

Primary hepatic stellate cells were isolated to investigate previously observed activation mechanisms and regulations on primary cell level. The hepatic stellate cell isolation procedure was initially based on the isolation protocol by Mederacke and Dapito (Mederacke et al., 2015) and was modified individually in the further course. All steps in the following isolation protocol are either based on the mentioned publication or individual modifications and own set-ups.

In the first step, the mouse is euthanized by cervical dislocation. Immediately afterward, median laparotomy is performed to expose the abdominal cave. Quick and immediate laparotomy and further steps are essential to avoid intrahepatic clotting and thus impaired homogenous liver perfusion and digestion. The stomach, intestine, seminary glands/ovaries, and urinary bladder are moved to the right side to expose the inferior vena cava (IVC) in its complete extension. Next, the liver (especially its inferior lobes) is elevated towards the diaphragm to expose the IVC further. Before continuing, the portal vein (PV) needs to be exposed to facilitate its cutting in the further course. With IVC and PV prepared and exposed, perfusion can be started. A 28 gauge butterfly attached to a pump is injected into the IVC at the junction level of the right renal vein with the IVC. The butterfly is fixed in position, and perfusion is started. Starting with a flow of 1ml/min, the flow speed is constantly increased up to 5ml/min within the first seconds of perfusion. With beginning discoloring of the liver and swelling of the PV, the PV is cut for pressure release and outflow. From then, the liver is perfused with EGTA (recipe see 2.1.1 buffers and solutions) for 2 min (perfusion speed 5ml/min), with Pronase (recipe see 2.1.1 buffers and solutions) for 5 min (perfusion speed 5ml/min) and Liberase (recipe see 2.1.1 buffers and solutions) for 5 min (perfusion speed 5ml/min). To ensure sufficient and complete perfusion, all lobes are carefully checked for complete discoloring not more than 2 minutes after the start of the perfusion. In further course, homogenous swelling of all lobes should be observed.

After the perfusion, the liver is removed from the mouse's abdominal cave and put into a 10cm culture dish to be minced. Before removal, the gallbladder is resected, ideally without puncturing the gallbladder or liver. Before mincing the resected liver, the liver's capsule is carefully removed to avoid contamination of the isolate with capsule tissue. The mincing is performed in some milliliters of GBBS/B to facilitate the collection of all

isolated cells. First, isolated liver cells are diluted in 40ml GBBS/B buffer (*recipe see 2.1.1 buffers and solutions*), then passed through a 70 μ m cell strainer into a 50mL tube. Afterward, 1% DNaseI solution (*recipe see 2.1.1 buffers and solutions*) is added, and the cell suspension is centrifuged at 580g, 4°C for 10 min. Next, the supernatant is discarded, resuspended with another 40ml GBBS/B, and 100 μ L DNaseI is added. The cell suspension is again centrifuged at 580g, 4°C for 10 min. Afterward, the supernatant is discarded again, and the pellet is resuspended in 32ml GBBS/B, 16ml Histodenz solution (*recipe see 2.1.1 buffers and solutions*), and 100 μ L DNaseI solution. The cell suspension is divided into four 15mL tubes, each filled with 12mL of the cell suspension. Then 1,5mL of GBBS/B is carefully layered on top of the 12mL cell suspension with a 1000 μ L pipette creating a sharp gradient between the cell suspension and the top layered GBBS/B. The tubes are then centrifuged for 17 minutes at 1380g and 4° Celsius without brakes to ensure the continued stability of the gradient.

After centrifugation, hepatic stellate cells float in the interface region between the initial cell suspension and the GBBS/B. They are carefully aspirated with a 1000 μ L pipette and then pipetted into a new 50mL tube. Cells are then resuspended in 50ml GBBS/B and centrifuged for 10 min at 580g and 4°C. After centrifugation, the supernatant is carefully discarded, and the pellet is resuspended with 2mL low glucose DMEM containing FCS and Pen/Strep (*recipe see cell 2.1.1 buffers and solutions*) to plate the cells then. Before plating, the cells are counted with a Neubauer counting chamber to ensure dense plating, which has proven crucial for the HSC's viability and attachment.

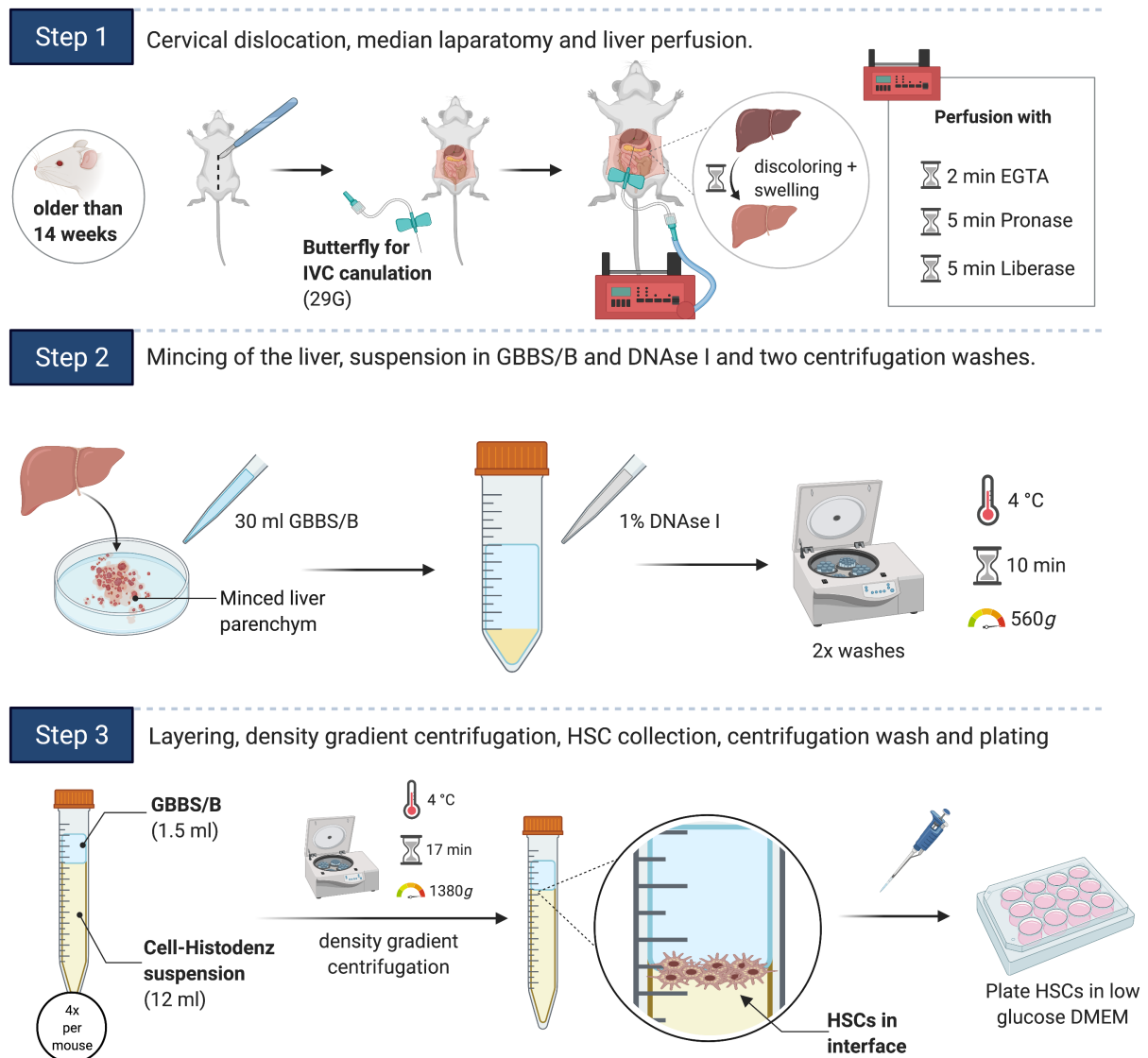


Figure 8 - HSC isolation overview

This figure gives an overview of the isolation's most crucial steps dividing the whole procedure into three main steps: **Step 1)** Cervical dislocation was performed to euthanize the mouse, followed by median laparotomy with scalpel or scissors. Afterward IVC is cannulated and perfusion with EGTA, Pronase and Liberase follows. **Step 2)** After the liver is resected, it is minced and suspended in 30ml of GBBS/B and 1 % DNase I in a 50ml tube. Two centrifuge washes with shown settings follow. **Step 3)** For each mouse four 15 ml tubes are filled up with 12 ml C-H suspension. 1.5 ml of GBBS/B are carefully layered on top to create sharp gradient in between the two phases. Density-based centrifugation with shown settings follows. Finally HSCs can be collected with a 1000 µl pipette from the interface and plated in a 12 well plate in low glucose DMEM. Further detailed description and information about the isolation protocol and specific steps can be found in paragraph 2.2.3 *Mouse experiments- HSC isolation*.

C-H suspension: cell-histodenz suspension; DMEM: Dulbecco modified eagle medium; GBBS: Grey's balanced buffer solution; HSCs: hepatic stellate cells; IVC: inferior vena cava

Created using BioRender.com

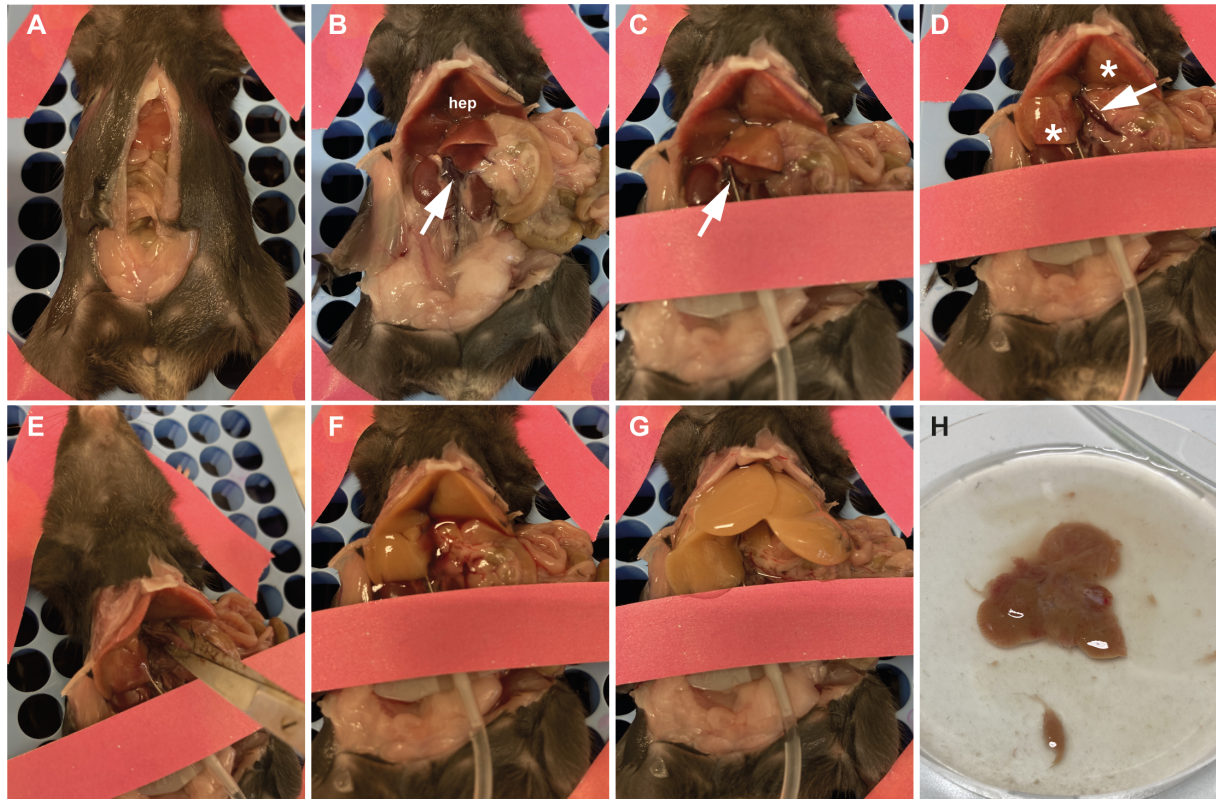


Figure 9 - HSC isolation, perfusion step

Pictures A-H display the liver perfusion step of the above described HSC isolation. (A) Median laparotomy. (B) Exposure of IVC (white arrow), the liver is marked by *hep*. (C) Cannulation of IVC (white arrow). (D) Swelling of PV (white arrow), discoloring of the liver (white asterisks). (E) Cutting of swollen PV. (F+G) Further discoloring and swelling of the perfused liver. (H) Removed and digested liver in Petri dish.

HSC: hepatic stellate cells; IVC: inferior vena cava; PV: portal vein.

Hepatic stellate cell isolation purity check

A fraction of isolated HSC's was used for a contamination check for all time points. All samples are checked for CD31 and CD45 on mRNA level to validate the isolate's purity and exclude potential contamination. Samples with comparatively high CD31 or CD45 levels were excluded from further analysis due to possible contamination with endothelial or immune cells.

2.2.4 Statistical analysis

All data presented is displayed as mean \pm SD. Single data points represent individual biological replicates. Each experiment was performed at least three times; actual repetitions are stated in respective figure legends. Discovered findings were considered significant when p was <0.05 . The exact performed statistical test is stated in the individual figure legends. In short; for all *ex vivo* experiments unpaired Mann-

Whitney test was performed for group comparisons, paired t-test was used to compare 0 to 9 days of HSC activation. For *in vitro* experiments, Gaussian distribution was assumed, and parametric t-tests were performed. Whenever previous experiments and findings suggested a one direction hypothesis, one-tailed tests were performed in accordance with the 3R's. Statistical analysis was performed with Prism, Version 9.1.1 (223) (Graph Pad). Asterisks were used as follows: * = $p < 0.05$, ** = $p < 0.01$, *** = $p < 0.001$, **** = $p < 0.0001$.

2.2.5 Bioinformatic analysis

Gene set enrichment analysis

To determine the association of SEMA3C with fibrosis respectively cirrhosis in patients, gene set enrichment analysis was performed. For gene set enrichment analysis (GSEA), data were processed using the GSEA software (Broad Institute, Cambridge, Massachusetts). GSEA was performed to determine gene expression levels in a priori defined patient sets and test them for significant differences with the help of the GSEA output. Differentially expressed genes (DEGs) are presented in an enrichment plot. The normalized enrichment score (NES) accounts for the gene set size. Further information included in GSEA is a p-value and the false discovery rate (FDR). The following publicly available gene sets for liver fibrosis and cirrhosis patients were included into the analysis: *NCBI GEO GSE45050*, *GSE61260*, *GSE103580*, *GSE83898*.

Overall survival analysis

To understand a potential association between SEMA3C expression and HCC overall survival analysis was done. Survival analysis was performed using the Kaplan Meier plotter (Györfy, 2021). The Kaplan Meier plotter was used to create a survival plot that compares two patient groups, split with regard to their expression levels of a certain gene. In this way, the prognostic value of a particular gene could be determined. The splitting into two groups was based on an automatically generated "best cutoff" - for this automatic cut-off selection, the software checks all possible cutoff values between the lower and upper quartile and selects the best performing threshold. The automatic cut off / threshold determination table is shown in the appendix. Comparison of patient collectives was performed with regard to patients' overall survival. For this thesis, the

KM plotter for liver cancer (Menyhárt et al., 2018) was used – plotting survival curves for a specific patient collective of hepatocellular carcinoma patients.

2.2.6 Ethical statement

Before starting to work autonomously, I successfully completed the course “Laboratory Animal Science and Methods of Animal Experimentation” after FELASA B. All experiments were performed according to the learnt guidelines, approved by the Regierungspräsidium Karlsruhe and executed in accordance with the three R’s.

3 RESULTS

3.1 The role of Semaphorin 3C in liver fibrosis

3.1.1 Semaphorin 3C is enriched in cirrhotic patients

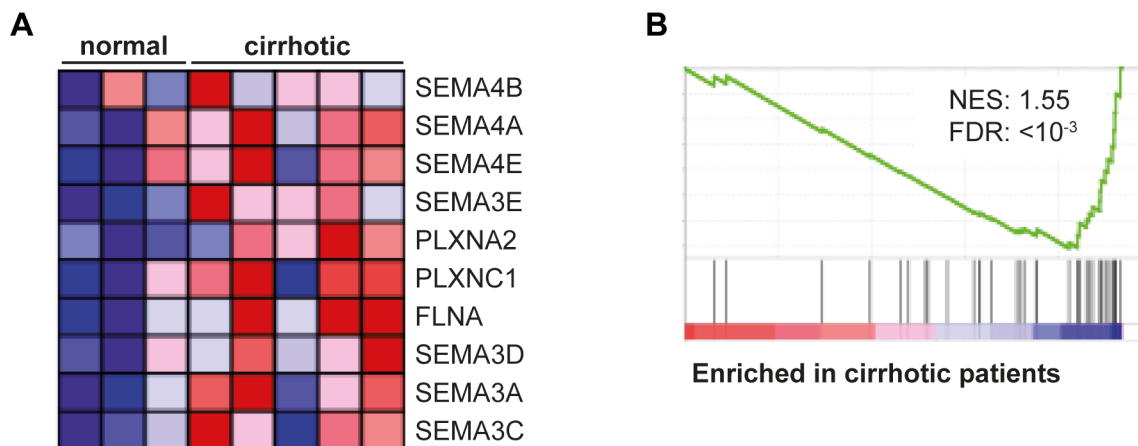


Figure 10 – Semaphorin and Plexin targets enriched in cirrhotic liver samples

Gene expression profiles from healthy donors and patients with liver cirrhosis (NCBI GEO dataset GSE45050) were used for GSEA. **(A)** Heatmap for most enriched Semaphorin and Plexin targets (Genset: GO_SEMAPHORIN_PLEXIN_SIGNALING_PATHWAY) (highest enrichment SEMA3C) comparing healthy donors (n=3) with cirrhotic patients (n=5) showing enrichment of all displayed SEMA and PLXN targets in cirrhotic patients. (blue: downregulated; red: upregulated). **(B)** Enrichment plot displaying the NES and FDS. **Figure created and provided by Lena Wiedmann, M.Sc.**

NES: normalized enrichment score; FDR: false discovery rate; SEMA: Semaphorin; PLXN: Plexin; FLNA: Filamin A

To understand gene expression levels of SEMAs and specifically SEMA3C in cirrhotic circumstances GSEA was performed on healthy patients (n=3) and patients with diagnosed liver cirrhosis (n=5). SEMA3C is the most enriched gene among all Semaphorin and Plexin targets (**Figure 10A**) suggesting the relevance of SEMA3C in the context of fibrotic and cirrhotic liver disease. The enrichment plot displays the enrichment of SEMA and PLXN targets in cirrhotic patients compared to healthy donors (**Figure 10B**). Additionally, we took the 500 most enriched genes in the liver cirrhosis samples from this GSEA and named it “cirrhosis signature”. In this signature, we found SEMA3C to be within the top 100 of most enriched genes, reinforcing the hypothesis of its possible importance in cirrhosis.

3.1.2 Semaphorin 3C correlates with worse fibrotic state in patients

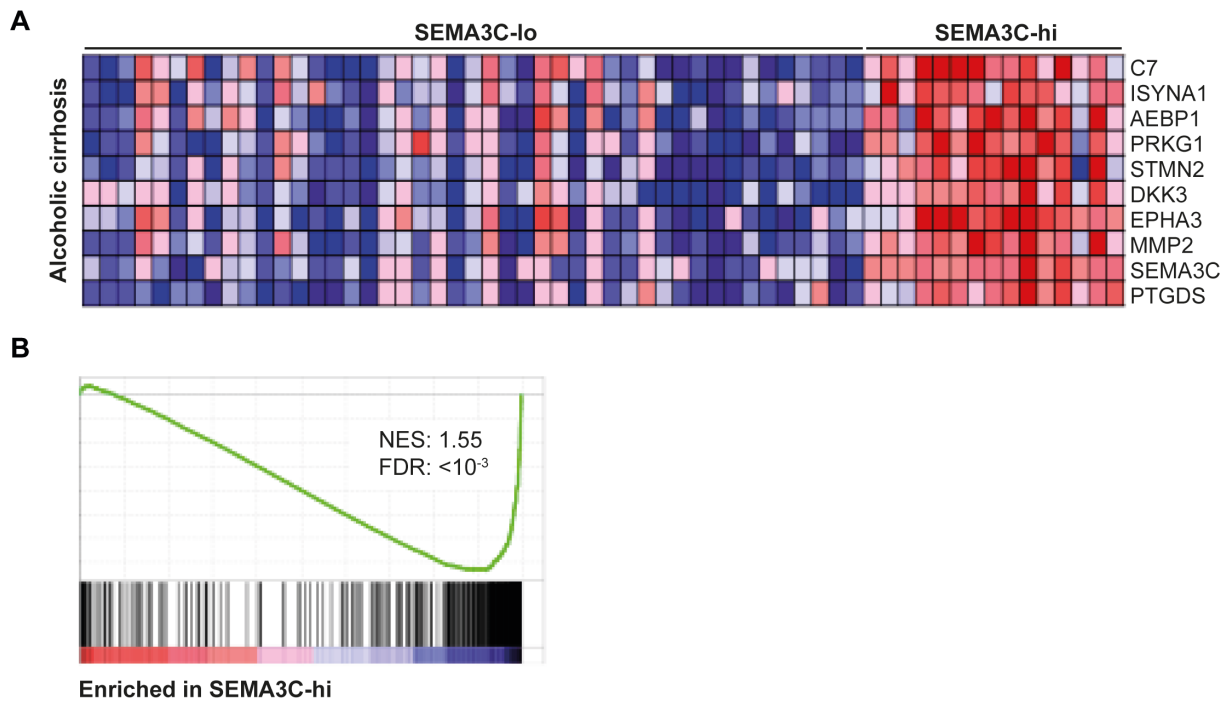


Figure 11 - Cirrhosis signature genes enriched in SEMA3C high expressing patients with alcoholic hepatitis

Gene expression profiles from patients with alcoholic liver cirrhosis (NCBI GEO dataset GSE103580) were used for GSEA. **(A)** Heatmap for genes of cirrhosis signature. Patients were assigned to their respective group according to their SEMA3C expression levels. SEMA3C-lo = SEMA3C expression level below mean and SEMA3C-hi = SEMA3C expression level above mean. (blue: downregulated; red: upregulated) **(B)** Enrichment plot displaying NES and FDR.

NES: normalized enrichment score; FDR: false discovery rate; SEMA3C lo: low SEMA3C expression levels; SEMA3C hi: high SEMA3C expression levels

To study the potential role and impact of SEMA3C on fibrotic respectively cirrhotic patients and the severity of their fibrotic or cirrhotic disease, GSEA was performed on a publicly available data set of alcoholic cirrhosis patients (dataset). Patients were grouped into SEMA3C low (SEMA3C-lo) and SEMA3C high (SEMA3C-hi) by the mean SEMA3C expression level and then compared using the a priori defined “cirrhosis signature”. Interestingly, the “cirrhosis signature” was enriched in the SEMA3C-hi cohort, suggesting that alcoholic hepatitis (AH) patients with higher SEMA3C levels have stronger cirrhosis than AH patients in the SEMA3C-lo group (**Figure 11A-B**).

3.2 The role of Semaphorin 3C in the activation of hepatic stellate cells

3.2.1 Semaphorin 3C exacerbates TGF- β signaling response in fibroblasts

The TGF- β pathway is known to be one of the key contributors to activation and fibrotic remodeling (Gressner et al., 2002; Roehlen et al., 2020). To investigate the potential interference of SEMA3C with TGF- β signaling SEMA3C was overexpressed in an activated HSC cell line (GRX).

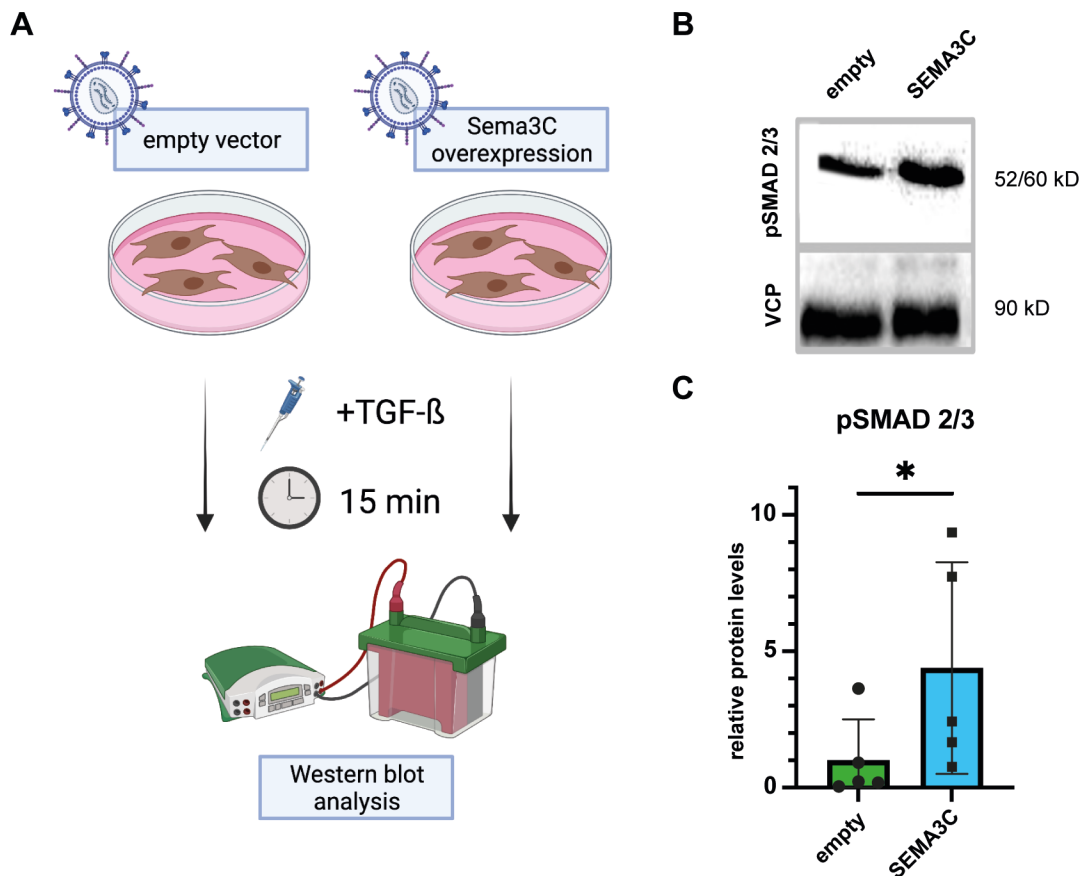


Figure 12 – GRX cells show elevated levels of TGF- β signaling upon SEMA3C overexpression

(A) Experimental set up: GRX control cells (empty) and GRX (SEMA3C) were starved, stimulated, lysed and analyzed for protein levels by Western blot. Created using BioRender.com **(B)** Empty and SEMA3C were stimulated with 10ng/ml of TGF- β for 15min. Figure shows representative image of pSMAD2/3 and VCP as loading control for empty and SEMA3C replicate (both stimulated with TGF- β) **(C)** Quantification of described Western blot analysis. Protein levels of TGF- β stimulated 'empty' replicates (n=5) were normalized to 1; relative protein levels of SEMA3C (n=5) were normalized 'empty' condition. One-tailed, non parametric t-test was performed to evaluate significance of displayed data. Data shown is mean \pm SD. * $p < 0.05$

kD: kilo Dalton; min: minutes; pSMAD2/3: phosphorylated SMAD 2/3; TGF- β : Transforming growth factor – beta; VCP: valosin containing protein

GRX cells infected with lentivirus containing an empty vector (empty) instead of SEMA3C were used as control condition. Empty and SEMA3C overexpressing cells were starved and then stimulated with TGF- β for 15 min (**Figure 12A**). To quantify the extent to which TGF- β response was triggered in cells phosphorylation of SMAD2/3 was analyzed. In accordance with literature TGF- β stimulation induced phosphorylation of SMAD2/3 in both conditions (Heldin et al., 1997; Nakao et al., 1997) (**Figure 12B**). Quantification of Western blots showed elevated levels of SMAD2/3 phosphorylation in GRX cells overexpressing SEMA3C: After stimulation with TGF- β pSMAD2/3 levels were more than four times higher in SEMA3C overexpressing GRX cells than in the control cells (**Figure 12C**).

3.2.2 Semaphorin 3C overexpression upregulates TGF- β related gene expression in activated fibroblasts

In order to understand the implications of exacerbated SMAD 2/3 phosphorylation in SEMA3C overexpressing cells in response to TGF- β stimulation, TGF- β related gene expression was analyzed in unstimulated and stimulated GRX control cells and GRX overexpressing SEMA3C. Cells were starved for 24h and then stimulated with TGF- β for 3, respectively 24 hours (**Figure 13A**). Then cells were lysed for mRNA isolation and subsequent RT-qPCR analysis checking expression of classic (fibroblast) activation marker genes *Pai-1*, *Tagln* (SM22 α) and *Acta2* (α SMA) to determine the extend to what the cells were responding to TGF- β stimulation. Gene expression levels of *Pai-1* and *Tagln* were significantly higher in the stimulated condition of SEMA3C overexpressing cells than in stimulated GRX control cells (**Figure 13B-C**) and gene expression levels of *Acta2* show a clear trend towards higher levels (**Figure 13D**). This indicates a higher state of activation and transdifferentiation in SEMA3C overexpressing GRX cells compared to the respective control.

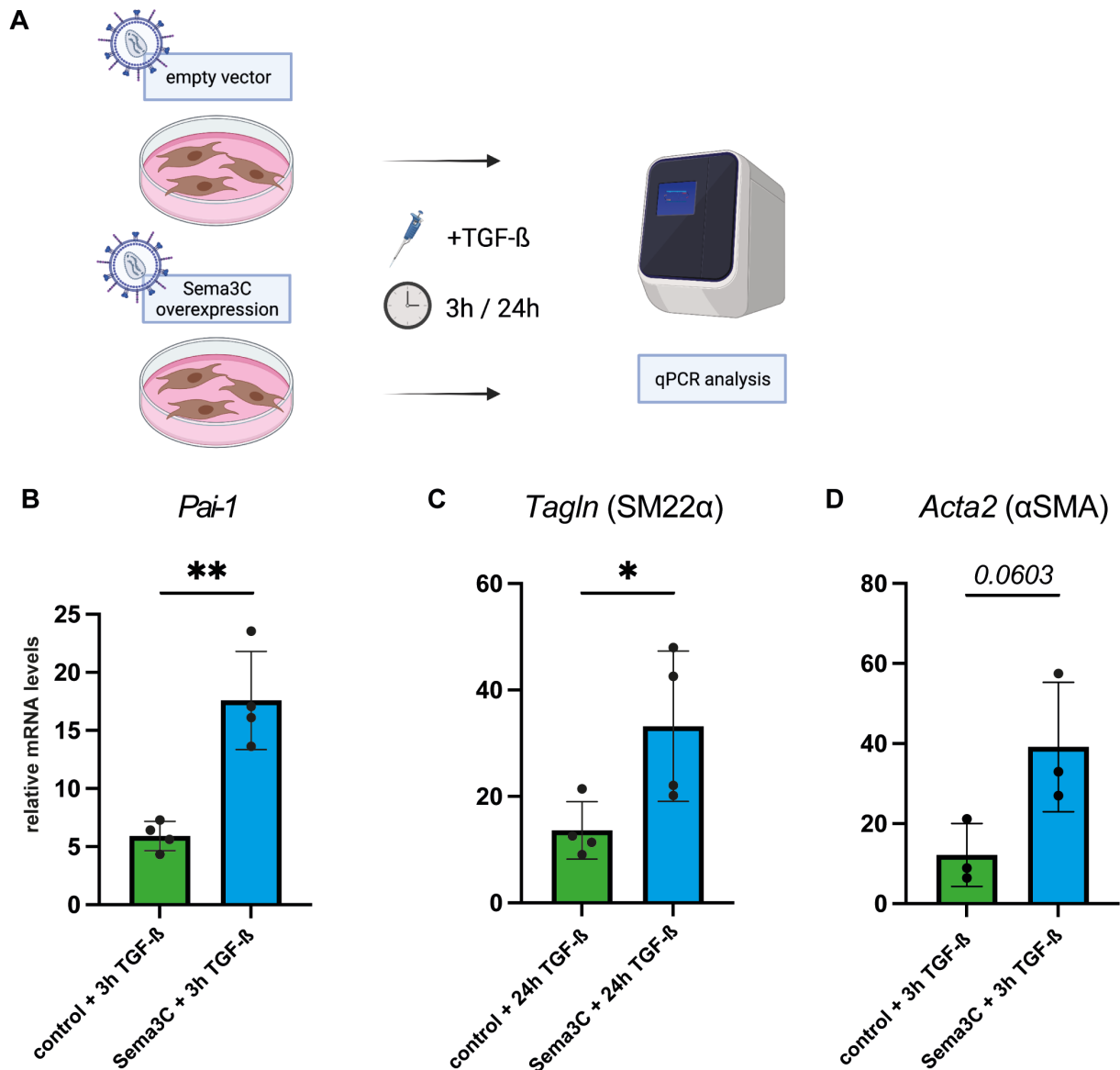


Figure 13 – SEMA3C overexpressing cells show elevated levels of TGF-β related gene expression

(A) Procedure of experiment: GRX control and SEMA3C overexpressing cells were cultured, starved, stimulated and then lysed for RT-qPCR analysis. Created using BioRender.com **(B-D)** Control displayed in green, SEMA3C overexpressing in blue. Control and SEMA3C overexpressing replicates were normalized to the unstimulated control. Displayed values are relative mRNA levels. **(B+C)** *Pai-1* and *Acta2* (αSMA) expression levels were analyzed after 3h of stimulation with 10ng/ml of TGF-β. **(D)** *Tagln* (SM22α) was analyzed after 24h of stimulation with 10ng/ml of TGF-β. Two-tailed, parametric t-test was performed to evaluate significance of displayed data. Data shown is mean ± SD. *p<0.05; **p<0.01;

3.2.3 Semaphorin 3C upregulation in activated hepatic stellate cells

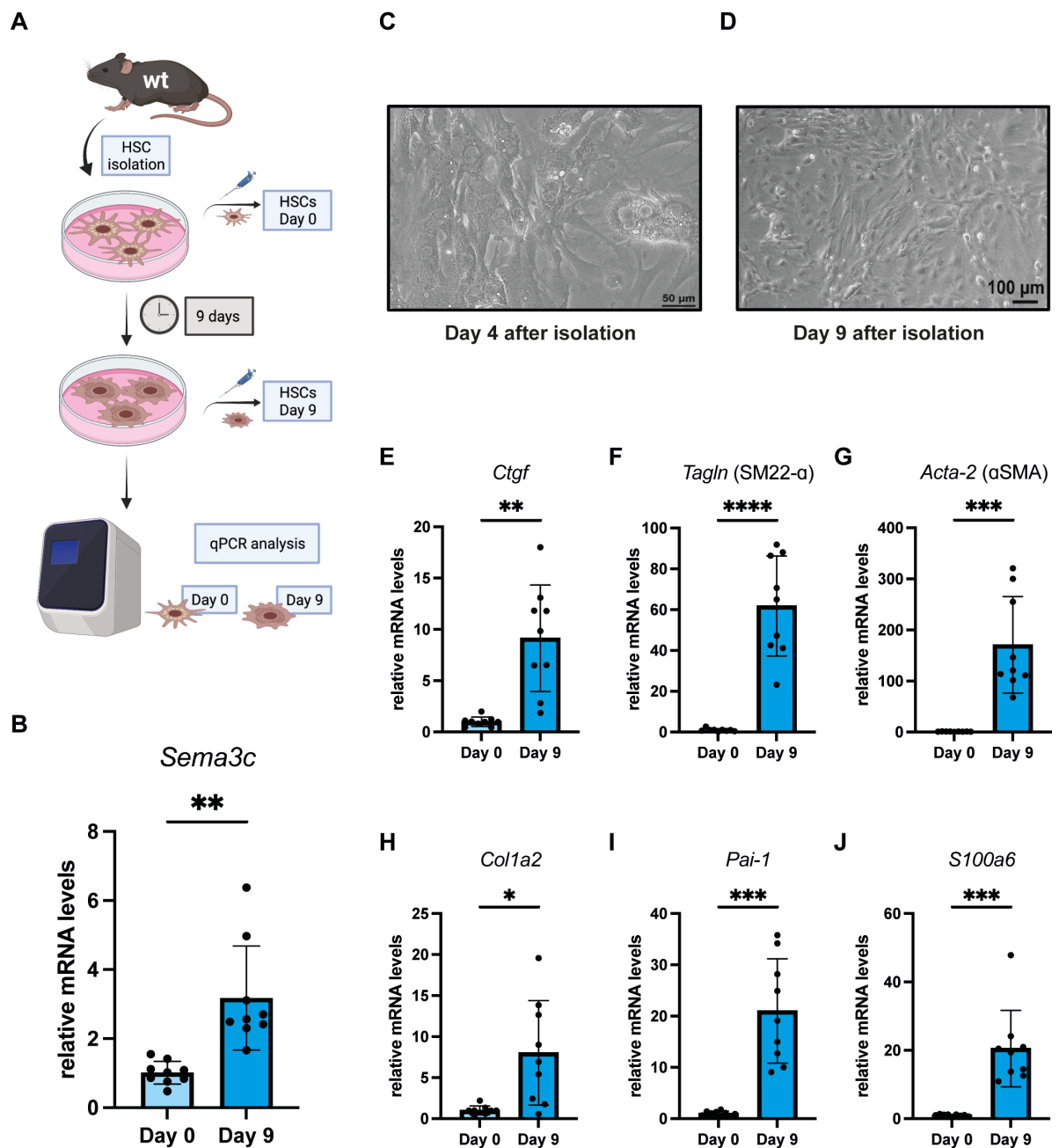


Figure 14 - Semaphorin 3C is upregulated in activated primary HSC upon activation by culture time

(A) Procedure of experiment: HSCs from Wildtype (wt) mice were isolated, cultured and analyzed by RT-qPCR. Created using BioRender.com (B; E-H) Graphs display relative gene expression levels of *SEMA3C*, *Ctgf*, *Tagln*, *Acta2*, *Col1a2*, *Pai-1*, *S100a6* at Day 0 and Day 9. (C-D) Light microscope pictures of cells were taken 4 and 9 days post isolation. Two tailed, paired, t-test was performed to evaluate significance of displayed data. Data shown is mean \pm SD. * $P < 0.05$; ** $P < 0.01$; *** $P < 0.001$; **** $P < 0.0001$.

To validate effects of SEMA3C that were observed in the GRX cell culture model, primary HSCs were isolated as described. HSCs from 14 – 20 weeks old C57BL/6J wildtype (wt) mice were isolated to confirm *Sema3c* upregulation upon activation of fibrosis mediating cells. After isolation, a fraction of HSCs was collected and directly lysed to check gene expression levels at Day 0. The remaining fraction of HSCs was cultured for 9 days to activate the isolated cells by culture time (**Figure 14A**). It has been shown that *in vitro* culturing is adequate to activate primary HSCs and trigger their transdifferentiation into myofibroblasts (El Taghdouini et al., 2015). Hence activation by culture time could be used as a sufficient model to investigate the regulation of SEMA3C upon activation.

After 9 days of culturing HSCs were lysed, mRNA was isolated and qPCR was performed. Gene expression levels of all genes were normalized to their respective expression levels at Day 0 (**Figure 14B, 14E-J**). qPCR showed upregulation of common activation and fibrosis markers such as *Ctgf*, *Acta2*, *Tagln* (SM22 α), *Col1a2*, *Pai-1* and *S100a6* and (**Figure 14E-J**) confirming successful activation of isolated wt HSCs by culture time. Also, 4 days post isolation HSCs still show retinoid lipid droplets (**Figure 14C**), whereas they were lost 9 days post isolation. Additionally a morphological change away from the stellate towards a myofibroblast phenotype can be observed (**Figure 14D**), demonstrating the HSC's transdifferentiation. Within the mentioned activation and transdifferentiation marker genes *Acta2* (α -SMA) and *Tagln* were most upregulated with relative increases of gene expression of 170-fold respectively 60-fold. Compared with levels at Day 0 *Sema3c* was upregulated at Day 9 up to sixfold. (**Figure 14B**).

3.2.4 Semaphorin 3C receptor downregulation in activated hepatic stellate cells

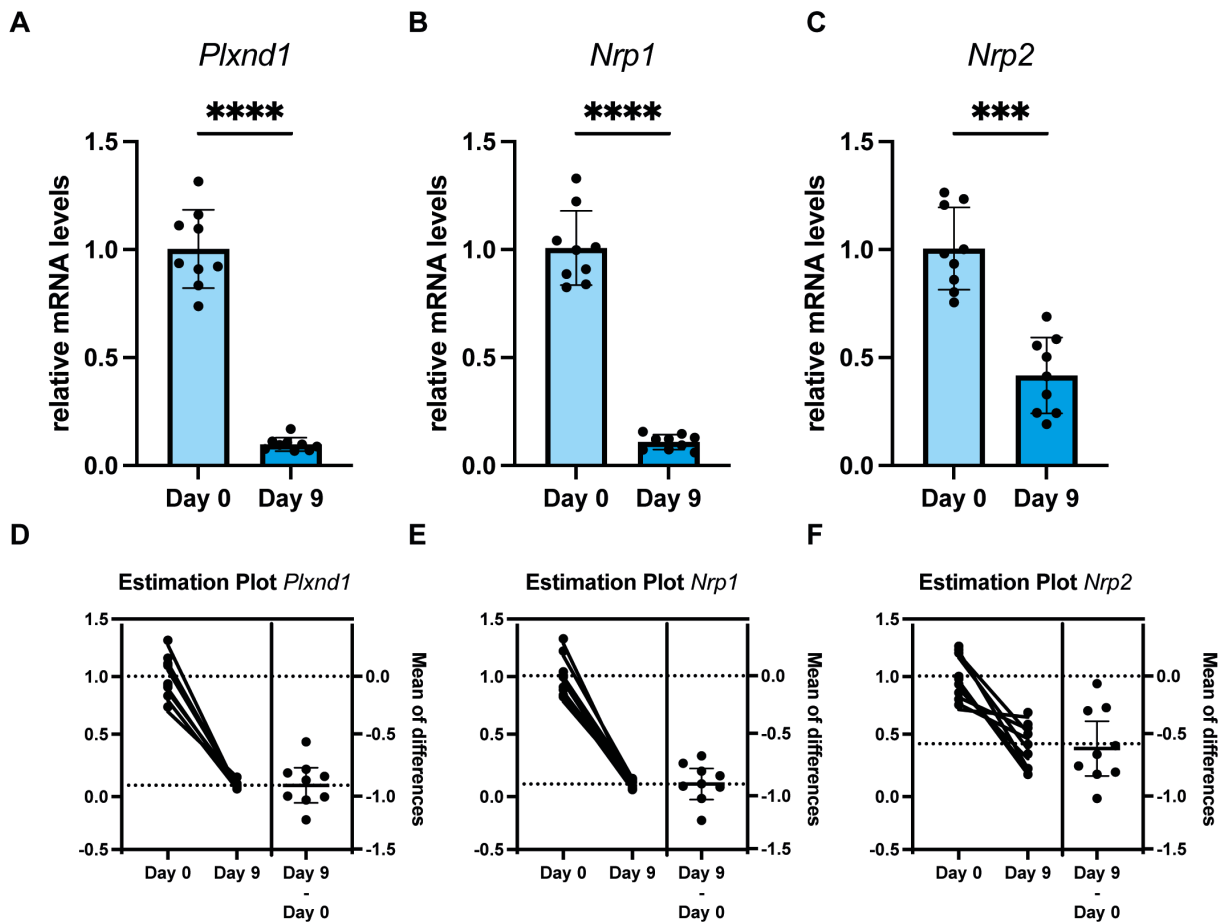


Figure 15 - *Nrp2* is maintained while *Nrp1* and *Plxnd1* are clearly downregulated upon activation
 Gene expression levels were measured in primary isolated murine HSCs at two timepoints. (A-C) Graphs display relative gene expression levels of *Plxnd1*, *Nrp1* and *Nrp2* at Day 0 and Day 9. (D-F) Estimation plots for *Plxnd1*, *Nrp1* and *Nrp2* show the corresponding pairs and display the means of difference between Day 0 and Day 9 for the respective receptors. Two tailed, paired, parametric t-test was performed to evaluate significance of displayed data. Data shown is mean \pm SD. *** $P < 0.001$; **** $P < 0.0001$.

Given that *Sema3c* is upregulated in activated primary HSCs (Figure 14B) it was crucial to investigate the regulation of different Semaphorin receptors upon activation. qPCR was performed on Day 0 and Day 9 samples from wildtype mice (see set up from 3.2.3). *Nrp1* and *Plxnd1* expression decreased ten- to twentyfold from Day 0 upon activation until Day 9 (Figure 15A-B; 15D-E). *Nrp2* however was only downregulated to levels between 0.6 and 0.3 (Figure 15C; 15F). These results indicate that expression of *Nrp2* is nearly maintained upon activation whilst *Nrp1* and *Plxnd1* are nearly completely downregulated. The findings led to further investigation of the effect

of specifically NRP2 on the activatability of hepatic stellate cells and its role as SEMA3C receptor.

3.2.5 Regulation of class 3 Semaphorins in activated hepatic stellate cells

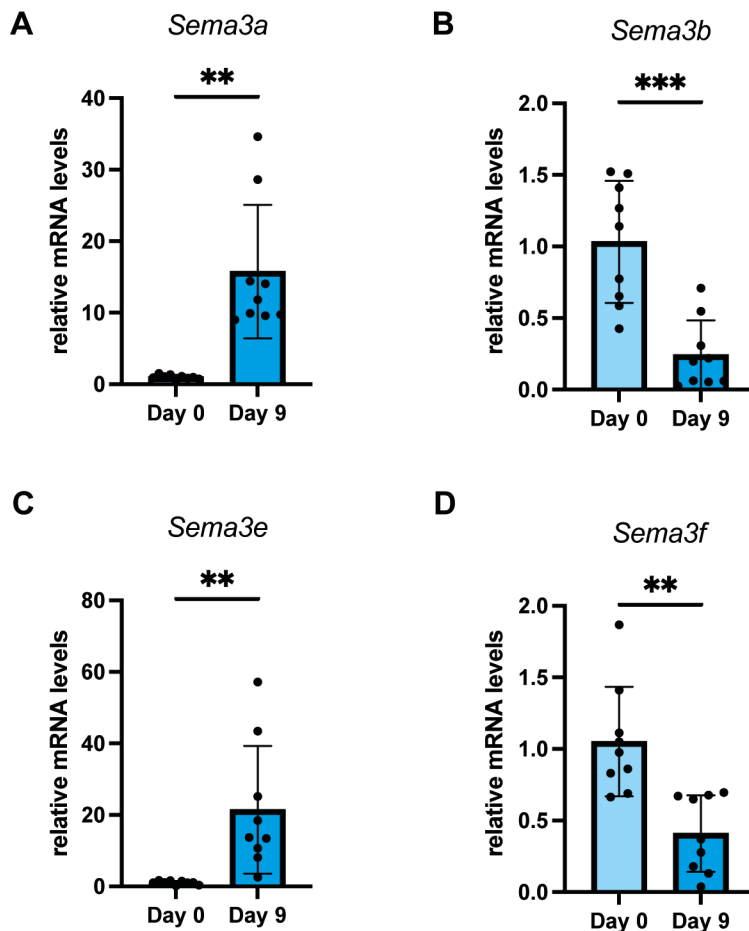


Figure 16 - *Sema3a* and *Sema3e* are upregulated, *Sema3b* and *Sema3f* downregulated in activated hepatic stellate cells

(A-E) Graphs display relative gene expression levels of *Sema3a*, *Sema3b*, *Sema3d*, *Sema3e* and *Sema3f* at Day 0 and Day 9. Two tailed, paired, parametric t-test was performed to evaluate significance of displayed data. Data shown is mean \pm SD. **P<0.01; ***P<0.001

As SEMA3C is part of a wider family of Semaphorin class 3 proteins (Goodman et al., 1999), mRNA isolates of activated hepatic stellate cells (HSCs) were analyzed by qPCR to understand the regulation of other class 3 Semaphorins in HSCs upon their activation. Experimental set up was the same as for SEMA3C analysis. Day 0 and Day 9 comparative analysis was performed for *Sema3a*, *Sema3b*, *Sema3e* and *Sema3f*. *Sema3a* and *Sema3e* were significantly upregulated in activated hepatic stellate cells

compared with their quiescent state. *Sema3e* was upregulated strongest with a relative increase of relative expression up to 21-fold on average (**Figure 16A**). *Sema3a* was increased up to 18-fold on average (**Figure 16D**). In contrast *Sema3b* and *Sema3f* were downregulated upon HSC activation (**Figure 16B; 16E**).

3.2.6 Semaphorin 3C knock out decreases activatability of hepatic stellate cells

In vitro experiments with GRX cells showed the promotion of activation and TGF- β related gene expression upon SEMA3C overexpression. To verify these *in vitro* results in an *ex vivo* setting and to investigate whether increased expression and presence of SEMA3C affects the activatability of primary hepatic stellate cells, 14 – 20 weeks old SM22 α ^{CRE}/SEMA3C^{fl/fl} (cre⁺) and their matching controls SEMA3C^{fl/fl} (cre⁻) were used for HSC isolation (**Figure 17A**).

Quiescent, inactivated hepatic stellate cells do not express SM22 α – however upon activation expression levels of SM22 α (*Tagln*) are increased(**Figure 17D**). Therefore the SEMA3C knock-out (ko) - with SM22 α as a driver gene - will only be induced during activation by culture time; at Day 0 before culturing the cells neither of the mentioned genotypes will have a SEMA3C knock out. Thus isolated HSCs from SM22 α ^{CRE}/SEMA3C^{fl/fl} and SEMA3C^{fl/fl} are compared with regard to their gene expression level after nine days of activation by culture time to understand the role of SEMA3C in the activation of HSCs. To do so HSCs were isolated as described from cre⁺ and cre⁻ mice. A fraction of isolated HSCs of both groups was directly lysed to perform the purity check as described. The remaining HSCs of both groups were plated, cultured for 9 days and then lysed for mRNA isolation and qPCR analysis (**Figure 17A**). Quantitative PCR analysis showed that HSCs from cre⁺ mice express significantly lower levels of *Acta2* (α SMA) and *Tagln* (SM22), *Ctgf* and *S100a6* (**Figure 17B-E**). This indicated lower degree of activation and slower progression of transdifferentiation of HSCs isolated from SM22 α ^{CRE}/SEMA3C^{fl/fl} (cre⁺) upon 9 days activation by culture time.

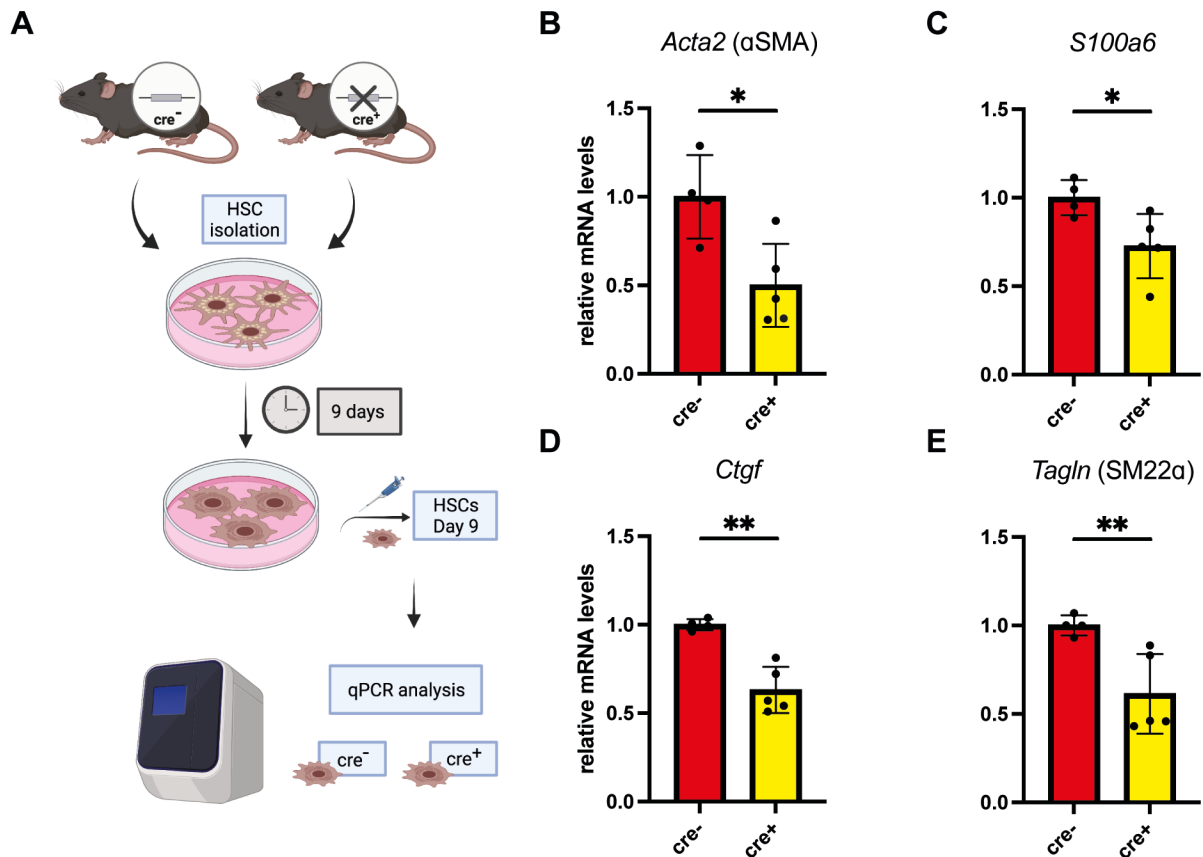


Figure 17 - HSCs with SEMA3C knock-out express lower levels of activation and transdifferentiation markers

(A) Procedure of experiment: HSCs from *SEMA3C^{fl/fl}* and *SM22α^{CRE}/SEMA3C^{fl/fl}* mice were isolated, cultured and analyzed by qPCR at day 9. Created using BioRender.com **(B-E)** Graphs display relative gene expression levels of *Acta2*, *S100a6*, *Ctgf* and *Tagln* for *cre⁻* and *cre⁺* group. One-tailed, non-parametric Mann-Whitney test was performed to evaluate significance of displayed data. Data shown is mean ± SD. *P<0.05; **P<0.01

3.3 The role of Neuropilin 2 in the activation of hepatic stellate cells

3.3.1 Neuropilin 2 alters Neuropilin 1 expression in fibroblasts

In contrast to the other two SEMA3C receptors (NRP1 and PLXND1) mRNA levels of *Nrp2* remained higher upon activation of HSCs. Hence the role of NRP2 for regulation of hepatic stellate cell activatability and transdifferentiation was to be further investigated. For this purpose GRX cells were infected with a lentivirus containing a plasmid coding for a small hairpin RNA (shRNA) targeting *Nrp2* (shNRP2). GRX cells infected with a vector containing a non-targeting shRNA (shControl). After the knock-

down was established in GRX cells, cells were stimulated with TGF- β and then lysed for Western blot analysis (**Figure 18A-C**). Displayed western blots are n=1 and hence data is only preliminary. (**Figure 18B**). For qPCR analysis cells were cultured, stimulated and lysed. *Nrp2* knock-down was confirmed in shNRP2 cells compared with control shRNA cells (Figure 18B, E). *Nrp1* levels were significantly decreased upon *Nrp2* knockdown (Figure 18C, E).

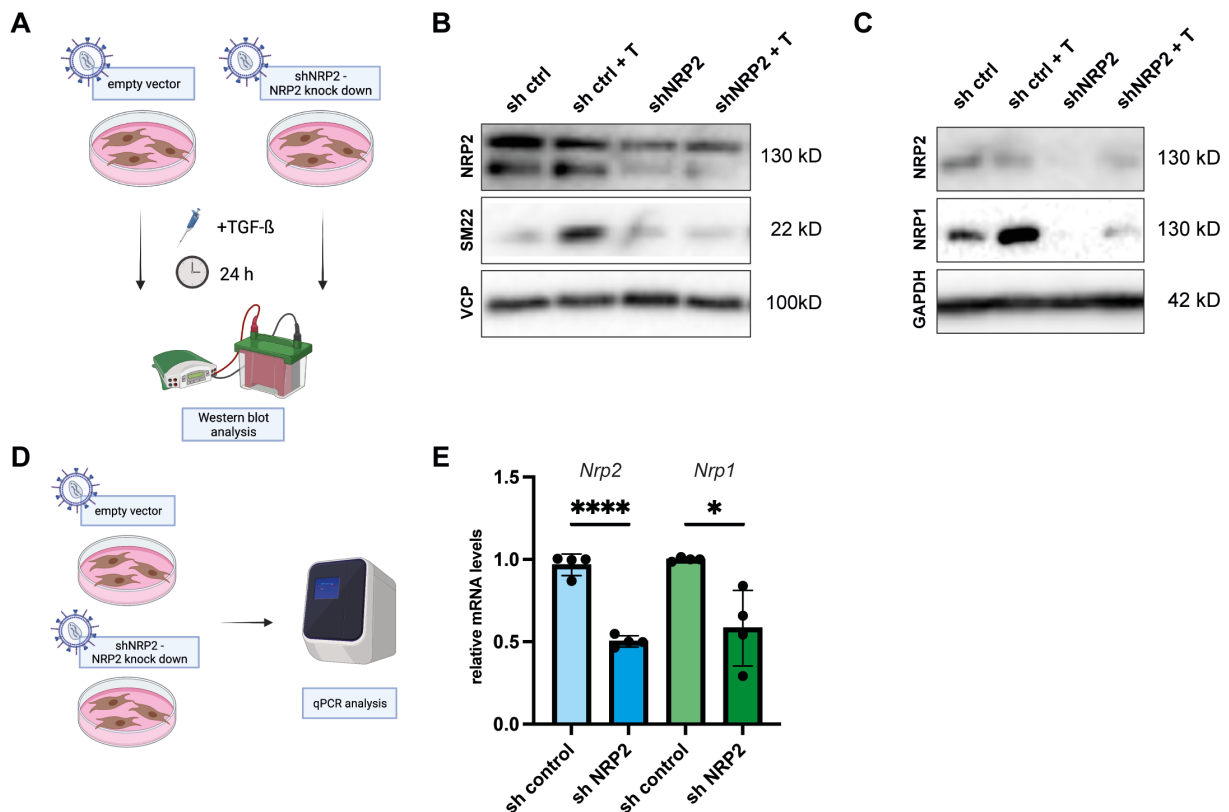


Figure 18 - Neuropilin 2 knock down alters activatability of fibroblasts and downregulates Neuropilin 1

(A) Procedure of experiment: control GRX cells (empty) and GRX treated with lentiviral vector for shNRP2 (shNRP2) were cultured, stimulated with 10ng/ml TGF- β , lysed and analyzed by Western blot. Created using BioRender.com (B-C) Figure shows preliminary data (n=1) representative Western blot of (B) NRP2, SM22 and VCP as loading control (C) respectively NRP2, NRP1 and GAPDH as loading control. (D) Procedure of experiment: control GRX cells (empty) and GRX treated with lentiviral vector for shNRP2 (shNRP2) were cultured, lysed and analyzed by qPCR. (E) Figure shows relative mRNA levels of *Nrp2* and *Nrp1* gene expression levels. Two tailed, unpaired, parametric t-test was performed to evaluate significance of displayed data. Data shown is mean \pm SD. *P<0.05; ****P<0.0001.

3.3.2 Neuropilin 2 alters activatability of hepatic stellate cells

To investigate a potential role of NRP2 on activation of HSCs, 14 – 20 weeks old SM22 α ^{CRE}/NRP2^{fl/fl} (*cre*⁺) and their matching controls NRP2^{fl/fl} (*cre*⁻) were used for HSC isolation (**Figure 19A**).

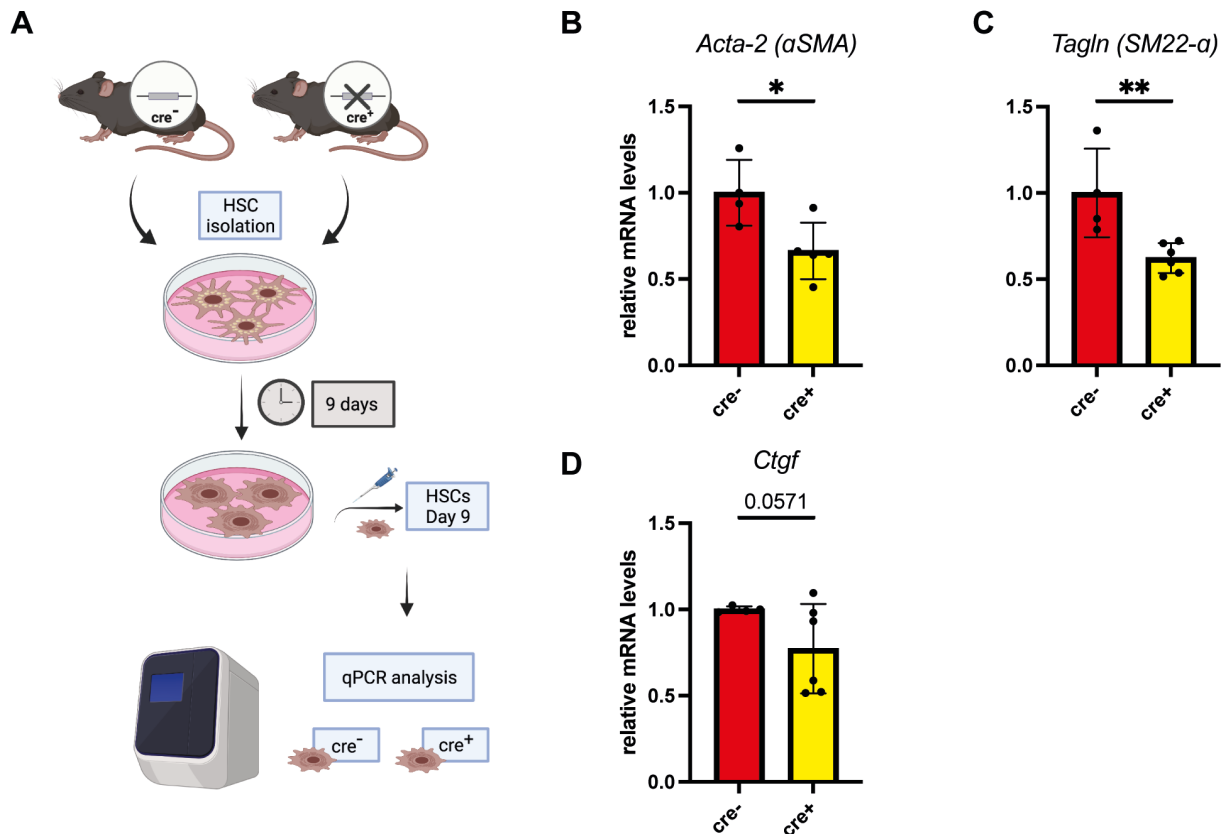


Figure 19 - HSCs with NRP2 knock out express lower levels of activation and transdifferentiation markers

(A) Procedure of experiment: HSCs from *cre*⁻ and *cre*⁺ mice were isolated at Day 9, cultured and analyzed by qPCR. Created using BioRender.com. (B-E) Graphs display relative gene expression levels of *Acta2*, *Tagln* and *Ctgf* for *cre*⁻ and *cre*⁺ group. One-tailed, non-parametric Mann-Whitney test was performed to evaluate significance of displayed data. Data shown is mean ± SD. *P<0.05; **P<0.01

Quantitative PCR analysis showed that HSCs from *cre*⁺ mice express significantly lower levels of *Acta2* (aSMA) and *Tagln* (SM22 α) and *Ctgf* than HSCs isolated from *cre*⁻ mice (**Figure 19B-D**). This indicated lower levels of activation and slower progression of transdifferentiation in HSCs isolated from SM22 α ^{CRE}/SEMA3C^{fl/fl} (*cre*⁺) upon 9 days activation by culture time in comparison with HSCs isolated from littermate controls.

3.4 Semaphorin 3C expression correlates with overall survival in patients with hepatocellular carcinoma

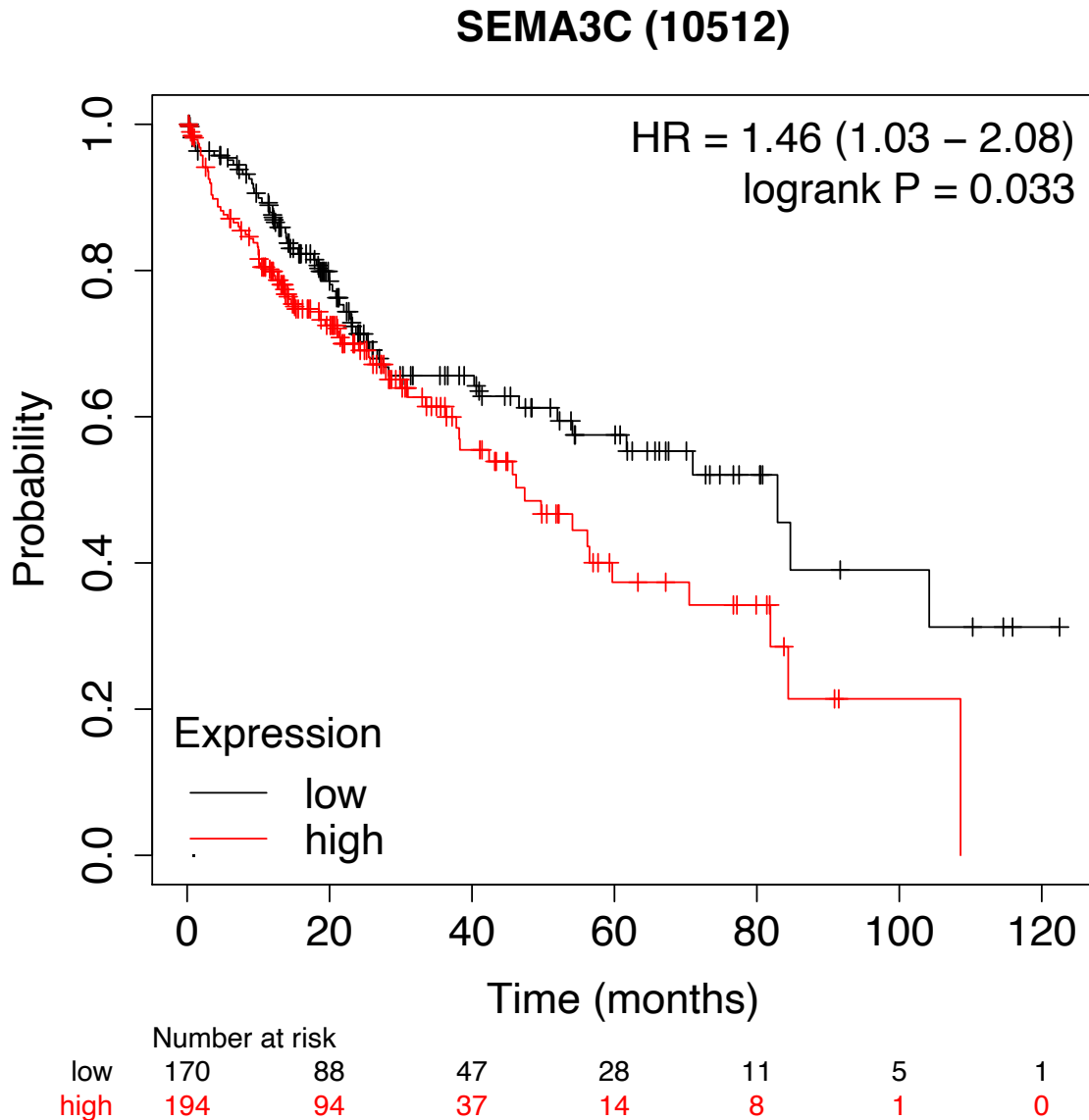


Figure 20 – SEMA3C low expressing patients show longer overall survival than SEMA3C high expressing patients

Kaplan-Meier plot based on Kaplan-Meier plotter (Menyhárt et al., 2018) SEMA3C low expressing patients (black line and crosses) and SEMA3C high expressing patients (red line and crosses) are compared with regard to their overall survival. Patients were grouped by automatically generated cut-off value.

HR: hazard ratio

Using the Kaplan Meier (KM) plotter for liver cancer (Menyhárt et al., 2018) comparative overall survival analysis was performed with regard to SEMA3C expression in patients diagnosed with hepatocellular carcinoma. The high and low

expression group was split at an automatically determined threshold (**Appendix Figure 21**). Patients with high SEMA3C expression levels were observed to have significantly shorter overall survival time than patients with low SEMA3C expression levels. Median survival for patients with low SEMA3C expression is 82.9 months, whilst the median survival for patients with high SEMA3C expression 47.4 months (**Figure 20**). The KM plotter's automatic cutoff determination generates the cutoff value grouping the patient collective into two sets. For the HCC patient collective at hand the cutoff value was determined to be 17 with a corresponding p-value of 0.033 and a hazard ratio of 1.46.

4 DISCUSSION

Central pathomechanism to liver fibrosis is the activation and transdifferentiation of hepatic stellate cells and subsequent myofibroblast-driven, fibrotic remodeling of the liver (Lee et al., 2015). Class 3 Semaphorins, such as SEMA3A and SEMA3E, are secreted proteins known to be involved in fibrotic diseases and specifically aggravate liver fibrosis (Jeon et al., 2020; Papic et al., 2018; Yagai et al., 2014). The main objective of this MD thesis was to investigate and understand whether SEMA3C correlates with fibrosis, and if so, whether and how it is involved in HSC activation and what mechanisms underly potential influence of SEMA3C on HSC activation and transdifferentiation.

4.1 Correlation of Semaphorin 3C and chronic liver disease

Publicly available data was used to perform GSEA on patients with liver cirrhosis, in many cases the end stage of liver fibrosis, and respective healthy control patients. The performed GSEA found several SEMA and PLXN family members enriched in cirrhotic patients compared with control patients such as SEMA3A, B, C, D and E, and SEMA4A, B, and E (**Figure 10 A-B**). This confirms the association of serum levels of specific SEMA proteins and specifically also SEMA3C with liver fibrosis (Papic et al). When checking gene expression levels in patients with liver cirrhosis compared to healthy donors, SEMA3C was the most enriched gene within the SEMA and PLXN targets (**Figure 10 A-B**), which set the focus of this study upon SEMA3C. GSEA was also used to generate a cirrhosis signature, including the comparatively 500 most enriched genes in cirrhotic patients.

To confirm not only an association, but also a correlation of SEMA3C and chronic liver disease, GSEA was then performed on a patient data set exclusively containing patients suffering from alcoholic hepatitis (**Figure 11**). Patients with low *SEMA3C* mRNA expression (*SEMA3C-lo*) showed far less enrichment of cirrhotic signature genes (determined in the former GSEA) than patients with high *SEMA3C* expression (*SEMA3C-hi*) (**Figure 11**). This leads to the conclusion that SEMA3C is associated with liver cirrhosis and correlates with the severity of liver cirrhosis and thus liver fibrosis. While it is impossible to deduce any mechanistic explanation from this mere correlation, it suggested further investigating potential SEMA3C mediated profibrotic

processes. Hepatic stellate cells are the main driver of fibrosis (Friedman, 2008), and a single cell analysis by Ramachandran showed that cells from the mesothelioma are the primary source of SEMA3C in the liver (Ramachandran et al., 2019). Therefore it was natural to focus the mechanistic investigation of the correlation between SEMA3C and fibrosis on the activation and transdifferentiation of hepatic stellate cells.

4.2 Role of Semaphorin 3C in fibroblast signaling and activation

The master profibrogenic cytokine TGF- β is widely regarded to conduct its fibrogenic effect as one of the most potent effectors in activating hepatic stellate cells (Chang and Li, 2020; Fabregat et al., 2016). At the same time, SEMA3C's receptors NRP1 and NRP2 are known to be involved in the amplification of TGF- β signaling leading to increased SMAD phosphorylation in colon cancer and liver fibrosis (Cao et al., 2010; Glinka et al., 2011; Grandclement et al., 2011b). Recent studies demonstrate that each Neuropilin enhances TGF- β mediated SMAD phosphorylation by binding TGF- β receptor 1 (T β RI) and by directly acting as a receptor for TGF- β 1 (Glinka et al., 2011; Grandclement et al., 2011a).

During this study, I hypothesized that the mechanism underlying the correlation between SEMA3C and fibrosis might originate from SEMA3C interfering with TGF- β signaling in hepatic stellate cells via its receptors NRP1 or NRP2. In fact, SEMA3C overexpression in GRX, an immortal, HSC derived, myofibroblast cell line, proper to mimic hepatic stellate cell behavior in culture (Borojevic et al., 1985; Herrmann et al., 2007), led to increased SMAD2/3 phosphorylation upon TGF- β stimulation compared to control GRX cells in Western blot analysis (**Figure 12 A-C**). Also, the stimulation with TGF- β led to significantly upregulated gene expression levels of *Pai-1*, *Acta2* (α SMA), and *Tagln* (SM22 α) in SEMA3C overexpressing cells compared with controls (**Figure 13**). SMAD2/3 is recognized as the main effector signaling pathway in TGF- β signaling (Hill, 2016; Kitamura and Ninomiya, 2003; Massagué, 2012) and *Pai-1*, *Acta2* (α SMA) and *Tagln* (SM22 α) are well established to be TGF- β induced genes (Duncan et al., 1999; Hu et al., 2003; Liu et al., 2013; Lund et al., 1987; Shafer and Towler, 2009). This indicates that SEMA3C actually mediates TGF- β signaling and subsequently augments SMAD 2/3 phosphorylation. The exact way SEMA3C mediates the enhanced TGF- β signaling response is still in question. For example, SEMA3C binding to its NRP receptors could lead to an intensified association of NRP1

and or NRP2 with T β Rs, further amplifying TGF- β -T β R mediated SMAD 2/3 phosphorylation and subsequent TGF- β related gene expression.

Enhanced TGF- β signaling and upregulated TGF- β related gene expression upon SEMA3C overexpression led me to conclude that SEMA3C is not only upregulated as a consequence of liver injury and inflammation but also actively contributes to the very progression of liver fibrosis itself. The expression of SEMA3C in early fibrosis could augment TGF- β response in involved HSCs and potentiate the fibrotic process and remodeling. These results and the subsequent assumptions regarding the mechanism are based on *in vitro* data from an immortalized cell line. Thus, it was crucial to investigate and validate obtained results in *ex vivo* experiments with primary HSCs.

4.3 The relevance of Semaphorin 3C in activation and transdifferentiation of hepatic stellate cells

Isolation of primary murine HSCs and subsequent HSC activation by culture time is a well-described and widely acknowledged model to study HSC biology and mimic their activation and transdifferentiation process (Friedman, 2003; Rombouts, 2015). Thus far, it was only known that general SEMA3C serum levels were elevated in association with liver fibrosis (Papic et al., 2018), and my study's results to that point were based on *in vitro* experiments on GRX cell line.

In the next step this project hence aimed to investigate the regulation of SEMA3C in isolated, primary HSCs upon activation by culture time. The significant upregulation of SEMA3C in HSCs after nine days of activation by culture time demonstrates that SEMA3C is not only generally associated with fibrosis, as Papic et al. indicate, but is a specific marker for HSCs activation (**Figure 14**).

To validate the activating and transdifferentiating effect of SEMA3C on GRX in primary HSCs, HSCs were isolated from SM22 α ^{CRE}xSEMA3C^{fl/fl}, and their littermate controls SEMA3C^{fl/fl}. **Figure 14F** demonstrates the massive upregulation of *Tagln* (SM22 α) in activated primary HSCs. As SM22 α is the driver gene in SM22 α ^{CRE}xSEMA3C^{fl/fl} mice, SEMA3C is deleted upon activation in HSCs isolated from these mice and retained in their littermate controls SEMA3C^{fl/fl}. After nine days of activation, HSCs isolated from SM22 α ^{CRE}xSEMA3C^{fl/fl} mice show significantly lower levels of activation and transdifferentiation markers *Pai-1*, *Acta2*, *Tagln*, and *S100a6* than HSCs isolated from their littermate controls (**Figure 17**). *Pai-1*, *Acta2* (α SMA), *Tagln* (SM22 α) and *S100a6*

are TGF- β -signaling induced genes, related to various characteristics of HSC derived myofibroblast in fibrosis such as contractility (*Acta2*) (Hu et al., 2003; Saab et al., 2002), fibrogenesis and altered matrix degradation (*Pai-1*) (Leyland et al., 1996). While overexpression of SEMA3C led to the amplification of TGF- β signaling and gene expression (**Figure 12-13**), SEMA3C deletion goes in hand with less contractility, fibrogenesis, and less factors altering matrix degradation (**Figure 17**). Based on these findings, I conclude that SEMA3C not only mediates HSC activation in HSC derived cell lines but also exacerbates TGF- β response in primary HSCs. Thereby SEMA3C triggers TGF- β related activation of primary HSCs. Vice versa, the observation of lower transcriptomic levels of transdifferentiation markers upon SEMA3C deletion (**Figure 17**), support the hypothesis that SEMA3C expression aggravates fibrosis development.

Data from GRX experiments that indicate the mediating role of SEMA3C in activation and transdifferentiation of HSCs left room for uncertainty regarding the mechanism of SEMA3C dependent signaling. To answer that uncertainty, I analyzed the regulation of SEMA3C receptors upon activation of HSCs (**Figure 15**). Interestingly NRP2 was the only SEMA3C receptor to be maintained (**Figure 15 C; F**), while Plexin D1 and NRP1 were nearly completely downregulated to levels between 2% and 10% compared to the day of isolation (**Figure 15 A-B; D-E**). This suggests eventual SEMA3C-dependent effects in the activation of primary HSCs to be mediated by NRP2, rather than Plexin D1 and NRP1. Hence it can be assumed that NRP2 functions as an individual modulator of HSC activation and TGF- β signaling augmentation, independent from Plexin D1 and seems to be the main receptor modulating SEMA3C's effects within the activation of HSCs.

To further explore the role of NRP2 in the regulation and eventual mediation of HSC activation, HSCs were isolated from SM22 α ^{CRE}xNRP2^{fl/fl}, and their littermate controls NRP2^{fl/fl}. Upon elimination of NRP2, HSCs isolated from SM22 α ^{CRE}xNRP2^{fl/fl} mice after nine days of culture activation show lower levels of *Acta2* (α SMA) and *Tagln* (SM22 α) and show a trend of reduced *Ctgf* levels (**Figure 19**). This supports my hypothesis that SEMA3C associated exacerbation of TGF- β signaling, gene expression, and activation of primary HSCs is mediated via NRP2. NRP1 is already known to exacerbate the activation of HSCs, enhancing TGF- β signaling (Cao et al., 2010). My findings suggest that NRP2 influences TGF- β -related HSC activation in a similar way. Potentially, NRP2

deletion mimics the effect of SEMA3C deletion as the underlying signaling mechanism of SEMA3C is disturbed, and hence the promoting effect of SEMA3C in HSCs isolated from NRP2^{fl/fl} mice does not unfold in HSCs isolated from SM22 α ^{CRE}xNRP2^{fl/fl} mice, leading to lower levels of HSC activation and transdifferentiation markers.

4.4 Other Class 3 semaphorins in activated hepatic stellate cells

Amongst several functions, other class 3 semaphorins than SEMA3C influence fibrosis and tumorigenesis (Gu et al., 2005; Rehman and Tamagnone, 2013; Toledano et al., 2019; Yagai et al., 2014). Remarkably SEMA3A and SEMA3E are extensively upregulated in primary HSC isolated from wildtype mice and activated by nine days of culture time (**Figure 15A; C**) while SEMA3B and SEMA3F are clearly downregulated (**Figure 15B;D**). Interestingly SEMA3A was already described to mediate fibrosis in corneal injury via amplifying TGF- β signaling (Jeon et al., 2020) and SEMA3A deletion ameliorated renal fibrosis (Jeon et al., 2020; Sang et al., 2021). SEMA3E triggers sinusoidal contractability in fibrosis and deletion of SEMA3E in rodent fibrosis model ameliorates fibrosis (Yagai et al., 2014). The upregulation of SEMA3A and SEMA3E in activated HSCs indicates a potential association if not correlation with and contribution to HSC activation of these two members of class 3 semaphorins. SEMA3A and SEMA3E upregulation is consistent with our current understanding of their respective role in fibrosis. Perspectively it will be interesting to investigate potential interaction of SEMA3A and SEMA3E with HSCs and to understand potential contribution of these two proteins to HSC activation and transdifferentiation. To what extent SEMA3C interacts or counteracts with other SEMA3s in context of liver fibrosis will be subject to discussion.

4.5 Semaphorin 3C in hepatocellular carcinoma

Overall survival (OS) of HCC patients is longer in SEMA3C low-expressing than in SEMA3C high-expressing patients (**Figure 20**). Tam et al. demonstrate that SEMA3C overexpression augments EMT markers in prostate cells, induces differentiation of cancer-promoting, stem-like population of cells, and increases invasiveness and dissemination of prostate cancer cells (Herman and Meadows, 2007; Tam et al., 2017). Additionally, it is known that SEMA3C promotes therapeutic resistance, metastasis,

cancer-like stem cell capacities, and vascularization of several types of cancer (Hao and Yu, 2018). I show the SEMA3C dependent augmentation of HSC activation and transdifferentiation, and the role of HSCs in promoting HCC is widely acknowledged (Amann et al., 2009; Barry et al., 2020; Dapito and Schwabe, 2015). Therefore it is possible that shorter OS in SEMA3C high-expressing HCC patients originates from HSC activation and thus HCC progression, vascularization, growth, and immune escape (**Figure 5**). It would be interesting to investigate comparable effects of SEMA3C in HCC cells to answer the question to what extent SEMA3C influences HCC development and uncover potential underlying mechanisms. Also, the role of other class 3 SEMAs should be evaluated. For example, SEMA3F and SEMA3B are known to contribute to tumor suppression and are downregulated in tumor entities such as breast neoplasia (Staton et al., 2011), melanoma (Bielenberg et al., 2004), and lung cancer (Lantuéjoul et al., 2003).

4.6 Study limitations

HSC activation has been studied *in vitro* with primary, isolated HSCs for a long time, simulating the HSC activation process *in vivo*. This model sufficiently upregulates characteristic activation markers and induces classic morphological changes like the loss of retinoid vacuoles. However, the *in vitro* activation process in a monoculture setting exposes primary HSCs to a somewhat unphysiological setting due to the lack of other parenchymal and non-parenchymal hepatic cell types, thus lacking interaction with these different cell types and the overwhelming effect of plastic and cell culture medium induced stimulation to the cultured HSCs (Mederacke et al., 2015). *In vitro* and *ex vivo* cell culture experiments that evaluate the activation of HSCs might therefore deliver slightly altered results due to unphysiological HSC environment and culture conditions. At the same time inhibitory effects, such as the deletion of SEMA3C and NRP2, are still regarded to display actual pathophysiological effect quite precisely. (Mederacke et al., 2015).

Regarding the GSEA, enrichment results were obtained from cirrhotic collectives. Cirrhosis is the end stage of fibrosis in most cases. However, enrichment data of fibrotic patients would of course display changes in actual fibrosis more precisely. Still it seems natural and justifiable to draw above-made conclusions from cirrhotic patients about enrichment and disease severity in fibrosis as well.

4.7 Conclusion and outlook

Proteins from the Semaphorin family are known to contribute, aggravate, and modulate fibrotic processes and diseases (Jeon et al., 2020; Peng et al., 2015; Reilkoff et al., 2013). This MD thesis project focused on understanding the potential role of Semaphorin 3C as a novel marker and promoter for the activation and transdifferentiation of hepatic stellate cells, ultimately leading to liver fibrosis. The project's working hypothesis was that Semaphorin 3C mediates and aggravates liver fibrosis by amplifying hepatic stellate cells activation and transdifferentiation.

The three main aims of this thesis and study were met as follows:

- I. **Correlation in patients:** *Semaphorin 3C is enriched in fibrotic patients, and high Semaphorin 3C expression in patients correlates with higher enrichment of typical fibrosis and cirrhosis marker genes.*
- II. **Mechanism in GRX cell line:** *Semaphorin 3C exacerbates TGF- β signaling and subsequently TGF- β related gene expression of activation and transdifferentiation markers, indicating Semaphorin 3C to be a driver for HSC activation, myofibroblast transdifferentiation, and thus liver fibrosis promotion.*
- III. **Effect confirmation in primary hepatic stellate cells:** *Semaphorin 3C's exacerbating effect on activation and transdifferentiation in GRX cells was confirmed in primary, isolated hepatic stellate cells. Semaphorin 3C is upregulated in activated primary hepatic stellate cells. Upon Semaphorin 3C knockout, primary HSCs show lower expression of activation and transdifferentiation markers. Upon Neuropilin 2 knockout, primary HSCs also show lower levels of activation and transdifferentiation markers.*

Considering these findings, this study identifies Semaphorin 3C as a novel marker and, more importantly, mediator for hepatic stellate cell activation and transdifferentiation and liver fibrosis. Semaphorin 3C augments TGF- β signaling and its downstream transduction via SMAD2/3 *in vitro* in GRX cells. Upon deletion of SEMA3C respectively

NRP2 in *ex vivo* experiments with primary HSCs, HSCs are less activated and show a weaker myofibroblast phenotype.

Presented results lay the foundation for SEMA3C to be investigated as a potential therapeutic target inhibiting hepatic stellate cell activation and transdifferentiation. NRP2 serves as an additional potential target, indirectly inhibiting SEMA3C signaling. It will be crucial to confirm the obtained results in murine fibrosis models and further rescue experiments. In the future it will be of interest to further investigate Semaphorin 3C dynamics in patients upon inflammation or injury as a stimulus.

As Semaphorin 3C also appears to correlate with overall survival in patients with hepatocellular carcinoma, it will be interesting to perform experiments on hepatocellular carcinoma cell lines and analyze biopsies of HCC patients with regard to Semaphorin 3C levels and their impact on hepatocellular carcinoma.

5 SUMMARY

In the developed world, close to 45% of all deaths are related to fibroproliferative pathologies with liver fibrosis, and in course, cirrhosis is one of the leading causes amongst those death numbers. Liver fibrosis is a pathological state arising from the organ's wound healing process, answering to liver injury and chronic inflammation. Constant inflammatory stimuli lead to excessive extracellular matrix secretion resulting in impaired metabolic and synthetic function. Ultimately the fibrosis progresses into liver cirrhosis, hepatocellular carcinoma, organ failure, and eventually even the patient's death. The activation and myofibroblast differentiation of hepatic stellate cells is a primary driver of fibrosis. To identify potential antifibrotic therapy targets, it is crucial to understand and further investigate the activation processes of hepatic stellate cells. One of the key drivers in hepatic stellate cell activation is TGF- β signaling, which is well known to mediate myofibroblast differentiation and extracellular matrix accumulation. Semaphorins are a group of secreted, membrane standing and transmembrane proteins influencing axonal guiding, angiogenesis, immune modulation. One member of this family is Semaphorin 3C, a secreted protein that binds to the extracellular matrix and signals through Neuropilin receptors 1 and 2.

Analysis of publicly available patient data sets confirmed that the Semaphorin 3C expression correlates with a worse fibrotic state. This correlation suggests a pivotal role of Semaphorin 3C in the development and progression of liver fibrosis. Given the critical role of hepatic stellate cells in fibrosis, the suspected role of Semaphorin 3C and its receptors in GRX cells (hepatic stellate cells derived cell line) and freshly isolated, primary hepatic stellate cells were analyzed to understand the potential role of Semaphorin3C in hepatic stellate cell activation further. Freshly isolated, primary hepatic stellate cells upregulate Semaphorin 3C, maintain Neuropilin 2 and downregulate Neuropilin 1 and Plexin D1 upon culture-induced activation, indicating Semaphorin 3C to be a marker for hepatic stellate cell activation.

To understand to what extent it mediates activation and transdifferentiation, Semaphorin 3C was overexpressed in GRX cells. *In vitro* overexpression exacerbates TGF- β response and augments SMAD2/3 phosphorylation. Characteristic, TGF- β related activation and transdifferentiation markers are upregulated in consequence. Neuropilin 2 is maintained in activated hepatic stellate cells, indicating Neuropilin 2-

Semaphorin 3C interaction to mediate the exacerbated TGF- β response. Upon deletion of Semaphorin 3C in primary, isolated hepatic stellate cells and their subsequent activation by culture time, lower levels of activation, and transdifferentiation markers such as *Acta2* (α SMA), *Pai-1*, *Tagln* (SM22 α) and *S100a6* are expressed. Deletion of Neuropilin 2 in primary, isolated hepatic stellate cells goes in hand with these observations, showing lower levels of activation and transdifferentiation markers than littermate controls. Ultimately Semaphorin 3C expression level is observed to correlate with shorter overall survival in hepatocellular carcinoma patients, indicating a potentially extended role of Semaphorin 3C not only in hepatic stellate cells in primary fibrosis but also hepatocellular carcinoma and carcinoma associated fibrosis.

The study postulates Neuropilin 2 - dependent modulation of TGF- β signaling in hepatic stellate cells by Semaphorin 3C to be the underlying, mechanistic foundation of the effect of Semaphorin 3C. This study identifies Semaphorin 3C as a novel marker and, more importantly, mediator for hepatic stellate cell activation and transdifferentiation and liver fibrosis. Also, it suggests a potential role of Semaphorin 3C in hepatocellular carcinoma progression.

6 ZUSAMMENFASSUNG

Fast 45 % aller Todesfälle in Industrieländern sind auf fibroproliferative Pathologien zurückzuführen, wobei Leberfibrose und in Folge die Leberzirrhose eine der Hauptursachen für diese Todesfälle sind. Leberfibrose ist ein pathologischer Zustand, der sich aus dem Wundheilungsprozess des Organs als Reaktion auf Leberverletzungen und chronische Entzündungen ergibt. Ständige Entzündungsreize führen zu einer übermäßigen Sekretion extrazellulärer Matrix, was zu einer Beeinträchtigung der metabolischen und synthetischen Funktion führt. Letztendlich führt die Leberfibrose zu Leberzirrhose, hepatozellulärem Karzinom, Organversagen und schließlich sogar zum Tod des Patienten. Es ist bekannt, dass die Aktivierung und myofibroblastische Differenzierung hepatischer Sternzellen eine der Hauptursachen für Leberfibrose ist. Für die Identifizierung potenziell antifibrotischer Therapieziele ist es daher von entscheidender Bedeutung, die Aktivierungsprozesse hepatischer Sternzellen zu verstehen und weiter zu untersuchen. Einer der wichtigsten Faktoren im Rahmen der Aktivierung hepatischer Sternzellen ist der TGF- β -Signalweg, der bekanntermaßen die Differenzierung von Myofibroblasten und die Akkumulation extrazellulärer Matrix vermittelt. Semaphorine sind eine Gruppe sekretierter, membranständiger und transmembranöser Proteine, die die axonale Entwicklung und Sprossung, Angiogenese und Immunmodulation beeinflussen. Ein Mitglied dieser Familie ist Semaphorin 3C, ein sekretiertes Protein, das an die extrazelluläre Matrix bindet und über Plexine und Neuropilin-Rezeptoren 1 und 2 Signale sendet.

Die Analyse veröffentlichter Patientendatensätze bestätigte, dass die Semaphorin 3C-Expression mit einem schlechteren fibrotischen Verlauf und Zustand der Patienten korreliert. Diese Korrelation deutet auf eine zentrale Rolle von Semaphorin 3C bei der Entwicklung und dem Fortschreiten der Leberfibrose hin. In Anbetracht der entscheidenden Rolle hepatischer Sternzellen im Rahmen von Leberfibrose wurde die vermutete Rolle Semaphorin 3Cs und seiner Rezeptoren in GRX-Zellen (von hepatischen Sternzellen abgeleitete Zelllinie) und frisch isolierten, primären hepatischen Sternzellen analysiert, um die potenzielle Rolle von Semaphorin 3C im Rahmen der Aktivierung hepatischer Sternzellen besser zu verstehen. Bei Zellkultur induzierter Aktivierung frisch isolierter, primärer hepatischer Sternzellen, regulieren diese die Expression Semaphorin 3Cs hoch, exprimieren weiterhin Neuropilin 2 und

regulieren die Expression von Neuropilin 1 und Plexin D1 bei kulturinduzierter Aktivierung herunter. Dies deutet darauf hin, dass Semaphorin 3C ein Marker für die Aktivierung und Transdifferenzierung hepatischer Sternzellen ist.

Um zu verstehen, inwieweit Semaphorin 3C die Aktivierung und Transdifferenzierung vermittelt, wurde Semaphorin 3C in GRX-Zellen überexprimiert. *In vitro* verstärkt die Überexpression Semaphorin 3Cs die TGF- β -Antwort und steigert die SMAD2/3-Phosphorylierung. Charakteristische, TGF- β -bezogene Aktivierungs- und Transdifferenzierungsmarker werden in Folge hochreguliert. Neuropilin 2 wird in aktivierten hepatischen Sternzellen weiterhin exprimiert, was darauf hindeutet, dass die Interaktion zwischen Neuropilin 2 und Semaphorin 3C die verstärkte TGF-Antwort vermittelt. Nach Deletion von Semaphorin 3C in primären, isolierten hepatischen Sternzellen und ihrer anschließenden Aktivierung durch Kulturzeit werden niedrigere Aktivierungsniveaus und Transdifferenzierungsmarker wie *Acta2* (α SMA), *Pai-1*, *Tagln* (SM22 α) und *S100a6* exprimiert. Die Deletion von Neuropilin 2 in primären, isolierten hepatischen Sternzellen geht mit ähnlichen Beobachtungen einher: auch in diesem Fall zeigen sich niedrigere Werte von Aktivierungs- und Transdifferenzierungsmarkern als in den jeweiligen Kontrollen. Schließlich wird beobachtet, dass die Semaphorin 3C - Expression mit einem kürzeren Gesamtüberleben bei Patienten mit hepatozellulärem Karzinom korreliert, was auf eine mögliche erweiterte Rolle Semaphorin 3Cs, nicht nur im Rahmen von Leberfibrose, sondern auch bei der Genese von hepatozellulärem Karzinom und karzinomassoziiertes Fibrose hindeutet.

Die vorliegende Dissertation postuliert, dass die Neuropilin-abhängige Modulation der TGF- β -Signalübertragung in hepatischen Sternzellen durch Semaphorin 3C die zugrundeliegende, mechanistische Grundlage für die Wirkung von Semaphorin 3C ist. Diese Studie identifiziert Semaphorin 3C als einen neuartigen Marker und als Mediator für die Aktivierung und Transdifferenzierung hepatischer Sternzellen und letztendlich die Entstehung und das Voranschreiten von Leberfibrose. Außerdem deutet sie auf eine mögliche Rolle von Semaphorin 3C bei der Progression des hepatozellulären Karzinoms hin.

7 REFERENCES

Adams, R.H., Lohrum, M., Klostermann, A., Betz, H., and Püschel, A.W. (1997). The chemorepulsive activity of secreted semaphorins is regulated by furin-dependent proteolytic processing. *EMBO J* 16, 6077-6086. [10.1093/emboj/16.20.6077](https://doi.org/10.1093/emboj/16.20.6077)

Amann, T., Bataille, F., Spruss, T., Mühlbauer, M., Gäbele, E., Schölmerich, J., Kiefer, P., Bosserhoff, A.K., and Hellerbrand, C. (2009). Activated hepatic stellate cells promote tumorigenicity of hepatocellular carcinoma. *Cancer Sci* 100, 646-653. [10.1111/j.1349-7006.2009.01087.x](https://doi.org/10.1111/j.1349-7006.2009.01087.x)

Appenrodt, B., and Lammert, F. (2018). Renal Failure in Patients with Liver Cirrhosis: Novel Classifications, Biomarkers, Treatment. *Visc Med* 34, 246-252. [10.1159/000492587](https://doi.org/10.1159/000492587)

Apte, R.S., Chen, D.S., and Ferrara, N. (2019). VEGF in Signaling and Disease: Beyond Discovery and Development. *Cell* 176, 1248-1264. <https://doi.org/10.1016/j.cell.2019.01.021>

Arthur, M.J., Friedman, S.L., Roll, F.J., and Bissell, D.M. (1989). Lipocytes from normal rat liver release a neutral metalloproteinase that degrades basement membrane (type IV) collagen. *J Clin Invest* 84, 1076-1085. [10.1172/jci114270](https://doi.org/10.1172/jci114270)

Asahina, K., Tsai, S.Y., Li, P., Ishii, M., Maxson, R.E., Jr., Sucov, H.M., and Tsukamoto, H. (2009). Mesenchymal origin of hepatic stellate cells, submesothelial cells, and perivascular mesenchymal cells during mouse liver development. *Hepatology* 49, 998-1011. [10.1002/hep.22721](https://doi.org/10.1002/hep.22721)

Asahina, K., Zhou, B., Pu, W.T., and Tsukamoto, H. (2011). Septum transversum-derived mesothelium gives rise to hepatic stellate cells and perivascular mesenchymal cells in developing mouse liver. *Hepatology* 53, 983-995. <https://doi.org/10.1002/hep.24119>

Asrani, S.K., Devarbhavi, H., Eaton, J., and Kamath, P.S. (2019). Burden of liver diseases in the world. *J Hepatol* 70, 151-171. <https://doi.org/10.1016/j.jhep.2018.09.014>

Bagnard, D., Lohrum, M., Uziel, D., Püschel, A.W., and Bolz, J. (1998). Semaphorins act as attractive and repulsive guidance signals during the development of cortical projections. *Development* 125, 5043-5053.

Barry, A.E., Baldeosingh, R., Lamm, R., Patel, K., Zhang, K., Dominguez, D.A., Kirton, K.J., Shah, A.P., and Dang, H. (2020). Hepatic Stellate Cells and Hepatocarcinogenesis. *Front Cell Dev Biol* 8, 709. [10.3389/fcell.2020.00709](https://doi.org/10.3389/fcell.2020.00709)

Bataller, R., and Brenner, D.A. (2005). Liver fibrosis. *The Journal of clinical investigation* 115, 209-218. 10.1172/JCI24282

Benvegnù, L., Gios, M., Boccato, S., and Alberti, A. (2004). Natural history of compensated viral cirrhosis: a prospective study on the incidence and hierarchy of major complications. *Gut* 53, 744-749. 10.1136/gut.2003.020263

Bielenberg, D.R., Hida, Y., Shimizu, A., Kaipainen, A., Kreuter, M., Kim, C.C., and Klagsbrun, M. (2004). Semaphorin 3F, a chemorepellent for endothelial cells, induces a poorly vascularized, encapsulated, nonmetastatic tumor phenotype. *J Clin Invest* 114, 1260-1271. 10.1172/jci21378

Borojevic, R., Monteiro, A.N., Vinhas, S.A., Domont, G.B., Mourão, P.A., Emonard, H., Grimaldi, G., Jr., and Grimaud, J.A. (1985). Establishment of a continuous cell line from fibrotic schistosomal granulomas in mice livers. *In Vitro Cell Dev Biol* 21, 382-390. 10.1007/bf02623469

Bosoi, C.R., and Rose, C.F. (2013). Brain edema in acute liver failure and chronic liver disease: Similarities and differences. *Neurochem Int* 62, 446-457. <https://doi.org/10.1016/j.neuint.2013.01.015>

Bray, F., Ferlay, J., Soerjomataram, I., Siegel, R.L., Torre, L.A., and Jemal, A. (2018). Global cancer statistics 2018: GLOBOCAN estimates of incidence and mortality worldwide for 36 cancers in 185 countries. *CA Cancer J Clin* 68, 394-424. 10.3322/caac.21492

Cao, S., Yaqoob, U., Das, A., Shergill, U., Jagavelu, K., Huebert, R.C., Routray, C., Abdelmoneim, S., Vasdev, M., Leof, E., *et al.* (2010). Neuropilin-1 promotes cirrhosis of the rodent and human liver by enhancing PDGF/TGF-beta signaling in hepatic stellate cells. *J Clin Invest* 120, 2379-2394. 10.1172/jci41203

Carthy, J.M. (2018). TGFβ signaling and the control of myofibroblast differentiation: Implications for chronic inflammatory disorders. *J Cell Physiol* 233, 98-106. 10.1002/jcp.25879

Chang, Y., and Li, H. (2020). Hepatic Antifibrotic Pharmacotherapy: Are We Approaching Success? *J Clin Transl Hepatol* 8, 222-229. 10.14218/jcth.2020.00026

Cubellis, M.V., Andreasen, P., Ragno, P., Mayer, M., Danø, K., and Blasi, F. (1989). Accessibility of receptor-bound urokinase to type-1 plasminogen activator inhibitor. *Proc Natl Acad Sci U S A* 86, 4828-4832. 10.1073/pnas.86.13.4828

D'Ambrosio, R., Aghemo, A., Rumi, M.G., Ronchi, G., Donato, M.F., Paradis, V., Colombo, M., and Bedossa, P. (2012). A morphometric and immunohistochemical study to assess the benefit of a sustained virological response in hepatitis C virus patients with cirrhosis. *Hepatology* 56, 532-543. 10.1002/hep.25606

Dapito, D.H., and Schwabe, R.F. (2015). Chapter 9 - Hepatic Stellate Cells and Liver Cancer. In *Stellate Cells in Health and Disease*, C.R. Gandhi, and M. Pinzani, eds. (Boston: Academic Press), pp. 145-162.

de Gouville, A.C., Boullay, V., Krysa, G., Pilot, J., Brusq, J.M., Loriolle, F., Gauthier, J.M., Papworth, S.A., Laroze, A., Gellibert, F., *et al.* (2005). Inhibition of TGF-beta signaling by an ALK5 inhibitor protects rats from dimethylnitrosamine-induced liver fibrosis. *Br J Pharmacol* 145, 166-177. 10.1038/sj.bjp.0706172

De Minicis, S., Seki, E., Uchinami, H., Kluwe, J., Zhang, Y., Brenner, D.A., and Schwabe, R.F. (2007). Gene expression profiles during hepatic stellate cell activation in culture and in vivo. *Gastroenterology* 132, 1937-1946. 10.1053/j.gastro.2007.02.033

De Winter, F., Holtmaat, A.J., and Verhaagen, J. (2002). Neuropilin and class 3 semaphorins in nervous system regeneration. *Adv Exp Med Biol* 515, 115-139. 10.1007/978-1-4615-0119-0_10

DeLeve, L.D. (2011). Vascular Liver Disease and the Liver Sinusoidal Endothelial Cell. In *Vascular Liver Disease: Mechanisms and Management*, L.D. DeLeve, and G. Garcia-Tsao, eds. (New York, NY: Springer New York), pp. 25-40.

Derynck, R., and Budi Erine, H. (2019). Specificity, versatility, and control of TGF- β family signaling. *Science Signaling* 12, eaav5183. 10.1126/scisignal.aav5183

Dewidar, B., Meyer, C., Dooley, S., and Meindl-Beinker, A.N. (2019). TGF- β in Hepatic Stellate Cell Activation and Liver Fibrogenesis-Updated 2019. *Cells* 8. 10.3390/cells8111419

Dong, C., Zhu, S., Wang, T., Yoon, W., and Goldschmidt-Clermont, P.J. (2002). Upregulation of PAI-1 is mediated through TGF-beta/Smad pathway in transplant arteriopathy. *J Heart Lung Transplant* 21, 999-1008. 10.1016/s1053-2498(02)00403-5

Duncan, M.R., Frazier, K.S., Abramson, S., Williams, S., Klapper, H., Huang, X., and Grotendorst, G.R. (1999). Connective tissue growth factor mediates transforming growth factor beta-induced collagen synthesis: down-regulation by cAMP. *FASEB J* 13, 1774-1786.

El Taghdouini, A., Najimi, M., Sancho-Bru, P., Sokal, E., and van Grunsven, L.A. (2015). In vitro reversion of activated primary human hepatic stellate cells. *Fibrogenesis Tissue Repair* 8, 14. 10.1186/s13069-015-0031-z

Ellis, E.L., and Mann, D.A. (2012). Clinical evidence for the regression of liver fibrosis. *J Hepatol* 56, 1171-1180. 10.1016/j.jhep.2011.09.024

Esselens, C., Malapeira, J., Colomé, N., Casal, C., Rodríguez-Manzaneque, J.C., Canals, F., and Arribas, J. (2010). The cleavage of semaphorin 3C induced by

ADAMTS1 promotes cell migration. *J Biol Chem* 285, 2463-2473. 10.1074/jbc.M109.055129

Fabregat, I., Moreno-Càceres, J., Sánchez, A., Dooley, S., Dewidar, B., Giannelli, G., and Ten Dijke, P. (2016). TGF- β signalling and liver disease. *Febs j* 283, 2219-2232. 10.1111/febs.13665

Falk, J., Bechara, A., Fiore, R., Nawabi, H., Zhou, H., Hoyo-Becerra, C., Bozon, M., Rougon, G., Grumet, M., Püschel, A.W., *et al.* (2005). Dual functional activity of semaphorin 3B is required for positioning the anterior commissure. *Neuron* 48, 63-75. 10.1016/j.neuron.2005.08.033

Fattovich, G., Giustina, G., Degos, F., Tremolada, F., Diodati, G., Almasio, P., Nevens, F., Solinas, A., Mura, D., Brouwer, J.T., *et al.* (1997). Morbidity and mortality in compensated cirrhosis type C: A retrospective follow-up study of 384 patients. *Gastroenterology* 112, 463-472. <https://doi.org/10.1053/gast.1997.v112.pm9024300>

Fattovich, G., Stroffolini, T., Zagni, I., and Donato, F. (2004). Hepatocellular carcinoma in cirrhosis: incidence and risk factors. *Gastroenterology* 127, S35-50. 10.1053/j.gastro.2004.09.014

Feiner, L., Webber, A.L., Brown, C.B., Lu, M.M., Jia, L., Feinstein, P., Mombaerts, P., Epstein, J.A., and Raper, J.A. (2001). Targeted disruption of semaphorin 3C leads to persistent truncus arteriosus and aortic arch interruption. *Development* 128, 3061-3070.

Ferrell, L. (2000). Liver Pathology: Cirrhosis, Hepatitis, and Primary Liver Tumors. Update and Diagnostic Problems. *Mod Pathol* 13, 679-704. 10.1038/modpathol.3880119

Friedman, S.L. (2003). Liver fibrosis – from bench to bedside. *J Hepatol* 38, 38-53. [https://doi.org/10.1016/S0168-8278\(02\)00429-4](https://doi.org/10.1016/S0168-8278(02)00429-4)

Friedman, S.L. (2008). Mechanisms of hepatic fibrogenesis. *Gastroenterology* 134, 1655-1669. 10.1053/j.gastro.2008.03.003

Friedman, S.L., Rockey, D.C., McGuire, R.F., Maher, J.J., Boyles, J.K., and Yamasaki, G. (1992). Isolated hepatic lipocytes and Kupffer cells from normal human liver: morphological and functional characteristics in primary culture. *Hepatology* 15, 234-243. 10.1002/hep.1840150211

Friedman, S.L., and Roll, F.J. (1987). Isolation and culture of hepatic lipocytes, Kupffer cells, and sinusoidal endothelial cells by density gradient centrifugation with Stractan. *Anal Biochem* 161, 207-218. 10.1016/0003-2697(87)90673-7

Friedman, S.L., Roll, F.J., Boyles, J., and Bissell, D.M. (1985). Hepatic lipocytes: the principal collagen-producing cells of normal rat liver. *Proc Natl Acad Sci U S A* 82, 8681-8685. 10.1073/pnas.82.24.8681

- Gard, A.L., White, F.P., and Dutton, G.R. (1985). Extra-neural glial fibrillary acidic protein (GFAP) immunoreactivity in perisinusoidal stellate cells of rat liver. *J Neuroimmunol* 8, 359-375. [10.1016/s0165-5728\(85\)80073-4](https://doi.org/10.1016/s0165-5728(85)80073-4)
- Geerts, A. (2001). History, heterogeneity, developmental biology, and functions of quiescent hepatic stellate cells. *Semin Liver Dis* 21, 311-335. [10.1055/s-2001-17550](https://doi.org/10.1055/s-2001-17550)
- Giampieri, M.P., Jezequel, A.M., and Orlandi, F. (1981). The lipocytes in normal human liver. A quantitative study. *Digestion* 22, 165-169. [10.1159/000198640](https://doi.org/10.1159/000198640)
- Ginès, P., and Schrier, R.W. (2009). Renal failure in cirrhosis. *N Engl J Med* 361, 1279-1290. [10.1056/NEJMra0809139](https://doi.org/10.1056/NEJMra0809139)
- Gitler, A.D., Lu, M.M., and Epstein, J.A. (2004). PlexinD1 and Semaphorin Signaling Are Required in Endothelial Cells for Cardiovascular Development. *Dev Cell* 7, 107-116. <https://doi.org/10.1016/j.devcel.2004.06.002>
- Glinka, Y., and Prud'homme, G.J. (2008). Neuropilin-1 is a receptor for transforming growth factor beta-1, activates its latent form, and promotes regulatory T cell activity. *J Leukoc Biol* 84, 302-310. [10.1189/jlb.0208090](https://doi.org/10.1189/jlb.0208090)
- Glinka, Y., Stoilova, S., Mohammed, N., and Prud'homme, G.J. (2011). Neuropilin-1 exerts co-receptor function for TGF-beta-1 on the membrane of cancer cells and enhances responses to both latent and active TGF-beta. *Carcinogenesis* 32, 613-621. [10.1093/carcin/bgq281](https://doi.org/10.1093/carcin/bgq281)
- Goodman, C.S., Kolodkin, A.L., Luo, Y., Püschel, A.W., and Raper, J.A. (1999). Unified Nomenclature for the Semaphorins/Collapsins. *Cell* 97, 551-552. [https://doi.org/10.1016/S0092-8674\(00\)80766-7](https://doi.org/10.1016/S0092-8674(00)80766-7)
- Grandclement, C., Pallandre, J.R., Valmary Degano, S., Viel, E., Bouard, A., Balland, J., Rémy-Martin, J.-P., Simon, B., Rouleau, A., Boireau, W., *et al.* (2011a). Neuropilin-2 Expression Promotes TGF- β 1-Mediated Epithelial to Mesenchymal Transition in Colorectal Cancer Cells. *PLoS One* 6, e20444. [10.1371/journal.pone.0020444](https://doi.org/10.1371/journal.pone.0020444)
- Grandclement, C., Pallandre, J.R., Valmary Degano, S., Viel, E., Bouard, A., Balland, J., Rémy-Martin, J.P., Simon, B., Rouleau, A., Boireau, W., *et al.* (2011b). Neuropilin-2 expression promotes TGF- β 1-mediated epithelial to mesenchymal transition in colorectal cancer cells. *PLoS One* 6, e20444. [10.1371/journal.pone.0020444](https://doi.org/10.1371/journal.pone.0020444)
- Gressner, A.M., Weiskirchen, R., Breitkopf, K., and Dooley, S. (2002). Roles of TGF-beta in hepatic fibrosis. *Front Biosci* 7, d793-807. [10.2741/a812](https://doi.org/10.2741/a812)
- Gu, C., Yoshida, Y., Livet, J., Reimert, D.V., Mann, F., Merte, J., Henderson, C.E., Jessell, T.M., Kolodkin, A.L., and Ginty, D.D. (2005). Semaphorin 3E and plexin-D1 control vascular pattern independently of neuropilins. *Science* 307, 265-268. [10.1126/science.1105416](https://doi.org/10.1126/science.1105416)

Gupta, T.K., Toruner, M., Chung, M.K., and Groszmann, R.J. (1998). Endothelial dysfunction and decreased production of nitric oxide in the intrahepatic microcirculation of cirrhotic rats. *Hepatology* 28, 926-931. 10.1002/hep.510280405

Guttmann-Raviv, N., Shraga-Heled, N., Varshavsky, A., Guimaraes-Sternberg, C., Kessler, O., and Neufeld, G. (2007). Semaphorin-3A and semaphorin-3F work together to repel endothelial cells and to inhibit their survival by induction of apoptosis. *J Biol Chem* 282, 26294-26305. 10.1074/jbc.M609711200

Györfy, B. (2021). Survival analysis across the entire transcriptome identifies biomarkers with the highest prognostic power in breast cancer. *Computational and Structural Biotechnology Journal* 19, 4101-4109. <https://doi.org/10.1016/j.csbj.2021.07.014>

Hao, J., and Yu, J.S. (2018). Semaphorin 3C and Its Receptors in Cancer and Cancer Stem-Like Cells. *Biomedicines* 6. 10.3390/biomedicines6020042

Harvey, A. (2012). Receptor complexes for each of the Class 3 Semaphorins. *Front Cell Neurosci* 6. 10.3389/fncel.2012.00028

Hasegawa, D., Wallace, M.C., and Friedman, S.L. (2015). Chapter 4 - Stellate Cells and Hepatic Fibrosis. In *Stellate Cells in Health and Disease*, C.R. Gandhi, and M. Pinzani, eds. (Boston: Academic Press), pp. 41-62.

Hazra, S., Xiong, S., Wang, J., Rippe, R.A., Krishna, V., Chatterjee, K., and Tsukamoto, H. (2004). Peroxisome proliferator-activated receptor gamma induces a phenotypic switch from activated to quiescent hepatic stellate cells. *J Biol Chem* 279, 11392-11401. 10.1074/jbc.M310284200

He, Z., and Tessier-Lavigne, M. (1997). Neuropilin Is a Receptor for the Axonal Chemorepellent Semaphorin III. *Cell* 90, 739-751. 10.1016/S0092-8674(00)80534-6

Heldin, C.-H., Miyazono, K., and ten Dijke, P. (1997). TGF- β signalling from cell membrane to nucleus through SMAD proteins. *Nature* 390, 465-471. 10.1038/37284

Heldin, C.-H., and Moustakas, A. (2016). Signaling Receptors for TGF- β Family Members. *Cold Spring Harb Perspect Biol* 8, a022053. 10.1101/cshperspect.a022053

Heldin, P., Pertoft, H., Nordlinder, H., Heldin, C.H., and Laurent, T.C. (1991). Differential expression of platelet-derived growth factor alpha- and beta- receptors on fat-storing cells and endothelial cells of rat liver. *Exp Cell Res* 193, 364-369. 10.1016/0014-4827(91)90108-7

Helmy, A., Jalan, R., Newby, D.E., Hayes, P.C., and Webb, D.J. (2000). Role of angiotensin II in regulation of basal and sympathetically stimulated vascular tone in early and advanced cirrhosis. *Gastroenterology* 118, 565-572. 10.1016/s0016-5085(00)70263-0

Hendriks, H.F., Verhoofstad, W.A., Brouwer, A., de Leeuw, A.M., and Knook, D.L. (1985). Perisinusoidal fat-storing cells are the main vitamin A storage sites in rat liver. *Exp Cell Res* 160, 138-149. 10.1016/0014-4827(85)90243-5

Herman, J.G., and Meadows, G.G. (2007). Increased class 3 semaphorin expression modulates the invasive and adhesive properties of prostate cancer cells. *Int J Oncol* 30, 1231-1238.

Herrmann, J., Gressner, A.M., and Weiskirchen, R. (2007). Immortal hepatic stellate cell lines: useful tools to study hepatic stellate cell biology and function? *J Cell Mol Med* 11, 704-722. 10.1111/j.1582-4934.2007.00060.x

Higashi, T., Friedman, S.L., and Hoshida, Y. (2017). Hepatic stellate cells as key target in liver fibrosis. *Adv Drug Deliv Rev* 121, 27-42. 10.1016/j.addr.2017.05.007

Hill, C.S. (2016). Transcriptional Control by the SMADs. *Cold Spring Harb Perspect Biol* 8. 10.1101/cshperspect.a022079

Hu, B., Wu, Z., and Phan, S.H. (2003). Smad3 mediates transforming growth factor-beta-induced alpha-smooth muscle actin expression. *Am J Respir Cell Mol Biol* 29, 397-404. 10.1165/rcmb.2003-0063OC

Huse, M., Chen, Y.G., Massagué, J., and Kuriyan, J. (1999). Crystal structure of the cytoplasmic domain of the type I TGF beta receptor in complex with FKBP12. *Cell* 96, 425-436. 10.1016/s0092-8674(00)80555-3

Irigoyen, J.P., Muñoz-Cánoves, P., Montero, L., Koziczak, M., and Nagamine, Y. (1999). The plasminogen activator system: biology and regulation. *Cell Mol Life Sci* 56, 104-132. 10.1007/pl00000615

Jalan, R., Gines, P., Olson, J.C., Mookerjee, R.P., Moreau, R., Garcia-Tsao, G., Arroyo, V., and Kamath, P.S. (2012). Acute-on chronic liver failure. *J Hepatol* 57, 1336-1348. 10.1016/j.jhep.2012.06.026

Jeon, K.I., Nehrke, K., and Huxlin, K.R. (2020). Semaphorin 3A potentiates the profibrotic effects of transforming growth factor- β 1 in the cornea. *Biochem Biophys Res Commun* 521, 333-339. 10.1016/j.bbrc.2019.10.107

Jepsen, P., Ott, P., Andersen, P.K., Sørensen, H.T., and Vilstrup, H. (2010). Clinical course of alcoholic liver cirrhosis: a Danish population-based cohort study. *Hepatology* 51, 1675-1682. 10.1002/hep.23500

Jiang, Q., Arnold, S., Heanue, T., Kilambi, K.P., Doan, B., Kapoor, A., Ling, A.Y., Sosa, M.X., Guy, M., Jiang, Q., *et al.* (2015). Functional loss of semaphorin 3C and/or semaphorin 3D and their epistatic interaction with *ret* are critical to Hirschsprung disease liability. *Am J Hum Genet* 96, 581-596. 10.1016/j.ajhg.2015.02.014

- Jiao, B., Liu, S., Tan, X., Lu, P., Wang, D., and Xu, H. (2021). Class-3 semaphorins: Potent multifunctional modulators for angiogenesis-associated diseases. *Biomed Pharmacother* 137, 111329. 10.1016/j.biopha.2021.111329
- Kim, S.U., Seo, Y.S., Lee, H.A., Kim, M.N., Lee, Y.R., Lee, H.W., Park, J.Y., Kim, D.Y., Ahn, S.H., Han, K.H., *et al.* (2019). A multicenter study of entecavir vs. tenofovir on prognosis of treatment-naïve chronic hepatitis B in South Korea. *J Hepatol* 71, 456-464. 10.1016/j.jhep.2019.03.028
- Kisseleva, T., and Brenner, D. (2021). Molecular and cellular mechanisms of liver fibrosis and its regression. *Nat Rev Gastroenterol Hepatol* 18, 151-166. 10.1038/s41575-020-00372-7
- Kisseleva, T., Cong, M., Paik, Y., Scholten, D., Jiang, C., Benner, C., Iwaisako, K., Moore-Morris, T., Scott, B., Tsukamoto, H., *et al.* (2012). Myofibroblasts revert to an inactive phenotype during regression of liver fibrosis. *Proc Natl Acad Sci U S A* 109, 9448-9453. 10.1073/pnas.1201840109
- Kitamura, Y., and Ninomiya, H. (2003). Smad expression of hepatic stellate cells in liver cirrhosis in vivo and hepatic stellate cell line in vitro. *Pathol Int* 53, 18-26. 10.1046/j.1440-1827.2003.01431.x
- Klaas, M., Kangur, T., Viil, J., Mäemets-Allas, K., Minajeva, A., Vadi, K., Antsov, M., Lapidus, N., Järvekülg, M., and Jaks, V. (2016). The alterations in the extracellular matrix composition guide the repair of damaged liver tissue. *Sci Rep* 6, 27398. 10.1038/srep27398
- Klagsbrun, M., Takashima, S., and Mamluk, R. (2002). The role of neuropilin in vascular and tumor biology. *Adv Exp Med Biol* 515, 33-48. 10.1007/978-1-4615-0119-0_3
- Knittel, T., Mehde, M., Kobold, D., Saile, B., Dinter, C., and Ramadori, G. (1999). Expression patterns of matrix metalloproteinases and their inhibitors in parenchymal and non-parenchymal cells of rat liver: regulation by TNF-alpha and TGF-beta1. *J Hepatol* 30, 48-60. 10.1016/s0168-8278(99)80007-5
- Kolodkin, A.L., Matthes, D.J., and Goodman, C.S. (1993). The semaphorin genes encode a family of transmembrane and secreted growth cone guidance molecules. *Cell* 75, 1389-1399. 10.1016/0092-8674(93)90625-z
- Krenkel, O., Hundertmark, J., Ritz, T.P., Weiskirchen, R., and Tacke, F. (2019). Single Cell RNA Sequencing Identifies Subsets of Hepatic Stellate Cells and Myofibroblasts in Liver Fibrosis. *Cells* 8. 10.3390/cells8050503
- Lantuéjoul, S., Constantin, B., Drabkin, H., Brambilla, C., Roche, J., and Brambilla, E. (2003). Expression of VEGF, semaphorin SEMA3F, and their common receptors neuropilins NP1 and NP2 in preinvasive bronchial lesions, lung tumours, and cell lines. *J Pathol* 200, 336-347. 10.1002/path.1367

- Lee, Y.A., Wallace, M.C., and Friedman, S.L. (2015). Pathobiology of liver fibrosis: a translational success story. *Gut* 64, 830-841. 10.1136/gutjnl-2014-306842
- Lewis, D.R., Chen, H.S., Cockburn, M.G., Wu, X.C., Stroup, A.M., Midthune, D.N., Zou, Z., Krapcho, M.F., Miller, D.G., and Feuer, E.J. (2017). Early estimates of SEER cancer incidence, 2014. *Cancer* 123, 2524-2534. 10.1002/cncr.30630
- Leyland, H., Gentry, J., Arthur, M.J., and Benyon, R.C. (1996). The plasminogen-activating system in hepatic stellate cells. *Hepatology* 24, 1172-1178. 10.1002/hep.510240532
- Lin, N., Meng, L., Lin, J., Chen, S., Zhang, P., Chen, Q., and Lin, Y. (2020). Activated hepatic stellate cells promote angiogenesis in hepatocellular carcinoma by secreting angiopoietin-1. *J Cell Biochem* 121, 1441-1451. 10.1002/jcb.29380
- Liu, Y., Liu, H., Meyer, C., Li, J., Nadalin, S., Königsrainer, A., Weng, H., Dooley, S., and Ten Dijke, P. (2013). Transforming growth factor- β (TGF- β)-mediated connective tissue growth factor (CTGF) expression in hepatic stellate cells requires Stat3 signaling activation. *J Biol Chem* 288, 30708-30719. 10.1074/jbc.M113.478685
- Lo, R.C., and Kim, H. (2017). Histopathological evaluation of liver fibrosis and cirrhosis regression. *Clin Mol Hepatol* 23, 302-307. 10.3350/cmh.2017.0078
- Lua, I., Li, Y., Zagory, J.A., Wang, K.S., French, S.W., Sévigny, J., and Asahina, K. (2016). Characterization of hepatic stellate cells, portal fibroblasts, and mesothelial cells in normal and fibrotic livers. *J Hepatol* 64, 1137-1146. 10.1016/j.jhep.2016.01.010
- Lund, L.R., Riccio, A., Andreasen, P.A., Nielsen, L.S., Kristensen, P., Laiho, M., Saksela, O., Blasi, F., and Danø, K. (1987). Transforming growth factor-beta is a strong and fast acting positive regulator of the level of type-1 plasminogen activator inhibitor mRNA in WI-38 human lung fibroblasts. *EMBO J* 6, 1281-1286.
- Marcellin, P., and Kutala, B.K. (2018). Liver diseases: A major, neglected global public health problem requiring urgent actions and large-scale screening. *Liver Int* 38 *Suppl* 1, 2-6. 10.1111/liv.13682
- Maslak, E., Gregorius, A., and Chlopicki, S. (2015). Liver sinusoidal endothelial cells (LSECs) function and NAFLD; NO-based therapy targeted to the liver. *Pharmacol Rep* 67, 689-694. <https://doi.org/10.1016/j.pharep.2015.04.010>
- Massagué, J. (2012). TGF β signalling in context. *Nat Rev Mol Cell Biol* 13, 616-630. 10.1038/nrm3434
- Matsushita, A., Götze, T., and Korc, M. (2007). Hepatocyte growth factor-mediated cell invasion in pancreatic cancer cells is dependent on neuropilin-1. *Cancer Res* 67, 10309-10316. 10.1158/0008-5472.Can-07-3256

Mederacke, I., Dapito, D.H., Affò, S., Uchinami, H., and Schwabe, R.F. (2015). High-yield and high-purity isolation of hepatic stellate cells from normal and fibrotic mouse livers. *Nat Protoc* 10, 305-315. 10.1038/nprot.2015.017

Mederacke, I., Hsu, C.C., Troeger, J.S., Huebener, P., Mu, X., Dapito, D.H., Pradere, J.P., and Schwabe, R.F. (2013). Fate tracing reveals hepatic stellate cells as dominant contributors to liver fibrosis independent of its aetiology. *Nat Commun* 4, 2823. 10.1038/ncomms3823

Menyhárt, O., Nagy, Á., and Gyórfy, B. (2018). Determining consistent prognostic biomarkers of overall survival and vascular invasion in hepatocellular carcinoma. *R Soc Open Sci* 5, 181006. 10.1098/rsos.181006

Miao, H.Q., Soker, S., Feiner, L., Alonso, J.L., Raper, J.A., and Klagsbrun, M. (1999). Neuropilin-1 mediates collapsin-1/semaphorin III inhibition of endothelial cell motility: functional competition of collapsin-1 and vascular endothelial growth factor-165. *J Cell Biol* 146, 233-242. 10.1083/jcb.146.1.233

Migdal, M., Huppertz, B., Tessler, S., Comforti, A., Shibuya, M., Reich, R., Baumann, H., and Neufeld, G. (1998). Neuropilin-1 is a placenta growth factor-2 receptor. *J Biol Chem* 273, 22272-22278. 10.1074/jbc.273.35.22272

Mihm, S. (2018). Danger-Associated Molecular Patterns (DAMPs): Molecular Triggers for Sterile Inflammation in the Liver. *Int J Mol Sci* 19. 10.3390/ijms19103104

Mikula, M., Proell, V., Fischer, A.N., and Mikulits, W. (2006). Activated hepatic stellate cells induce tumor progression of neoplastic hepatocytes in a TGF-beta dependent fashion. *J Cell Physiol* 209, 560-567. 10.1002/jcp.20772

Mokdad, A.A., Lopez, A.D., Shahrzad, S., Lozano, R., Mokdad, A.H., Stanaway, J., Murray, C.J., and Naghavi, M. (2014). Liver cirrhosis mortality in 187 countries between 1980 and 2010: a systematic analysis. *BMC Med* 12, 145. 10.1186/s12916-014-0145-y

Morales-Ruiz, M., Rodríguez Vita, J., Jimenez, W., and Ribera, J. (2015). Pathophysiology of Portal Hypertension. In, pp. 3631-3665.

Nakao, A., Imamura, T., Souchelnytskyi, S., Kawabata, M., Ishisaki, A., Oeda, E., Tamaki, K., Hanai, J., Heldin, C.H., Miyazono, K., *et al.* (1997). TGF-beta receptor-mediated signalling through Smad2, Smad3 and Smad4. *EMBO J* 16, 5353-5362. 10.1093/emboj/16.17.5353

Nasarre, P., Gemmill, R.M., and Drabkin, H.A. (2014). The emerging role of class-3 semaphorins and their neuropilin receptors in oncology. *Onco Targets Ther* 7, 1663-1687. 10.2147/ott.S37744

Neufeld, G., Mumblat, Y., Smolkin, T., Toledano, S., Nir-Zvi, I., Ziv, K., and Kessler, O. (2016). The semaphorins and their receptors as modulators of tumor progression. *Drug Resistance Updates* 29, 1-12. <https://doi.org/10.1016/j.drug.2016.08.001>

Papic, N., Zidovec Lepej, S., Gorenc, L., Grgic, I., Gasparov, S., Filipic Kanizaj, T., and Vince, A. (2018). The association of semaphorins 3C, 5A and 6D with liver fibrosis stage in chronic hepatitis C. *PLoS One* 13, e0209481. 10.1371/journal.pone.0209481

Pasterkamp, R.J., and Giger, R.J. (2009). Semaphorin function in neural plasticity and disease. *Curr Opin Neurobiol* 19, 263-274. 10.1016/j.conb.2009.06.001

Peng, H.Y., Gao, W., Chong, F.R., Liu, H.Y., and Zhang, J.I. (2015). Semaphorin 4A enhances lung fibrosis through activation of Akt via PlexinD1 receptor. *J Biosci* 40, 855-862. 10.1007/s12038-015-9566-9

Pinzani, M. (2015). Chapter 3 - Hepatic Fibrosis: A Global Clinical Problem. In *Stellate Cells in Health and Disease*, C.R. Gandhi, and M. Pinzani, eds. (Boston: Academic Press), pp. 29-39.

Pinzani, M., and Gandhi, C.R. (2015). Chapter 1 - History and Early Work. In *Stellate Cells in Health and Disease*, C.R. Gandhi, and M. Pinzani, eds. (Boston: Academic Press), pp. 1-13.

Pinzani, M., and Macias-Barragan, J. (2010). Update on the pathophysiology of liver fibrosis. *Expert Rev Gastroenterol Hepatol* 4, 459-472. 10.1586/egh.10.47

Pinzani, M., Milani, S., Grappone, C., Weber, F.L., Jr., Gentilini, P., and Abboud, H.E. (1994). Expression of platelet-derived growth factor in a model of acute liver injury. *Hepatology* 19, 701-707. 10.1002/hep.1840190323

Potiron, V.A., Roche, J., and Drabkin, H.A. (2009). Semaphorins and their receptors in lung cancer. *Cancer Lett* 273, 1-14. 10.1016/j.canlet.2008.05.032

Puche, J.E., Saiman, Y., and Friedman, S.L. (2013). Hepatic stellate cells and liver fibrosis. *Compr Physiol* 3, 1473-1492. 10.1002/cphy.c120035

Püschel, A.W., Adams, R.H., and Betz, H. (1995). Murine semaphorin D/collapsin is a member of a diverse gene family and creates domains inhibitory for axonal extension. *Neuron* 14, 941-948. 10.1016/0896-6273(95)90332-1

Racanelli, V., and Rehmann, B. (2006). The liver as an immunological organ. *Hepatology* 43, S54-62. 10.1002/hep.21060

Racine-Samson, L., Rockey, D.C., and Bissell, D.M. (1997). The role of alpha1beta1 integrin in wound contraction. A quantitative analysis of liver myofibroblasts in vivo and in primary culture. *J Biol Chem* 272, 30911-30917. 10.1074/jbc.272.49.30911

- Ramachandran, P., Dobie, R., Wilson-Kanamori, J.R., Dora, E.F., Henderson, B.E.P., Luu, N.T., Portman, J.R., Matchett, K.P., Brice, M., Marwick, J.A., *et al.* (2019). Resolving the fibrotic niche of human liver cirrhosis at single-cell level. *Nature* 575, 512-518. 10.1038/s41586-019-1631-3
- Rehman, M., and Tamagnone, L. (2013). Semaphorins in cancer: Biological mechanisms and therapeutic approaches. *Semin Cell Dev Biol* 24, 179-189. <https://doi.org/10.1016/j.semcdb.2012.10.005>
- Reilkoff, R.A., Peng, H., Murray, L.A., Peng, X., Russell, T., Montgomery, R., Feghali-Bostwick, C., Shaw, A., Homer, R.J., Gulati, M., *et al.* (2013). Semaphorin 7a+ regulatory T cells are associated with progressive idiopathic pulmonary fibrosis and are implicated in transforming growth factor- β 1-induced pulmonary fibrosis. *Am J Respir Crit Care Med* 187, 180-188. 10.1164/rccm.201206-1109OC
- Reynaert, H., Thompson, M.G., Thomas, T., and Geerts, A. (2002). Hepatic stellate cells: role in microcirculation and pathophysiology of portal hypertension. *Gut* 50, 571-581. 10.1136/gut.50.4.571
- Roehlen, N., Crouchet, E., and Baumert, T.F. (2020). Liver Fibrosis: Mechanistic Concepts and Therapeutic Perspectives. *Cells* 9, 875. 10.3390/cells9040875
- Rojkind, M., Giambrone, M.A., and Biempica, L. (1979). Collagen types in normal and cirrhotic liver. *Gastroenterology* 76, 710-719.
- Rombouts, K. (2015). Chapter 2 - Hepatic Stellate Cell Culture Models. In *Stellate Cells in Health and Disease*, C.R. Gandhi, and M. Pinzani, eds. (Boston: Academic Press), pp. 15-27.
- Rosmorduc, O., and Housset, C. (2010). Hypoxia: a link between fibrogenesis, angiogenesis, and carcinogenesis in liver disease. *Semin Liver Dis* 30, 258-270. 10.1055/s-0030-1255355
- Ruiz-Ortega, M., Rodríguez-Vita, J., Sanchez-Lopez, E., Carvajal, G., and Egido, J. (2007). TGF-beta signaling in vascular fibrosis. *Cardiovasc Res* 74, 196-206. 10.1016/j.cardiores.2007.02.008
- Saab, S., Tam, S.P., Tran, B.N., Melton, A.C., Tangkijvanich, P., Wong, H., and Yee, H.F. (2002). Myosin mediates contractile force generation by hepatic stellate cells in response to endothelin-1. *J Biomed Sci* 9, 607-612. 10.1007/BF02254988
- Sánchez-Valle, V., Chávez-Tapia, N.C., Uribe, M., and Méndez-Sánchez, N. (2012). Role of oxidative stress and molecular changes in liver fibrosis: a review. *Curr Med Chem* 19, 4850-4860. 10.2174/092986712803341520
- Sang, Y., Tsuji, K., Fukushima, K., Takahashi, K., Kitamura, S., and Wada, J. (2021). Semaphorin3A inhibitor ameliorates renal fibrosis through the regulation of JNK signaling. *Am J Physiol Renal Physiol* 321, F740-f756. 10.1152/ajprenal.00234.2021

- Schirmacher, P., Geerts, A., Pietrangelo, A., Dienes, H.P., and Rogler, C.E. (1992). Hepatocyte growth factor/hepatopoietin A is expressed in fat-storing cells from rat liver but not myofibroblast-like cells derived from fat-storing cells. *Hepatology* 15, 5-11. 10.1002/hep.1840150103
- Schuppan, D., Ruehl, M., Somasundaram, R., and Hahn, E.G. (2001). Matrix as a modulator of hepatic fibrogenesis. *Semin Liver Dis* 21, 351-372. 10.1055/s-2001-17556
- Schwamborn, J.C., Fiore, R., Bagnard, D., Kappler, J., Kaltschmidt, C., and Püschel, A.W. (2004). Semaphorin 3A stimulates neurite extension and regulates gene expression in PC12 cells. *J Biol Chem* 279, 30923-30926. 10.1074/jbc.C400082200
- Shafer, S.L., and Towler, D.A. (2009). Transcriptional regulation of SM22alpha by Wnt3a: convergence with TGFbeta(1)/Smad signaling at a novel regulatory element. *J Mol Cell Cardiol* 46, 621-635. 10.1016/j.yjmcc.2009.01.005
- Shang, L., Hosseini, M., Liu, X., Kisseleva, T., and Brenner, D.A. (2018). Human hepatic stellate cell isolation and characterization. *J Gastroenterol* 53, 6-17. 10.1007/s00535-017-1404-4
- Sheth, K., and Bankey, P. (2001). The liver as an immune organ. *Curr Opin Crit Care* 7, 99-104. 10.1097/00075198-200104000-00008
- Smolkin, T., Nir-Zvi, I., Duvshani, N., Mumblat, Y., Kessler, O., and Neufeld, G. (2018). Complexes of plexin-A4 and plexin-D1 convey semaphorin-3C signals to induce cytoskeletal collapse in the absence of neuropilins. *J Cell Sci* 131. 10.1242/jcs.208298
- Spill, F., Reynolds, D.S., Kamm, R.D., and Zaman, M.H. (2016). Impact of the physical microenvironment on tumor progression and metastasis. *Curr Opin Biotechnol* 40, 41-48. 10.1016/j.copbio.2016.02.007
- Stamenkovic, I. (2003). Extracellular matrix remodelling: the role of matrix metalloproteinases. *J Pathol* 200, 448-464. 10.1002/path.1400
- Staton, C.A., Shaw, L.A., Valluru, M., Hoh, L., Koay, I., Cross, S.S., Reed, M.W., and Brown, N.J. (2011). Expression of class 3 semaphorins and their receptors in human breast neoplasia. *Histopathology* 59, 274-282. 10.1111/j.1365-2559.2011.03922.x
- Takahashi, T., Fournier, A., Nakamura, F., Wang, L.-H., Murakami, Y., Kalb, R.G., Fujisawa, H., and Strittmatter, S.M. (1999). Plexin-Neuropilin-1 Complexes Form Functional Semaphorin-3A Receptors. *Cell* 99, 59-69. [https://doi.org/10.1016/S0092-8674\(00\)80062-8](https://doi.org/10.1016/S0092-8674(00)80062-8)
- Tam, K.J., Hui, D.H.F., Lee, W.W., Dong, M., Tombe, T., Jiao, I.Z.F., Khosravi, S., Takeuchi, A., Peacock, J.W., Ivanova, L., *et al.* (2017). Semaphorin 3C drives epithelial-to-mesenchymal transition, invasiveness, and stem-like characteristics in prostate cells. *Sci Rep* 7, 11501. 10.1038/s41598-017-11914-6

Tamagnone, L., Artigiani, S., Chen, H., He, Z., Ming, G.-I., Song, H.-j., Chedotal, A., Winberg, M.L., Goodman, C.S., Poo, M.-m., *et al.* (1999a). Plexins Are a Large Family of Receptors for Transmembrane, Secreted, and GPI-Anchored Semaphorins in Vertebrates. *Cell* 99, 71-80. [https://doi.org/10.1016/S0092-8674\(00\)80063-X](https://doi.org/10.1016/S0092-8674(00)80063-X)

Tamagnone, L., Artigiani, S., Chen, H., He, Z., Ming, G.I., Song, H., Chedotal, A., Winberg, M.L., Goodman, C.S., Poo, M., *et al.* (1999b). Plexins are a large family of receptors for transmembrane, secreted, and GPI-anchored semaphorins in vertebrates. *Cell* 99, 71-80. 10.1016/s0092-8674(00)80063-x

Tannapfel, A., and Klöppel, G., eds. (2020). *Pathologie : Leber, Gallenwege und Pankreas*, 3rd ed. 2020. edn (Berlin, Heidelberg: Springer Berlin Heidelberg).

Toledano, S., Lu, H., Palacio, A., Ziv, K., Kessler, O., Schaal, S., Neufeld, G., and Barak, Y. (2016). A Sema3C Mutant Resistant to Cleavage by Furin (FR-Sema3C) Inhibits Choroidal Neovascularization. *PLoS One* 11, e0168122. 10.1371/journal.pone.0168122

Toledano, S., Nir-Zvi, I., Engelman, R., Kessler, O., and Neufeld, G. (2019). Class-3 Semaphorins and Their Receptors: Potent Multifunctional Modulators of Tumor Progression. *Int J Mol Sci* 20. 10.3390/ijms20030556

Tran, T.S., Kolodkin, A.L., and Bharadwaj, R. (2007). Semaphorin regulation of cellular morphology. *Annu Rev Cell Dev Biol* 23, 263-292. 10.1146/annurev.cellbio.22.010605.093554

Trefts, E., Gannon, M., and Wasserman, D.H. (2017). The liver. *Curr Biol* 27, R1147-R1151. <https://doi.org/10.1016/j.cub.2017.09.019>

Tsuchida, T., and Friedman, S.L. (2017). Mechanisms of hepatic stellate cell activation. *Nat Rev Gastroenterol Hepatol* 14, 397-411. 10.1038/nrgastro.2017.38

Villanueva, C., Albillos, A., Genescà, J., Abraldes, J.G., Calleja, J.L., Aracil, C., Bañares, R., Morillas, R., Poca, M., Peñas, B., *et al.* (2016). Development of hyperdynamic circulation and response to β -blockers in compensated cirrhosis with portal hypertension. *Hepatology* 63, 197-206. 10.1002/hep.28264

Wake, K. (1971). "Sternzellen" in the liver: perisinusoidal cells with special reference to storage of vitamin A. *Am J Anat* 132, 429-462. 10.1002/aja.1001320404

Wang, L., Feng, Y., Xie, X., Wu, H., Su, X.N., Qi, J., Xin, W., Gao, L., Zhang, Y., Shah, V.H., *et al.* (2019). Neuropilin-1 aggravates liver cirrhosis by promoting angiogenesis via VEGFR2-dependent PI3K/Akt pathway in hepatic sinusoidal endothelial cells. *EBioMedicine* 43, 525-536. 10.1016/j.ebiom.2019.04.050

Weiskirchen, R., and Tacke, F. (2016). Liver Fibrosis: From Pathogenesis to Novel Therapies. *Dig Dis* 34, 410-422. 10.1159/000444556

- Weiskirchen, S., Tag, C.G., Sauer-Lehnen, S., Tacke, F., and Weiskirchen, R. (2017). Isolation and Culture of Primary Murine Hepatic Stellate Cells. *Methods Mol Biol* 1627, 165-191. 10.1007/978-1-4939-7113-8_11
- West, D.C., Rees, C.G., Duchesne, L., Patey, S.J., Terry, C.J., Turnbull, J.E., Delehedde, M., Heegaard, C.W., Allain, F., Vanpouille, C., *et al.* (2005). Interactions of multiple heparin binding growth factors with neuropilin-1 and potentiation of the activity of fibroblast growth factor-2. *J Biol Chem* 280, 13457-13464. 10.1074/jbc.M410924200
- Worzfeld, T., and Offermanns, S. (2014a). Semaphorins and plexins as therapeutic targets. *Nat Rev Drug Discov* 13, 603-621. 10.1038/nrd4337
- Worzfeld, T., and Offermanns, S. (2014b). Semaphorins and plexins as therapeutic targets. *Nature Reviews Drug Discovery* 13, 603-621. 10.1038/nrd4337
- Yagai, T., Miyajima, A., and Tanaka, M. (2014). Semaphorin 3E secreted by damaged hepatocytes regulates the sinusoidal regeneration and liver fibrosis during liver regeneration. *Am J Pathol* 184, 2250-2259. 10.1016/j.ajpath.2014.04.018
- Yamashita, N., Morita, A., Uchida, Y., Nakamura, F., Usui, H., Ohshima, T., Taniguchi, M., Honnorat, J., Thomasset, N., Takei, K., *et al.* (2007). Regulation of spine development by semaphorin3A through cyclin-dependent kinase 5 phosphorylation of collapsin response mediator protein 1. *J Neurosci* 27, 12546-12554. 10.1523/jneurosci.3463-07.2007
- Yang, W.J., Hu, J., Uemura, A., Tetzlaff, F., Augustin, H.G., and Fischer, A. (2015). Semaphorin-3C signals through Neuropilin-1 and PlexinD1 receptors to inhibit pathological angiogenesis. *EMBO Mol Med* 7, 1267-1284. 10.15252/emmm.201404922
- Yata, Y., Gotwals, P., Koteliansky, V., and Rockey, D.C. (2002). Dose-dependent inhibition of hepatic fibrosis in mice by a TGF-beta soluble receptor: implications for antifibrotic therapy. *Hepatology* 35, 1022-1030. 10.1053/jhep.2002.32673
- Yin, C., Evason, K.J., Asahina, K., and Stainier, D.Y. (2013). Hepatic stellate cells in liver development, regeneration, and cancer. *J Clin Invest* 123, 1902-1910. 10.1172/jci66369
- Yokoi, Y., Namihisa, T., Kuroda, H., Komatsu, I., Miyazaki, A., Watanabe, S., and Usui, K. (1984). Immunocytochemical detection of desmin in fat-storing cells (Ito cells). *Hepatology* 4, 709-714. 10.1002/hep.1840040425
- Zhang, C.Y., Yuan, W.G., He, P., Lei, J.H., and Wang, C.X. (2016). Liver fibrosis and hepatic stellate cells: Etiology, pathological hallmarks and therapeutic targets. *World J Gastroenterol* 22, 10512-10522. 10.3748/wjg.v22.i48.10512

Zhao, W., Zhang, L., Xu, Y., Zhang, Z., Ren, G., Tang, K., Kuang, P., Zhao, B., Yin, Z., and Wang, X. (2014). Hepatic stellate cells promote tumor progression by enhancement of immunosuppressive cells in an orthotopic liver tumor mouse model. *Lab Invest* 94, 182-191. 10.1038/labinvest.2013.139

Zipprich, A., Garcia-Tsao, G., Rogowski, S., Fleig, W.E., Seufferlein, T., and Dollinger, M.M. (2012). Prognostic indicators of survival in patients with compensated and decompensated cirrhosis. *Liver Int* 32, 1407-1414. 10.1111/j.1478-3231.2012.02830.

8 APPENDIX

Clinical trials links:

PPAR α / δ agonist: <https://clinicaltrials.gov/ct2/show/NCT02704403> (Access date: 04.12.2021)

FXR agonists: <https://clinicaltrials.gov/ct2/show/NCT02548351> (Access date: 04.12.2021)

LOXL 2 inhibitors: <https://clinicaltrials.gov/ct2/show/NCT03028740> (Access date: 04.12.2021)

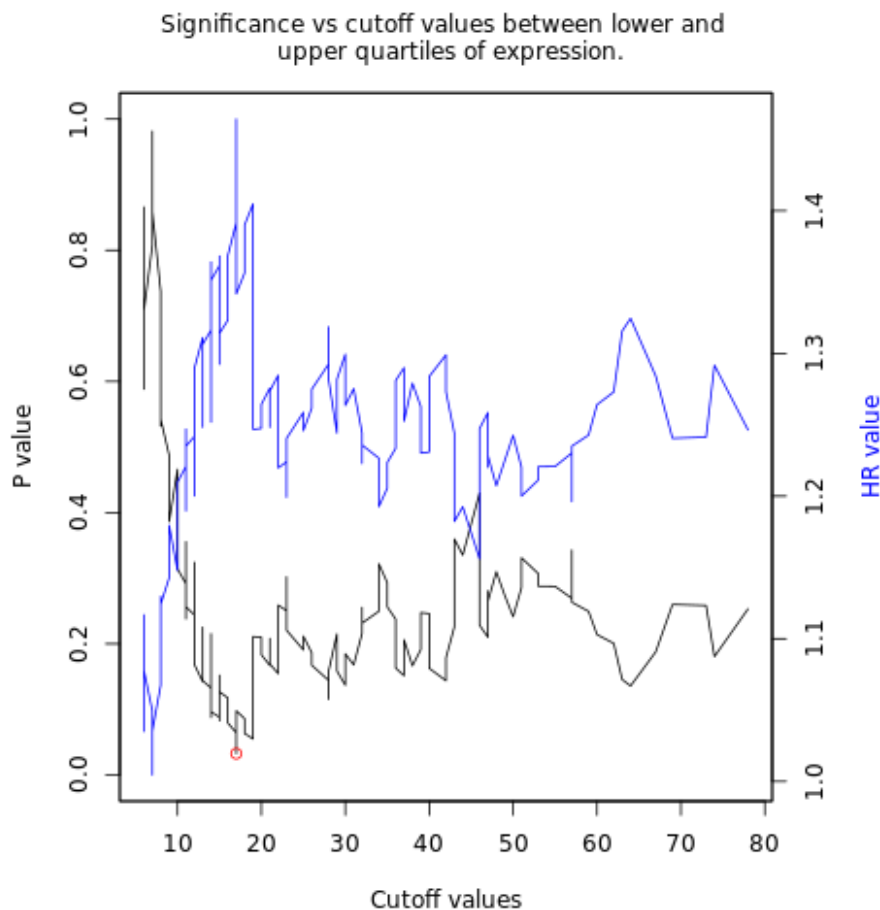


Figure 21 - Automatic cutoff determination of KM OS plot in HCC patients

Cut-off values plot based on Kaplan-Meier plotter for HCC (Menyhárt et al., 2018). Automatic cutoff determines the ideal cutoff for grouping the patients into high and low expressing collectives. The y-axes show p-value and hazard ratio. Different corresponding p-values are displayed by the black line and are shown on the left y-axis. Corresponding hazard ratio values are displayed by the blue line and shown on the right y-axis. The automatically determined cut-off value is 17 (marked by red circle), corresponding p-value=0.03255, corresponding HR=1.46.

HCC: Hepatocellular carcinoma; HR: hazard ratio

9 CURRICULUM VITAE

PERSONALIEN

Name und Vorname:	Hubert, Max Ole
Geburtsdatum:	19.03.1998
Geburtsort:	Neuss
Vater:	Dr. Oliver Hubert
Mutter:	Dr. Dörte Hubert

SCHULISCHER WERDEGANG

8/2007 – 6/2015	Albert Einstein-Gymnasium, Kaarst
6/2015	Abitur Note: 1,0

UNIVERSITÄRER WERDEGANG

WS 2015/16	Economics & Management, King's College London
WS 2016/17	Humanmedizin, Ruprecht-Karls Universität Heidelberg
9/2018	1. Abschnitt Ärztliche Prüfung Note: sehr gut
10/2022	2. Abschnitt Ärztliche Prüfung Note: gut
12/2023	3. Abschnitt Ärztliche Prüfung Note: sehr gut
Dezember 2023	Approbation, Ruprecht-Karls Universität Heidelberg Note: sehr gut

10 DANKSAGUNG

Abschließend möchte ich die Gelegenheit nutzen mich bei allen Personen zu bedanken, die mich während meiner Zeit am DKFZ begleitet und unterstützt haben und zum erfolgreichen Abschluss dieser Dissertation beigetragen haben.

Ein großes Dankeschön gilt meinem Doktorvater und Arbeitsgruppenleiter Prof. Andreas Fischer. Danke für die Möglichkeit als Medizinstudent in Deinem Labor in die Welt der Grundlagenwissenschaft einzusteigen, für zahlreiche richtungswesende Treffen während meiner Laborzeit, die erfolgreiche Unterstützung bei Stipendienbewerbungen und die perfekte und schnelle Kommunikation im Rahmen der Einreichung meiner Dissertation.

Das größte Danke richte ich an meine Betreuerin Lena. Ohne Dich, Deine bedingungslose Unterstützung, Geduld, Beharrlichkeit und Motivation würde ich heute wohl nicht mit dieser fertigen Arbeit in den Händen dastehen. Sowohl in den täglichen Gesprächen über Experimente und wissenschaftliche Unklarheiten als auch in persönlichen Gesprächen war auf Dich immer zu 100% Verlass. Das werde ich für immer zu schätzen wissen.

Außerdem möchte ich Jon und Francesca hervorheben – vielen Dank für Eure Betreuung, Euren immer wertvollen Rat und Eure wissenschaftliche und persönliche Unterstützung. Danke für die Zeit, die wir uns als Projektteam durch all die Unwegsamkeiten und Herausforderungen unseres Sema-Projekts gekämpft haben. Danke auch an die anderen Mitglieder des Fischer-Labors (Sana, Ronja, Iris, Jacqueline, Elisenda, Mag und Tara) für Eure Hilfe, Beratung und all die aufmunternden, lustigen und abwechslungsreichen Kaffee Sessions, Casino Lunches, Online Quiz Abende und Lab Meetings.

Meinen Eltern und Schwestern bin ich unglaublich dankbar für zahlreiche Telefonate und Gespräche, die die Motivation aufrecht gehalten, Frustrationen bei Seite gewischt und Zweifel entkräftet haben. Auf Euch ist immer Verlass – habe Euch sehr lieb!

Zuletzt geht ein Dank an meine Freunde Josh, Felix, Pablo, Luki, Luki, David, Tim, Till, Endrit, Krille, David, Greg, Jules, Sophie und Kathi. Ihr habt für die nötige Ablenkung, Leichtigkeit und Positivität gesorgt, die ich an Heidelberg und unserer Gruppe so liebe.